

7. REGIONAL CLIMATES—P. Bissolli, C. Ganter, T. Li, A. Mekonnen, and A. Sánchez-Lugo, Eds.

a. Overview

This chapter provides summaries of the 2017 temperature and precipitation conditions across seven broad regions: North America, Central America and the Caribbean, South America, Africa, Europe, Asia, and Oceania. In most cases, summaries of notable weather events are also included. Local scientists provided the annual summary for their respective regions and, unless otherwise noted, the source of the data used is typically the agency affiliated with the authors. Please note that different nations, even within the same section, may use unique periods to define their normals. Section introductions will typically define the prevailing practices for that section, and exceptions will be noted within the text. In a similar way, many contributing authors use languages other than English as their primary professional language. To minimize additional loss of fidelity through re-interpretation after translation, editors have been conservative and careful to preserve the voice of the author. In some cases, this may result in abrupt transitions in style from section to section.

b. North America

This section is divided into three subsections: Canada, the United States, and Mexico. All anomalies are with respect to the 1981–2010 base period, unless otherwise noted.

Much of North America had warmer-than-average conditions during 2017. The annual temperatures for each country were among the 10 warmest years for their respective records, with Mexico having its warmest year on record. Precipitation varied greatly across the continent, with the United States and Mexico recording near-average national precipitation totals. Annual precipitation across Canada was mostly near to below average, with only parts of the east experiencing above-average conditions. Warm, dry conditions across the west contributed to the development of one of the earliest and largest fires ever recorded in Canada. Over the course of the year, the U.S. experienced 16 weather and climate events that each caused over \$1 billion (U.S. dollars), tying with 2011 as the highest number since records began in 1980.

1) CANADA—L. A. Vincent, R. Whitewood, D. Phillips, and V. Isaac

In Canada, 2017 was characterized by higher-than-average winter mean temperatures from the Yukon to Atlantic Canada, followed by spring, sum-

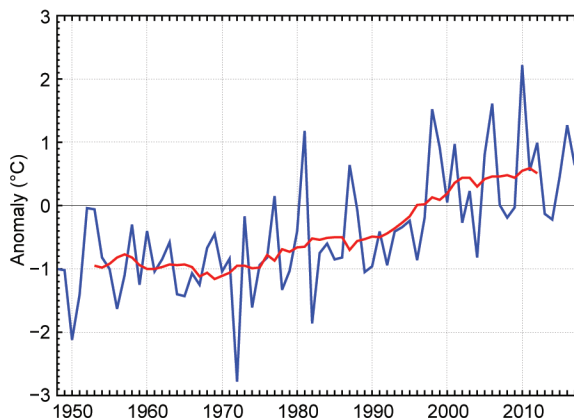


FIG. 7.1. Annual average temperature anomalies (°C; 1981–2010 base period) in Canada for 1948–2017. Red line is the 11-year running mean. (Source: Environment and Climate Change Canada.)

mer, and autumn mean temperatures near or below average across the country. Precipitation measured at 28 available stations indicates wetter-than-average spring conditions across the country and drier-than-average summer conditions mainly in southern British Columbia.

(i) Temperature

The annual average temperature in 2017 for Canada was 0.7°C above the 1981–2010 national average, its tenth warmest year since nationwide records began in 1948 (Fig. 7.1). Four of the ten warmest years have occurred during the last decade, with 2010 being the record warmest (+2.2°C). The national annual average temperature has increased by 1.8°C over the past 70 years. Spatially, annual departures above +2.0°C were recorded in the north (Fig. 7.2a), which resulted in two provinces/territories reporting annual average temperatures among their ten highest: Northwest Territories (fifth highest) and Nunavut (seventh highest).

Seasonally, winter (December–February) 2016/17 was 1.8°C above average—the seventh warmest winter on record. The national winter average temperature has increased by 3.4°C over the past 70 years. Winter anomalies above +3.0°C were recorded from the northwest to the Atlantic coast, and five provinces/territories had winter average temperatures among their ten highest: Northwest Territories (third highest), Nunavut (fourth highest), Ontario (fifth highest), Manitoba (sixth highest), and Saskatchewan (ninth highest). During the spring (March–May), near- to below-average temperatures were recorded from the Pacific to the Atlantic coast across southern Canada while above-average temperatures were observed in the north. The nationally averaged temperature for

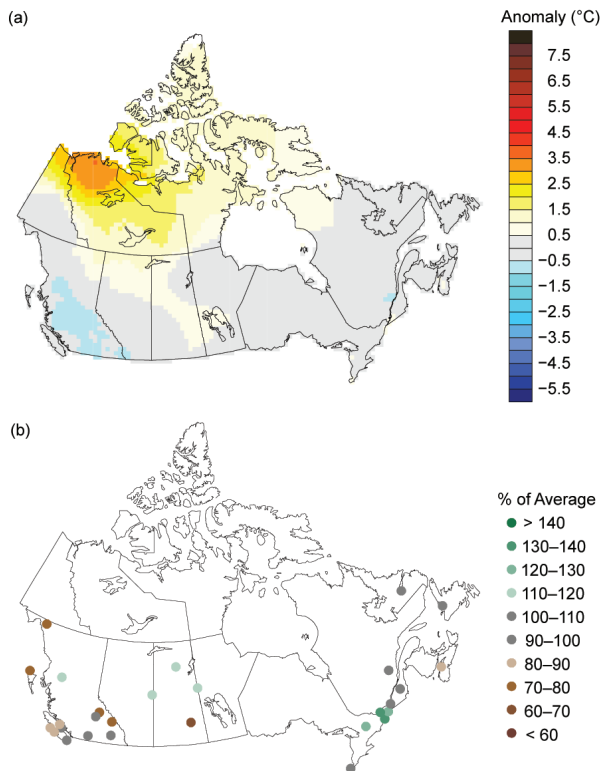


FIG. 7.2. Annual (a) average temperature anomalies (°C) and (b) total precipitation (% of average) in Canada for 2017. Base period: 1981–2010. (Source: Environment and Climate Change Canada.)

spring 2017 was 0.3°C below the 1981–2010 average and the 27th highest in the 70-year record. The national spring temperature has increased by 1.7°C over the past 70 years. None of the provinces/territories experienced an average spring temperature that ranked among their ten highest or lowest on record (since 1948).

Summer (June–August) was 0.4°C above average and the 13th warmest since 1948. Most of the Yukon, Northwest Territories, and southern Nunavut experienced summer anomalies greater than +1.0°C; Northwest Territories and Yukon reported their seventh and eighth warmest summer on record, respectively. Summer temperatures were below average for the regions extending from southern Manitoba to the Atlantic provinces, and were near average for the remainder of the country. The national summer temperature has increased by 1.5°C over the past 70 years. Autumn (September–November) was 0.6°C above average and the 19th highest since 1948. Above-average temperatures were experienced in the north and in the eastern provinces, from eastern Ontario to Atlantic Canada, which resulted in two Maritimes provinces, New Brunswick and Nova Scotia, each having their third warmest autumn since 1948. Near- or below-

average temperatures were experienced in the western provinces, from southern Yukon to western Ontario. The national autumn temperature has increased by 1.7°C over the past 70 years. December 2017 was 2.0°C above average with most of the north experiencing above-average conditions, while Ontario and southern Quebec had below-average temperatures.

(ii) Precipitation

Over the past decade, precipitation monitoring technology has evolved and Environment and Climate Change Canada and its partners implemented a transition from manual observations to using automatic precipitation gauges. Extensive data integration is required to link the current precipitation observations to the long-term historical manual observations. While this data reconciliation due to changing monitoring technology and methods is in progress, this report presents the analysis based on only 28 stations which have sufficient precipitation observations from similar instrumentation over the period 1981–2017; most of these stations are located in the southern regions of the country.

Annual precipitation was near to below average across western Canada, with near to above-average precipitation across eastern Canada (Fig. 7.2b). Seasonally, drier-than-average conditions were experienced at several stations located in the western provinces during the winter 2016/17 and summer 2017; wetter-than-average conditions were observed at most stations across the country during the spring 2017; near-average conditions were found at most stations otherwise.

(iii) Notable events and impacts

In 2017, the southern British Columbia interior experienced its longest and most severe wildfire season in the province’s history. After a wet spring, the region had its driest summer on record. One of the earliest and largest fires ever recorded in Canada burned west of Kamloops in the Ashcroft–Cache Creek–Clinton area. The towns of Ashcroft, Kamloops, and Kelowna each received less than 10 mm of total precipitation during the entire summer. A province-wide state of emergency, the first in 15 years and the province’s longest one, began on 7 July and lasted until 15 September. In total, the British Columbia Wildfire Service reported 1265 fires that destroyed 1.2 million hectares of timber, bush, and grassland, exceeding the previous record for burned land by 30%. Total firefighting costs exceeded half a billion Canadian dollars and insured property losses reached close to \$130 million Canadian dollars (\$103 million U.S.

dollars). This memorable season follows the equally memorable extreme Fort McMurray wildfire in May 2016 in neighboring Alberta province (Kochtubajda et al. 2017).

In May, eastern Ontario and southern Quebec each experienced one of their worst spring flooding events on record. Several rivers exceeded the maximum amount of water released in the past and overflowed from Gananoque to Gaspésie. In Montréal, April rainfall totaled 156.2 mm—its second wettest April in 147 years. Both Ottawa and Montréal had their wettest spring on record—with 400 mm or more at each location (records date back to the 1870s). Spring flooding forced 4000 people to evacuate their homes from the Ottawa region to near Quebec City. Many towns and cities declared states of emergency, including Gatineau, Laval, and Montréal. According to the Insurance Bureau of Canada, spring flooding in April and May resulted in 15 750 claims and \$223 million Canadian dollars (\$177 million U.S. dollars) in property damages. In total, more than 5000 residences were flooded, 550 roads were washed or swept away by floods or landslides, and—tragically—on 6 May, two people were swept away by the swollen Sainte-Anne River in the Gaspé region.

2) UNITED STATES—J. Crouch, A. Smith, C. Fenimore, and R. R. Heim Jr.

The annual average temperature in 2017 for the contiguous United States (CONUS) was 12.5°C or 1.0°C above the 1981–2010 average—its third warmest year since records began in 1895, 0.2°C cooler than 2016 and 0.4°C cooler than 2012 (Fig. 7.3). The annual CONUS temperature over the 123-year period of record is increasing at an average rate of 0.1°C

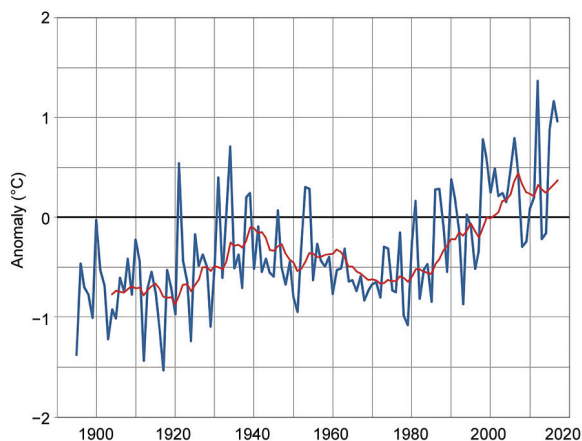


FIG. 7.3. Annual mean temperature anomalies (°C; 1981–2010 base period) for the contiguous United States for 1895–2017. Red line is the 10-year running mean. (Source: NOAA/NCEI.)

decade⁻¹, with the trend increasing since 1970 to 0.3°C decade⁻¹. The nationally averaged precipitation total during 2017 was 104% of average, the 20th wettest year in the historical record. The annual CONUS precipitation total is increasing at an average rate of 4.3 mm decade⁻¹. Outside the CONUS, Alaska had its seventh warmest year (+1.2°C departure) since statewide records began in 1925, and near-median precipitation (104% of average). Complete U.S. temperature and precipitation maps are available at www.ncdc.noaa.gov/cag/.

(i) Temperature

For the CONUS, ten months in 2017 were warmer than their respective 1981–2010 average. Every state, except Washington, had a warmer-than-average annual temperature (Fig. 7.4a). Arizona, Georgia, New Mexico, North Carolina, and South Carolina were each record warm.

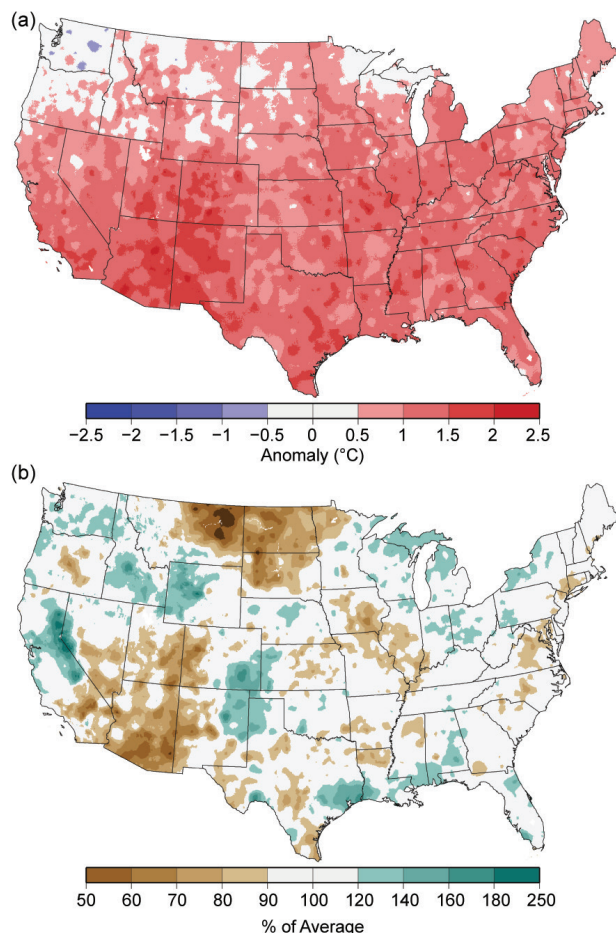


FIG. 7.4. Annual (a) average temperature anomalies (°C) and (b) total precipitation (% of average) in the contiguous United States for 2017. Base period: 1981–2010. (Source: NOAA/NCEI.)

The winter (December–February) 2016/17 CONUS temperature was sixth highest at 1.3°C above average, driven largely by the second warmest February on record. The Rockies to the East Coast were warmer than average, while the Northwest was cooler than average. The CONUS spring (March–May) temperature was 0.9°C above average, its eighth warmest spring on record. Above-average temperatures spanned the nation with near-average conditions in the Northwest and Northeast. The summer (June–August) CONUS temperature was 0.4°C above average, its 15th warmest summer on record. Above-average conditions were observed in the West and along parts of the East Coast. California and Nevada experienced a record-warm summer. The south-central CONUS was cooler than average. The autumn (September–November) temperature was 0.9°C above average, the tenth warmest such period on record for the CONUS. Record warmth occurred in parts of the Southwest and Northeast. December 2017 was 0.6°C above average with the first half of the month having record and near-record warmth across much of the nation and a significant cold wave impacting the East the last week of the month.

(ii) Precipitation

Locations across the West, Great Plains, Great Lakes, Deep South, Midwest, and Northeast had a wetter-than-average year in 2017, while areas of the Northern Rockies and Plains were drier than average (Fig. 7.4b). Six states had annual precipitation totals above their 90th percentile, including Michigan, which was record wet, while only North Dakota was below its 10th percentile. Areas of the West, particularly California, experienced significant drought relief in early 2017, with a multiyear drought nearly eradicated due to the heavy winter precipitation. However, the wet winter allowed vegetation to flourish, creating an abundance of fuels for wildfires during the subsequent dry season. In the Northern Plains, a dry spring and summer set the stage for a rapidly expanding and intensifying drought. The year began and ended with about one-quarter of the contiguous U.S. in drought.

The CONUS winter precipitation was 120% of average, its wettest since 1997/98 and ninth wettest on record. Above-average winter precipitation occurred across the West and parts of the Northern Plains and Midwest. Nevada and Wyoming each had their wettest winter. Spring 2017 was tenth wettest for the CONUS, with 119% of average precipitation. Above-average precipitation occurred across the Northwest, Central Plains, Midwest, Northeast,

and Mid-Atlantic. A record-breaking flood event impacted the mid-Mississippi Valley in late April. The Northern Plains were drier than average with drought conditions developing by the end of the season. Summer precipitation for the CONUS was 112% of average, its 13th wettest on record. Above-average precipitation fell across the Southeast, Great Lakes, and Northeast. In August, Hurricane Harvey brought record rainfall to parts of Louisiana and Texas (see Sidebar 4.3 for more details). Below-average precipitation fell across the Northwest, Northern Rockies, and Plains. For autumn, the CONUS precipitation total was 94% of average, which is near the median value. Above-average precipitation fell across the Northwest, Northern Rockies, Midwest, and Northeast. Above-average precipitation also fell in Florida where Hurricane Irma made landfall in September (see Sidebar 4.1 for more details). Below-average autumn precipitation occurred across parts of the Southwest, Southern Plains, and Lower Mississippi Valley. Arkansas had its driest autumn on record. By the end of the season, drought covered much of the southern CONUS. December 2017 was the 11th driest on record for the CONUS and driest since 1989 with 68% of average precipitation. Drier-than-average conditions stretched from coast to coast with nearly one-third of the CONUS having precipitation totals below the 10th percentile.

(iii) Notable events and impacts

There were 16 weather and climate events with losses exceeding \$1 billion (U.S. dollars) each across the United States (Fig. 7.5) in 2017, including three tropical cyclones, eight severe storms, two inland floods, a crop freeze, drought, and wildfires. The 2017 total tied with 2011 as highest annual number of U.S. billion-dollar disasters (adjusted for inflation) since records began in 1980. Cumulatively, these events led to 362 fatalities and caused \$306 billion U.S. dollars in total, direct costs—a new U.S. annual cost record. The previous costliest year for the U.S. was 2005 with losses of \$215 billion. One of the more noteworthy events included the western wildfire season, with total costs of \$18 billion, tripling the previous U.S. annual wildfire cost record set in 1991. Overall, wildfires burned over 4.0 million hectares across the United States during 2017, which is well above the 2000–10 average of 2.7 million hectares. Hurricane Harvey had total costs of \$125 billion, second only to Hurricane Katrina in the 38-year period of record for billion-dollar disasters. Hurricanes Maria and Irma had total costs of \$90 billion and \$50 billion, respectively. Hurricane Maria now ranks as the third

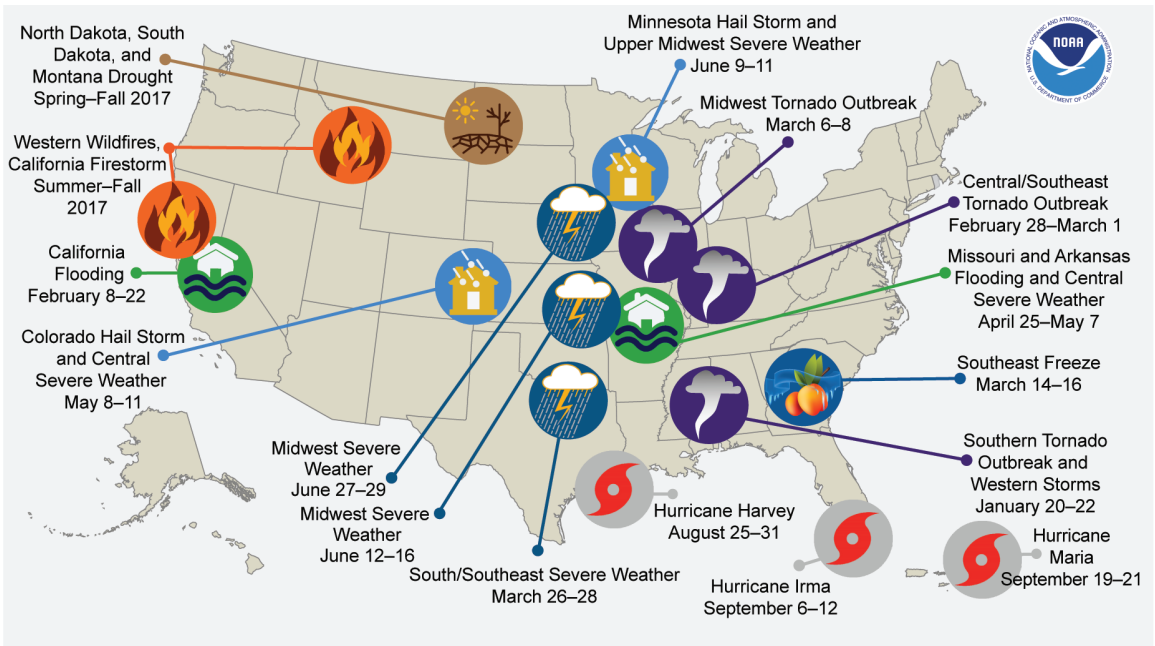


FIG. 7.5. Map depicting date, approximate location, and type of the 16 weather and climate disasters in the U.S. in 2017 with losses exceeding \$1 billion U.S. dollars. (Source: NOAA/NCEI.)

costliest weather and climate disaster on record for the nation, and Irma ranks as the fifth costliest.

Tornado activity during 2017 was above average for the first time since 2011 with 1400 tornadoes confirmed, compared to the 1991–2010 annual average of approximately 1250. There were 34 tornado-related fatalities, well below the 30-year average of 110.

3) MEXICO—R. Pascual Ramirez and A. Albanil

The 2017 mean temperature for Mexico was the highest since national temperature records began in 1971, marking the fourth consecutive year that a new national annual temperature has been tied or broken. Precipitation during 2017 varied greatly across the country; however, the 2017 national precipitation total was near average at 99.4% of normal.

(i) Temperature

The 2017 mean temperature for Mexico was the highest since national temperature records began in 1971 at 22.6°C, or 1.6°C above its 1981–2010 average. This surpassed the previous record set in 2016 by 0.2°C and 2014 and 2015 by 0.5°C, which at the time had been reported as the warmest years on record (Fig. 7.6). The year 2017 also marks the 14th consecutive year with an above-average annual temperature. The national daily mean, maximum, and minimum temperatures were close to two standard deviations above average during much of January–October (Fig. 7.7), resulting in above-average monthly tem-

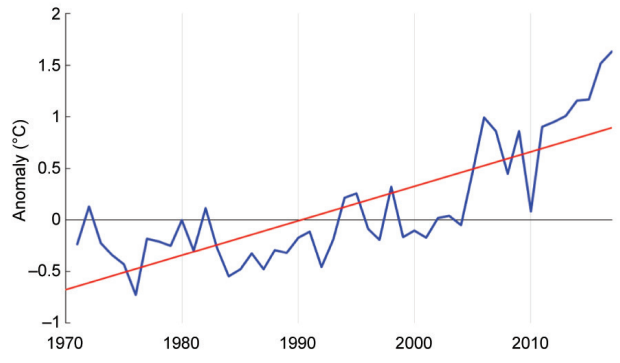


FIG. 7.6. Annual mean temperature anomalies (°C; 1981–2010 base period) for Mexico for 1971–2017. The red line represents the linear trend over this period. (Source: Meteorological Service of Mexico.)

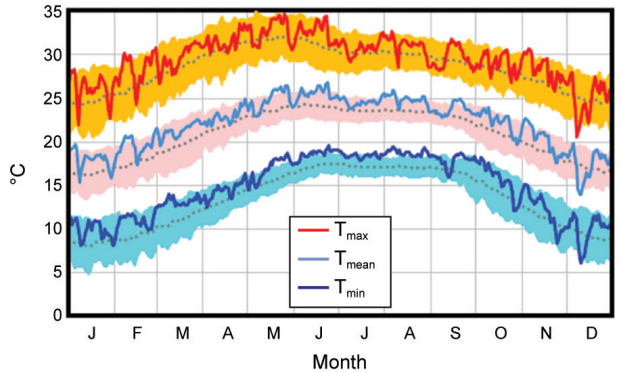


FIG. 7.7. Nationwide daily temperatures (°C; 1981–2010 base period) for Mexico in 2017. Shaded areas represent the ±2 std dev. Solid lines represent daily values for the three temperature parameters and dotted lines are the climatology. (Source: National Meteorological Service of Mexico.)

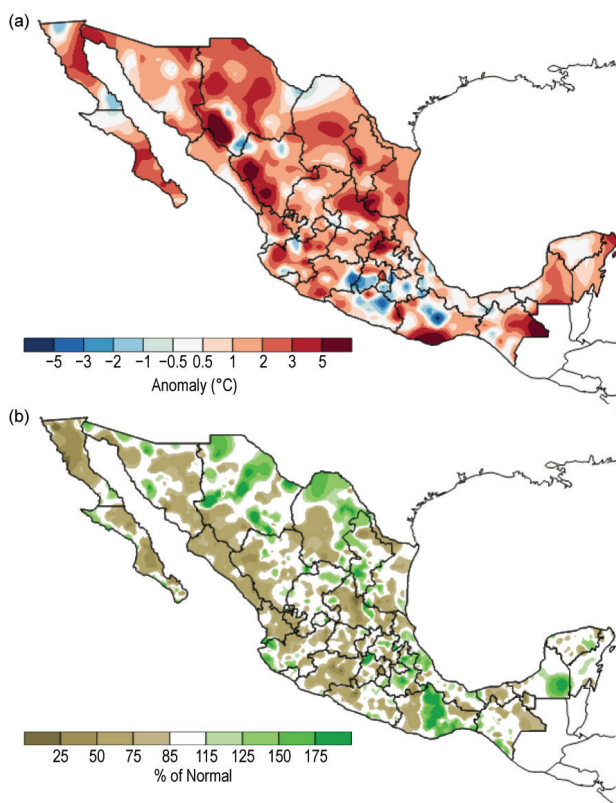


FIG. 7.8. 2017 annual (a) mean temperature anomalies (°C) over Mexico and (b) precipitation anomalies (% of normal). Base period: 1981–2010. (Source: National Meteorological Service of Mexico.)

peratures for 2017. March, June, and November were each warmest on record for their respective months.

Temperatures were above average across most of the country, with small areas in the middle of the country experiencing cooler-than-average conditions (Fig. 7.8a). Eight of Mexico’s 31 states reported their warmest year on record. With the exception of Quintana Roo, located in the south, the remaining record-setting states are located across the northern half of Mexico (Durango, Sinaloa, Nuevo León, Jalisco, Hidalgo, San Luis Potosí, and Tamaulipas).

(ii) Precipitation

Rainfall anomalies varied across Mexico, with above-average conditions in northern Chihuahua and Coahuila, coastal Jalisco, northern Puebla and Veracruz, some areas of Oaxaca, and most of the Yucatan Peninsula. The rest of the country had below-average conditions, with the most notable precipitation deficit of 50% of normal precipitation in Sonora, Sinaloa, and a portion in the central-west (Fig. 7.8b).

Climatologically, September is typically the wettest month of the year, contributing about 18.4% of the annual total rainfall. September 2017 provided

21.7% of the annual rainfall. During the month, four tropical cyclones (Tropical Storms Lidia and Pilar from the Pacific; Hurricane Max in the Pacific; and Hurricane Katia in the Gulf of Mexico) impacted the nation with heavy rain. Three of those four tropical cyclones made landfall, while Pilar stayed off shore, along Mexico’s Pacific coastline. The last time four cyclones came close to or made landfall in Mexico was in September 1974. Four is the highest number of cyclones to come close to or make landfall in Mexico for any month, according to available hurricane data since 1949.

March is typically the driest month of the year, providing only 1.8% of the annual rainfall; however, February was the driest month of 2017, contributing only 1.6% to the annual rainfall total.

Northwestern Mexico typically receives nearly 60% of its total annual rainfall during the four-month period of June–September. However, in 2017, precipitation associated with the monsoon and Tropical Storm Lidia caused the region to receive 60%–68% of its annual rainfall total in just one week.

(iii) Notable events and impacts

Ten tropical cyclones affected Mexico in 2017, five fewer than the 1971–2012 average of fifteen. Six tropical cyclones were near land or made landfall from the Pacific basin, and four from the Caribbean basin/Gulf of Mexico. The Pacific number was fewer than the average of ten, and the Caribbean/Gulf of Mexico number was near the average of five.

Of note, Caribbean Hurricane Franklin (Category 1 on the Saffir–Simpson scale) produced the year’s highest 24-hour precipitation total for Mexico when 404 mm fell in Veracruz upon landfall on 9 August. This value ranks among the top 20 highest daily precipitation totals recorded in the country, according to the Mexican National Meteorological Service.

Drought conditions, which commenced during spring (March–May) 2016, continued to affect southern Mexico in 2017, in particular the Isthmus of Tehuantepec in Oaxaca. Drought conditions deteriorated during the first five months of 2017 due to the warmer- and drier-than-average conditions affecting the area. However, heavy precipitation associated with Tropical Storms Beatriz and Calvin, which made landfall in the affected area, helped ameliorate the long-term drought. These two storms impacted the same area within two weeks of each other (1 June and 12 June, respectively), producing much-needed precipitation and relief for the agriculture sector, but causing damage to infrastructure, such as damaged roads and bridges due to landslides. Drought also af-

ected southern Sinaloa, in northwest Mexico, causing agricultural and livestock losses, and a shortage of drinking water in more than 400 rural communities.

Several heat waves affected eastern Mexico, notably the Huastecas (an area that encompasses the states of San Luis Potosi, Hidalgo, and Veracruz) from 26–30 April and again from 5–8 June. During both heat waves, the maximum temperature reached 50°C, breaking the previous record of 49°C in Huejutla, Hidalgo, set in April 2013. These heat waves were produced by a broad high pressure system located over northeastern Mexico, inhibiting cloudiness and thus increasing temperature. Another major heat wave affected the municipality of Aldama, Chihuahua, during 11–20 June.

c. Central America and the Caribbean

1) CENTRAL AMERICA—J. A. Amador, H. G. Hidalgo, E. J. Alfaro, B. Calderón, and N. Mora

For this region, nine stations from five countries were analyzed (Fig. 7.9). Stations on the Caribbean slope are: Philip Goldson International Airport, Belize; Puerto Barrios, Guatemala; Puerto Lempira, Honduras; and Puerto Limón, Costa Rica. Stations located on the Pacific slope are: Tocumen International Airport and David, Panamá; Liberia, Costa Rica; Choluteca, Honduras; and Puerto San José, Guatemala. The station distribution covers the relevant precipitation regimes located on the Caribbean and Pacific slopes of Central America (Magaña et al. 1999). Precipitation and temperature records for the stations analyzed were provided by Central American

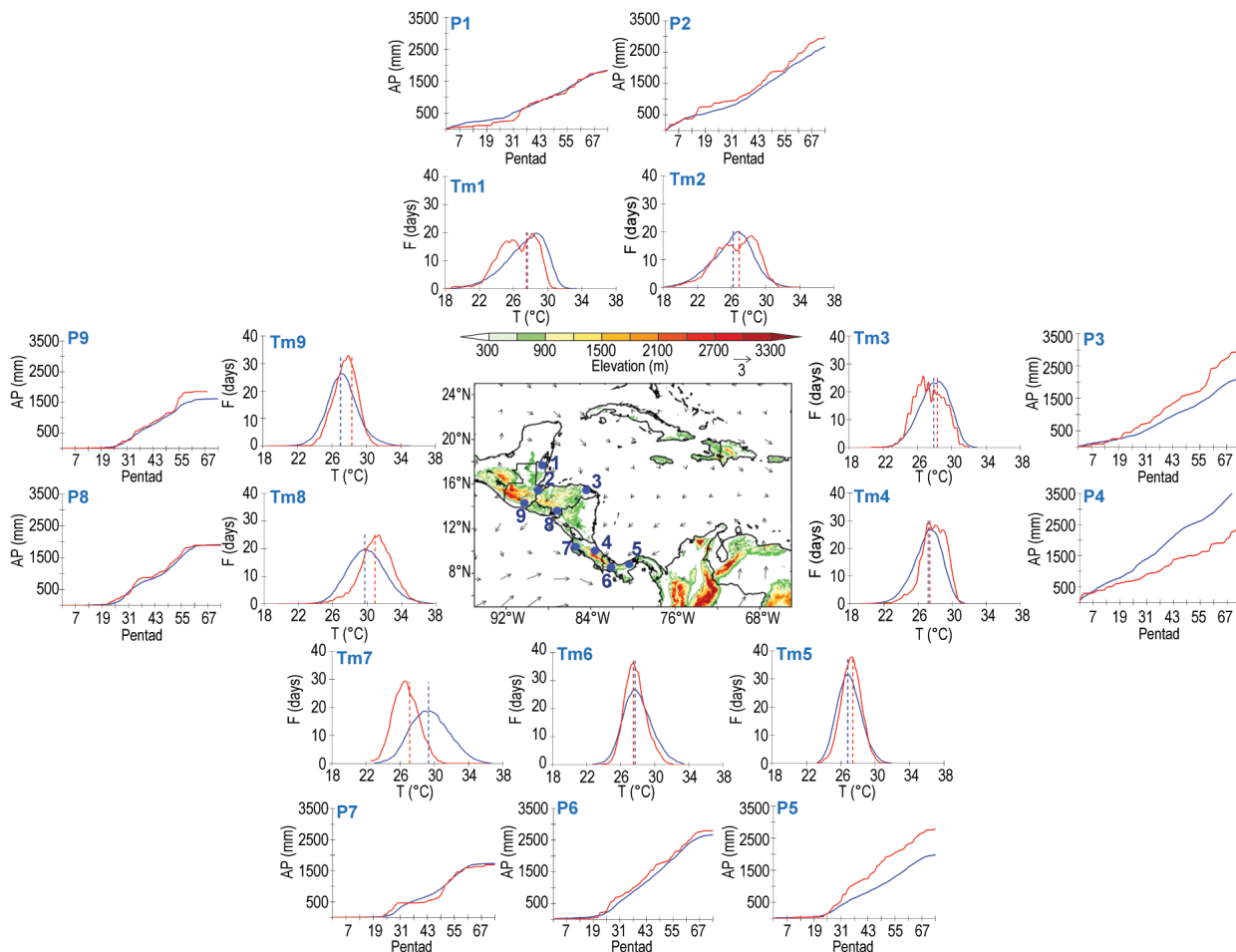


FIG. 7.9. Mean surface temperature (T_m ; °C) frequency (F ; days) and accumulated pentad precipitation (AP ; mm) time series are shown for nine stations (blue dots) in Central America: (1) Philip Goldson International Airport, Belize; (2) Puerto Barrios, Guatemala; (3) Puerto Lempira, Honduras; (4) Puerto Limón, Costa Rica; (5) Tocumen International Airport, Panamá; (6) David, Panamá; (7) Liberia, Costa Rica; (8) Choluteca, Honduras; and (9) Puerto San José, Guatemala. The blue solid line represents the 1981–2010 average values and the red solid line shows 2017 values. Vertical dashed lines show the mean temperature for 2017 (red) and the 1981–2010 period (blue). Vectors indicate July wind anomalies at 925 hPa (1981–2010 base period). Shading depicts regional elevation (m). (Sources: NOAA/NCEI and CA-NWS.)

National Weather Services (CA-NWS) or by NOAA. Anomalies are reported using a 1981–2010 base period and were calculated using CA-NWS data. The methodologies used for all variables can be found in Amador et al. (2011).

(i) Temperature

The mean temperature (Tm) frequency distribution for the climatology and for 2017 for all stations is shown in Fig. 7.9. Five stations on the Caribbean slope and northern Central America (Tm2, Tm3, Tm5, Tm8, and Tm9) had a higher annual mean temperatures than the base period. The largest annual mean temperature occurred at Puerto San José and Choluteca (Tm8 and Tm9, respectively), which were about 1.0°C above normal. Three stations (Tm1, Tm4, and Tm6) had a mean annual temperature similar to the reference period, and the Liberia Station (Tm7) mean annual temperature was colder by 2.0°C. On the Caribbean side, three stations (Tm1, Tm2, and Tm3) depicted a bi-modal temperature distribution during 2017.

(ii) Precipitation

The accumulated pentad precipitation (P; mm) time series for the nine stations in Central America are presented in Fig. 7.9. Puerto San José (P9) was close to normal until pentad 55, when storms produced above-average conditions that continued through pentad 59, followed by a sparse rain period that lasted for over 2 months. This was sufficient to yield above-normal precipitation accumulations at the end of the year. Choluteca (P8) was generally near-normal all year but had a light mid-summer drought from pentad 35 to 41. Liberia (P7) started with significantly above-average conditions during the first part of its rainy season, then experienced a deep midsummer drought (Magaña et al. 1999) and a near-normal second part of the rainy season that resulted in near-normal annual accumulations. During most of the year, David (P6) recorded slightly-above-average conditions, while Puerto Barrios (P2) and Tocumen (P5) were wetter than normal during most of the year, and extremely wet from pentad 32, with values that surpassed the normal average at the 95% confidence level. Belize (P1) had considerable rainfall deficit until pentad 35, after which it recuperated due to wetter-than-average conditions and remained normal until the end of the year. Lempira (P3) recorded conditions during most of the year that were significantly higher than normal at the 95% confidence level, while Puerto Limón (P4) was the only station that had below-average conditions during 2017. Low-level

circulations in the region showed a slightly stronger-than-average Caribbean low-level jet (Amador 1998) during summer (July vectors in Fig. 7.9), a condition usually associated with wetter (drier and more intense mid-summer drought) conditions in the Caribbean (Pacific) slope of Central America.

(iii) Notable events and impacts

Tropical storms were very active in the Caribbean basin (6°–24°N, 92°–60°W) during 2017. There were eight named storms: five tropical storms (Bret, Franklin, Harvey, Nate, and Phillipe) and three major hurricanes (Irma, José, and María). Tropical Storm Nate made landfall in Nicaragua and crossed Honduras on 5–6 October. Nate induced indirect cyclonic circulations (Peña and Douglas 2002) over the isthmus, impacting the Pacific slope of Costa Rica. According to the Costa Rica National Emergency Commission (CNE, its Spanish acronym), Nate caused more than \$540 million U.S. dollars in damages, the highest amount in the country's documented history of natural disasters since 1996. This information is based on a CNE study (Hidalgo 2017) of economic losses including Tropical Storms Alma (2008) and Nate (2017) and Hurricanes Cesar (1996), Mitch (1998), Tomas (2010), and Otto (2016). As with Tropical Depression 12-E in 2011 (Amador et al. 2012), the relative position of Nate with respect to highly vulnerable areas in Central America is as important as tropical storm intensity. Tropical Storm Selma developed in the eastern tropical Pacific and affected Central America during 27–28 October. Selma made landfall in El Salvador on 28 October, marking the first time on record a tropical storm made landfall in El Salvador. For additional information on regional impacts from hydrometeorological events during the year, please refer to Online Table 7.1.

2) CARIBBEAN—T. S. Stephenson, M. A. Taylor, A. R. Trotman, C. J. Van Meerbeeck, V. Marcellin, K. Kerr, J. D. Campbell, J. M. Spence, G. Tamar, M. Hernández Sosa, and K. Stephenson

(i) Temperature

Normal to above-normal annual mean temperatures were recorded across the Caribbean in 2017 (Fig. 7.10a). Some locations in the northern Caribbean (including southern Cuba and Bahamas) experienced below-normal surface temperatures during January–June. In the latter half of the year, above-normal surface temperatures (+0.2° to +1.0°C) were spread across the entire region.

Trinidad reported its tenth warmest annual mean temperature (28.0°C) since records began in 1946;

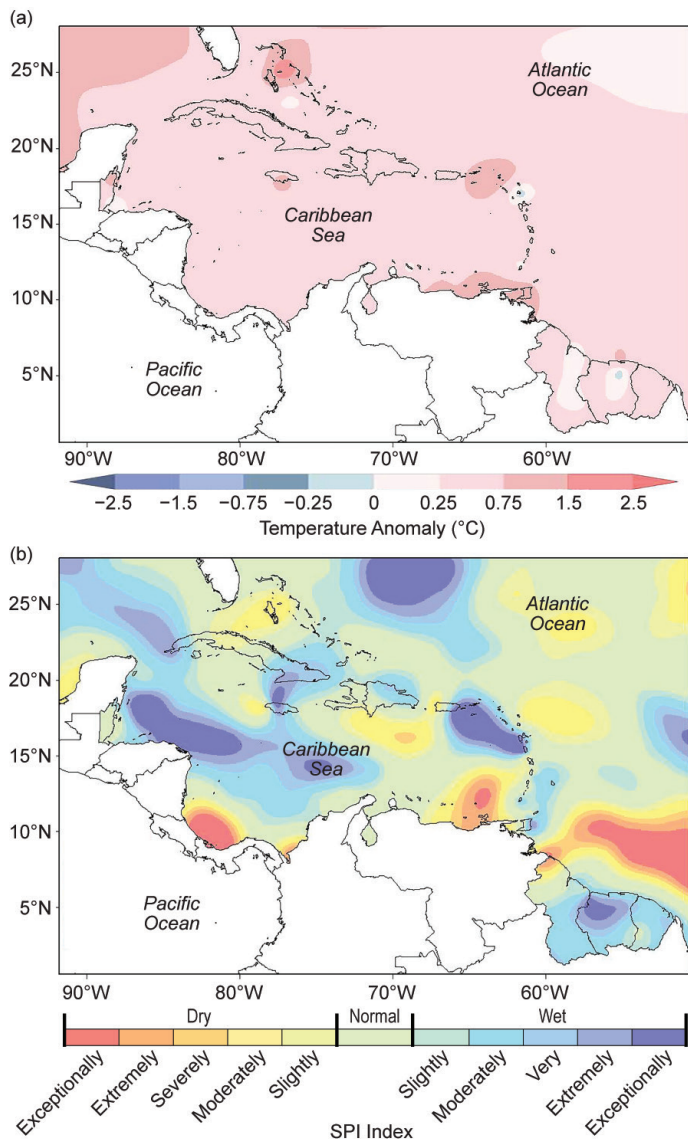


FIG. 7.10. (a) 2017 Annual mean temperature anomalies (°C; 1981–2010 base period) and (b) 2017 annual rainfall pattern as characterized using the standardized precipitation index across the Caribbean. [Source: Caribbean Climate Outlook Forum (CariCOF) and NCEP/NCAR Reanalysis Data. Prepared by the Caribbean Institute for Meteorology and Hydrology (CIMH).]

TABLE 7.1. Extreme annual maximum temperatures (°C) for some Caribbean locations.				
Country	Station Name/ Location	Start Year of Records	Max temp (°C)	2017 Rank
Aruba	Bea	1985	32.1	9
Bahamas	Freeport	1971	29.0	5
Bahamas	LPIA	1971	30.1	3
Belize	Airport	1971	30.5	8
Jamaica	Sangster	1973	32.0	4
Jamaica	Worthy Park	1973	30.8	2
Martinique	Lamentin	1971	30.7	4
Trinidad	Piarco	1946	32.4	7

second highest mean maximum temperature in August (33.6°C), which tied with August 2015 and 2016; and highest daily maximum temperature for August (35.8°C) set on 23 August. San Juan, Puerto Rico, had its third warmest mean temperature in both February (26.4°C) and September (29.2°C) since records began in 1898. Grenada had its highest May mean maximum temperature on record as temperatures soared to 31.1°C in Point Salines. Several locations across the Caribbean had annual maximum temperatures among their nine highest on record (Table 7.1).

(ii) Precipitation

The year brought normal to above-normal annual rainfall totals to much of the Caribbean (Fig. 7.10b). This was observed in association with above-normal annual and seasonal Caribbean SSTs (Chen and Taylor 2002; Taylor et al. 2002; Spence et al. 2004). During the first quarter of the year, most islands experienced predominantly near-normal conditions. However, some islands—including Tobago, Aruba, Curacao, Dominica, parts of Puerto Rico, Dominican Republic, and Jamaica—observed above-normal rainfall, while severely dry conditions were observed in some areas of Puerto Rico. For the April–June period, apart from Tobago where moderately dry conditions were recorded in some areas, rainfall over the islands of the eastern Caribbean was normal to above normal. Mixed conditions were observed over the northern islands. Notably, extremely wet conditions were observed in central regions of Jamaica.

Above-normal rainfall dominated much of the Caribbean between July and September.

This was likely related to the passage of a number of storms through the region, including Hurricanes Irma (see Sidebar 4.1), Jose, and María (see Sidebar 7.1), and favorable atmospheric and oceanic conditions in the region enabled by a La Niña event in the Pacific Ocean. Barbados, Dominica, Guadeloupe, St. Kitts, northern Dominican Republic, and eastern Cuba were extremely wet. In contrast, western areas of Jamaica were extremely dry. During the final three months

of the year, mixed rainfall conditions were experienced across the region. Parts of Trinidad and Tobago and central Jamaica experienced very wet conditions, while parts of Martinique and Guadeloupe were severely dry.

Two locations (Cave Valley, Jamaica, and Sainte Marie, Martinique) each observed their wettest year using records available since 1971, with 2961.2 mm and 2923.0 mm of precipitation, respectively. Port-au-Prince (Haiti) recorded its driest year (588.3 mm) using records available since 1971. Cyril E. King Airport in St. Thomas had its second wettest March (148.1 mm). Jamaica experienced its seventh heaviest mean rainfall across the island in March (248.0 mm) using records available since 1881. San Juan International Airport, Puerto Rico, recorded its wettest September (401.1 mm) since records began in 1898. Christiansted, Henry E. Rohlsen Airport, U.S. Virgin Islands, experienced its wettest March (162.6 mm) and second wettest September (282.4 mm)

since records commenced in 1951. The September extreme anomalies were observed in relation to the passage of Hurricanes Irma and María.

(iii) Notable events and impacts

Category 5 Hurricane Irma severely impacted the Caribbean during 5–8 September. Some of the impacts of Irma on the islands included: 14 deaths and over 50 000 residents without electrical power in the Turks and Caicos; one death and total destruction in Barbuda; several deaths reported in St. Martin; one death and severe damage in Anguilla; damage to property in St. Kitts; five deaths and extensive damage in the U.S. Virgin Islands; four deaths and severe impacts in the British Virgin Islands; major power outages over eastern Puerto Rico; more than 2000 homes damaged in the Dominican Republic; and flooding in some northern coastal areas in Cuba. See Sidebars 4.1 and 7.1 for more detailed information about Irma.

SIDEBAR 7.1: IMPACTS FROM HURRICANES IRMA AND MARIA IN THE CARIBBEAN—O. MARTINEZ-SÁNCHEZ

September 2017 featured the passage of two major hurricanes across the Caribbean: Irma and María. Both hurricanes caused extensive to catastrophic damages across the eastern and northeastern Caribbean islands, where buildings, roads, homes, and the electrical grids were left in ruins.

Hurricane Irma had sustained winds of 160 kt (82 m s^{-1}) with higher wind gusts, torrential rain, and destructive storm surge just as it made landfall on the islands of Barbuda, Saint Martin, and the British Virgin Islands (BVI). Reports indicated that at least 95% of Barbuda's infrastructure was damaged or destroyed. The catastrophic damage that occurred in Barbuda forced a mandatory evacuation of the entire island, with residents brought to the island of Antigua. In the aftermath of Irma, 22.5% of the population in Tortola (BVI) was displaced. Even though the center of Irma passed just north of St. Thomas and St. John (U.S. Virgin Islands; USVI), wind gusts greater than 117 kt (60 m s^{-1}) were reported as the southern eyewall clipped the USVI, causing catastrophic damage and five confirmed deaths. Hurricane Irma delivered the first powerful punch to the electrical grid, structures, and roads across the northern USVI and eastern Puerto Rico.

Two weeks later, Hurricane María made landfall in Dominica as a category 5 storm. María maintained category 5 strength as it continued its path towards the USVI and Puerto Rico (Fig. SB7.1). María made landfall on the southeastern coast of Puerto Rico as a category 4 hurricane with sustained winds of 134 kt (69 m s^{-1}). Unfortunately, most wind sensors were

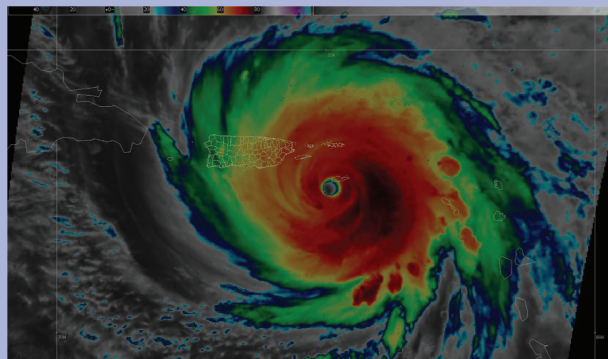


FIG. SB7.1. Satellite image of the center of Hurricane María located southeast of St. Croix, USVI on 20 September 2017. (Source: NOAA/NWS.)

damaged by María before making landfall, resulting in no land-based wind observations that would record the maximum winds affecting the island. María's strong winds also destroyed the FAA-NWS radar, which was designed to endure maximum sustained winds of 116 kt (60 m s^{-1}). Although the lack of observations was an issue for the post-hurricane assessment, there is no doubt that María was much more severe than Irma as the center moved west-northwestward from southeastern Puerto Rico through the interior and into the northwestern sections of the island. Most trees were defoliated, and many were either broken or uprooted. Citizens reported the ground and their houses shaking, and most were amazed by the force of the

Hurricane María made landfall in Dominica as a Saffir–Simpson category 5 intensity level storm on 18 September and struck southeastern Puerto Rico at category 4 intensity on 20 September (see Sidebar 7.1). In Dominica approximately 15 deaths were associated with María, with an additional 20 persons missing. The hurricane destroyed much of the island’s infrastructure, removed vegetation, cut off communication and access to the island, and resulted in food and water shortages. Approximately 80% of agriculture crops were ruined in Puerto Rico and the power grid was destroyed, leaving 3.4 million residents without electricity.

Remarkably Hurricanes Irma, Jose (which peaked as a top end category 4), and María traversed the region over a two-week period. Largely as a result of these three hurricanes, the accumulated cyclone energy (ACE) index (Bell et al. 2000; see also Section 4f2 for an explanation of ACE) for September 2017

was 175×10^4 kt²—the highest value for any month for the Atlantic basin since 1851.

Multiple extreme rainfall events were observed in Jamaica throughout the year. A surface to upper-level trough over the western Caribbean resulted in heavy rain over parts of Jamaica during 13–15 May, causing major flooding and landslides. Impacts include destroyed bridges, multiple damaged roads, and stranded communities. (Clarendon was the worst affected parish; flooding was also observed in nine other parishes.) On 8–10 September, a trough induced by Hurricane Irma across the western Caribbean resulted in heavy thundershowers and flooding over the eastern and central parishes. An accompanying lightning strike on the Jamaica Civil Aviation Authority facility in Kingston on 8 September resulted in damage to radar and communication equipment, resulting in the shutdown of Jamaica’s airspace for more than 24 hours and for 12-hour periods on 10–11 September.

unprecedented strong winds. While most structures across the island are built of concrete and are generally strong enough to withstand strong winds, countless homes and buildings suffered some type of structural damage. Nearly all commercial signs, traffic lights, and roads signs were destroyed. All communications—cellphones and landlines, radio, and television—were largely disrupted; an estimated 95% of the cell towers were out of service in Puerto Rico. The electrical grid was also destroyed, causing 100% of the island to lose electric power. The damage to the electrical grid was so extensive that 5 months later 25% of residents in Puerto Rico were still without power.

The flash flooding due to Hurricane María’s extreme heavy rainfall was catastrophic. The 48-hour rainfall accumulations were generally between 380 and 500 mm with isolated higher amounts. As a result, 30 rivers reached major flood stage, with 13 of those at or above record-flood stage. Numerous bridges were destroyed by the strong currents, isolating many rural communities. The La Plata River, across north central and northeastern Puerto Rico, flooded its entire alluvial valley, including the municipality of Toa Baja where hundreds of families had to be rescued from their rooftops in Barrios Ingenio and Levittown. Across northwestern Puerto Rico, excessive runoff moving across the dam at the Guajataka Lake compromised the stability of the dam, resulting in communities along the Guajataka River below the dam being displaced due to the risk of dam failure. The excessive rainfall also resulted

in widespread landslides across the Island, making thousands of roads impassable, especially across the mountainous areas of Puerto Rico. The blocked roads disrupted the ability of rescue workers to distribute food, water, medical supplies, and fuel for stranded communities. The damage was so bad that <8% of roads were open and usable a month following María’s passage over Puerto Rico. Damage due to beach erosion and coastal flooding was also observed along the shorelines, particularly across western Puerto Rico, where waves destroyed dozens of houses. Storm surge observations across the local islands ranged from 2–3 meters with wave heights greater than 6 meters. Winds, waves, and the storm surge across eastern Puerto Rico sank more than 300 boats.

María was the strongest hurricane to impact Puerto Rico since 1928, when Hurricane San Felipe II (also known as Hurricane Okeechobee) made landfall over the island as a category 5. The official death toll for María stands at 64, although many believe the number is much higher. The catastrophic damage caused thousands of Puerto Ricans to move to the U.S. mainland after the storm. NOAA’s National Centers for Environmental Information (NCEI), in consultation with the National Hurricane Center (NHC), classified Hurricane María as the third costliest U.S. tropical cyclone on record, with \$90 billion U.S. dollars in damages across Puerto Rico and the U.S. Virgin Islands (www.nhc.noaa.gov/news/UpdatedCostliest.pdf).

d. South America

Warmer-than-normal conditions engulfed much of South America during 2017, with anomalies $+1.0^{\circ}\text{C}$ or higher. However, below-normal minimum temperatures were observed across Suriname, French Guiana, a small area in northern Colombia, and across parts of southern Brazil. During 2017, wetter-than-normal conditions prevailed over much of the region, with the largest positive anomalies across the coast of Peru. Drier-than-normal conditions persisted across northeastern Brazil and across parts of southern South America.

Anomalies in this section are all with respect to the 1981–2010 average, unless otherwise noted.

I) NORTHERN SOUTH AMERICA—R. Martínez, L. López, D. Marín, S. Mitro, R. Hernández, E. Zambrano, and J. Nieto

The northern South America region includes Ecuador, Colombia, Venezuela, Guyana, Suriname, and French Guiana.

(i) Temperature

Most of northern South America had above-normal temperatures during 2017. Colombia, Ecuador, Suriname, and Venezuela had annual maximum temperatures that were 0.5° – 1.5°C above normal and, in some isolated areas, greater than $+2.0^{\circ}\text{C}$. Below-normal maximum temperatures for 2017 were limited to small areas across northern South America (Fig. 7.11a). Most of northern South America also experienced above-normal annual minimum temperatures that were $+1.5^{\circ}\text{C}$ or more, although Suriname, French Guiana, and a small area in northern Colombia observed below-normal minimum temperatures during 2017 (Fig. 7.11b). During 2017, August had the high-

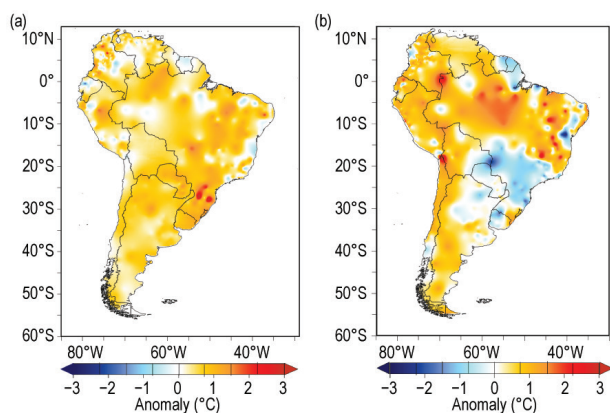


FIG. 7.11. Annual anomalies of 2017 (a) maximum and (b) minimum temperature ($^{\circ}\text{C}$; 1981–2010 base period). (Source: Data from the NMHSs of Argentina, Colombia, Chile, Brazil, Ecuador, Paraguay, Peru, Suriname, and Venezuela; processed by CIIFEN, 2018.)

est positive maximum and minimum temperature anomalies ($+2^{\circ}\text{C}$) across the region.

Cooler-than-normal conditions were limited to Colombia and Venezuela during January and March. However, on 8 February, Bogota, Colombia, set a new maximum temperature of 25.1°C , surpassing the previous record of 24.9°C set in 1995.

(ii) Precipitation

Most of northern South America had above-normal precipitation during 2017 (Fig. 7.12). During January–March 2017, the presence of the coastal El Niño caused above-normal precipitation in the coastal region of Ecuador and southern Colombia (Fig. 7.13). The extreme rainfall events triggered deadly landslides (see Notable events and impacts section). These locations received 150–300 mm (180%–230%) of their normal precipitation from January to March.

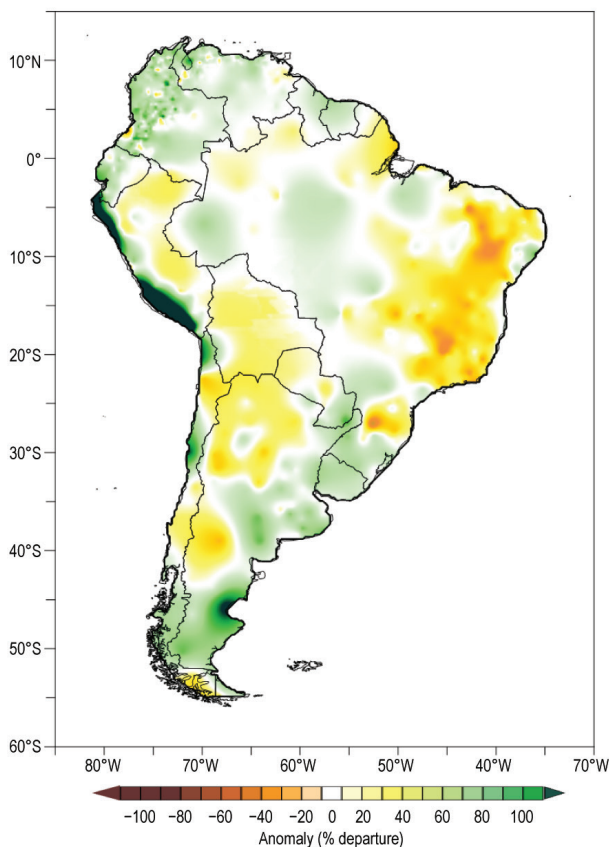


FIG. 7.12. Annual anomalies of 2017 precipitation (%; 1981–2010 base period). (Source: Data from the NMHSs of Argentina, Colombia, Chile, Brazil, Ecuador, Paraguay, Peru, Suriname, and Venezuela; processed by CIIFEN, 2018.)

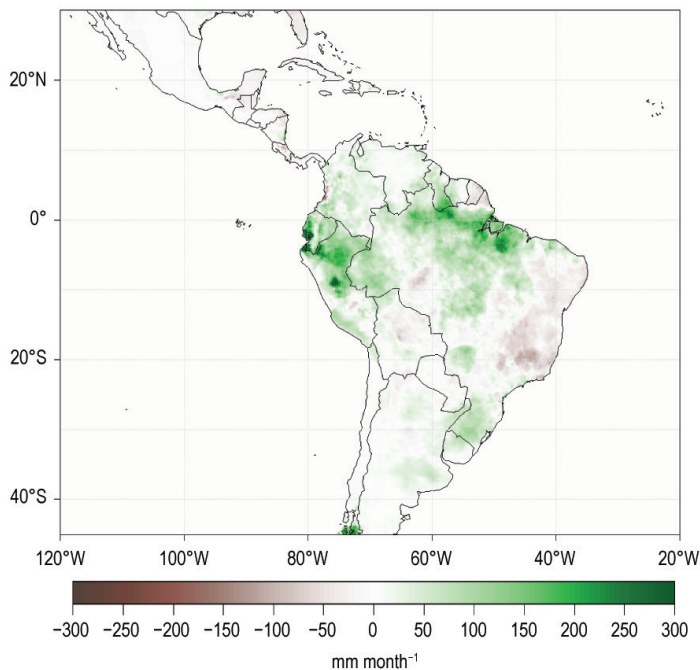


FIG. 7.13. Precipitation anomalies (mm month⁻¹; 1981–2010 base period) during Jan–Mar 2017. (Source: UCSB CHIRPS v2; processed by CIIFEN, 2018.)

(iii) Notable events and impacts

During the first quarter of 2017, regional climate was highly influenced by sea surface temperature warming of the coastal El Niño (Sidebar 7.2). The sudden warming in the eastern equatorial Pacific was different from the typical development of El Niño events. Although its impacts in the Andean countries varied, the most significant effects of the intense and quick coastal El Niño were mainly associated with extreme precipitation events and subsequent flooding and landslides.

From January to April, rainfall exceeded normal conditions in a large part of the coastal region of Ecuador and most of Colombia, Suriname, and Venezuela. Heavy rain during February–April produced floods in Ecuador, which were responsible for more than two dozen fatalities and over 127 000 people affected in the provinces of Guayas and Manabi. Some locations set new precipitation records during March. In Mocoa, Colombia, extreme rainfall (130 mm in 3 hours) in late March fell in areas that were already saturated by heavy rain earlier in the month, causing flash floods and a landslide that killed more than 250 people and left over 300 people injured. During March–May, devastating floods affected the departments of Antioquia, Cundinamarca, and Choco in Colombia.

In Venezuela, above-normal precipitation fell during August–September, triggering the most devastat-

ing floods in more than a decade in the states of Bolívar and Delta Amacuro. The 5-day accumulated rainfall of 120 mm at the end of August caused flash floods and a landslide in Río Mercedes (State of Aragua), affecting hundreds of people and causing four fatalities.

2) CENTRAL SOUTH AMERICA—J. A. Marengo, J. C. Espinoza, L. M. Alves, J. Ronchail, J. Báez, K. Takahashi, and W. Lavado-Casimiro

The central South America region includes Brazil, Peru, Paraguay, and Bolivia.

(i) Temperature

The first half of 2017 was characterized by extreme high temperatures (2°–3°C above normal) in Bolivia, Paraguay, northern Peru, and southern Brazil. Warmer-than-normal conditions continued to affect the region from June through September, with temperatures ranging from 1° to 3°C above normal over Bolivia, Paraguay, and northeastern Brazil. Near-normal temperatures were recorded across the region during October–December.

Several cold episodes occurred from April through July. The passage of a cold front on 20 June brought cold temperatures to the southern half of Brazil, with some regions recording minimum temperatures <0°C. São Joaquim and Bom Jesus (located in the state of Rio Grande do Sul; climatologies of 5.9°C and 8.0°C, respectively) reported minimum temperatures as low as -3°C and -2.6°C, respectively. A polar air intrusion during 17–19 July (see Notable events and impacts section) brought cooler-than-normal conditions to parts of southern and eastern Brazil and in western Amazonia, resulting in monthly minimum temperatures 1°–3°C below normal.

(ii) Precipitation

The first half of 2017 was characterized by below-normal precipitation in Bolivia and west-central and northeastern Brazil. Above-normal precipitation was observed in northwestern Amazonia, southern Brazil, and along the northern Peruvian coast during the second half of the year.

The dry conditions observed in 2016 in Bolivia and northeastern Brazil (Marengo et al. 2017) persisted through 2017. Most of central South America east of the Andes experienced below-normal rainfall (100–150 mm month⁻¹; Fig. 7.14) from January through April, with only weak episodes of the South Atlantic convergence zone (SACZ)—a summertime circulation pattern associated with rainfall in the

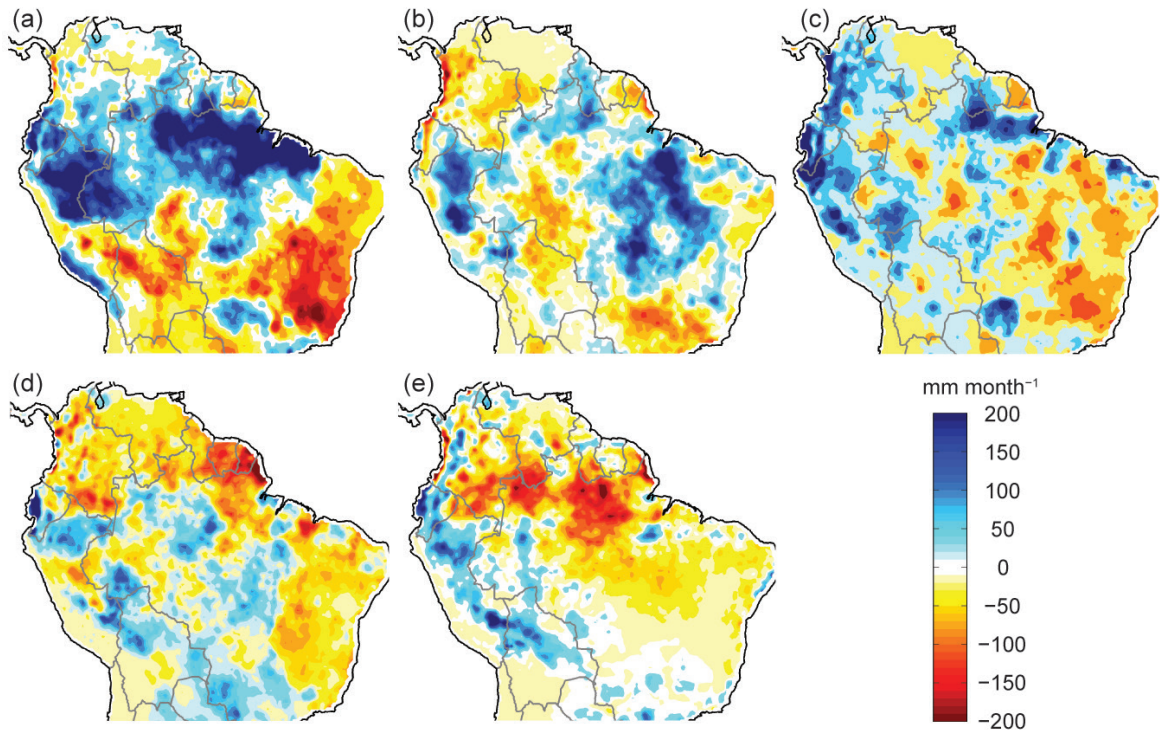


FIG. 7.14. Monthly rainfall anomalies (mm month⁻¹; 1981–2010 base period) for Jan–May 2017. [Source: Climate Hazards group Infrared Precipitation with Stations (CHIRPS) dataset.]

region. The extreme dry conditions were ideal for the development of wildfires. According to the Brazilian National Institute for Space Research, the total number of wildfires for the Amazon region in 2017 was 272 000, the highest number since records began in 1999, which burned over 986 000 hectares. In December, a SACZ episode caused heavy rainfall over southeastern Brazil, Paraguay, and Bolivia, resulting in high river levels for Amazonas-Solimões and Negro River basins. Floods affected the cities of Trinidad and Santa Cruz de la Sierra (Bolivia), as well as soybean crops and livestock in the lowlands of Bolivia.

(iii) Notable events and impacts

Heavy rains that fell in Peru during January–May (Fig. 7.14) were triggered by the coastal El Niño present in the eastern tropical Pacific Ocean (see Sidebar 7.2). Torrential rainfall triggered flash floods and landslides that affected over 625 000 people in the regions of Tumbes, Piura, Lambayeque, La Libertad, Ancash, Ica, and Arequipa and claimed nearly 100 lives. Losses include 242 bridges, 13 227 km of rural and main roads (1.5% of the national road system), 45 335 km of agricultural irrigation channels, and 60 400 ha of crops. In the suburbs of Lima, landslides (“huaycos”) destroyed houses, and the highway

between Lima and the Andean cities was inaccessible for several days.

The January 2017 precipitation total for the city of São Paulo was 453.8 mm, 179% of normal for the month, and its wettest January since 2011. The copious rain prompted flash floods in several locations across the city.

In the city of Maceio, located on the coast in the state of Alagoas in northeast Brazil, a state of emergency was declared due to torrential rains that produced landslides and flash flooding on 27 May, killing three people. By 29 May, over 8400 families were affected, and more than 16 500 people were left homeless. Total rainfall in May 2017 was 742.4 mm (more than twice the monthly normal of 344.7 mm), with 169.6 mm recorded on the 27th.

During the first two weeks of June, well-above-normal rainfall was observed in the eastern portion of the state of Santa Catarina (southern Brazil) due to the passage of a cold front. Torrential rains affected more than 28 800 people and, in some districts, a state of emergency was declared due to floods. The same cold front caused heavy rainfall and flash floods in Rio de Janeiro, and the total rainfall measured on 20 June was almost 247 mm (June climatology is 461.8 mm). This event affected public transportation in the city and flooded some neighborhoods.

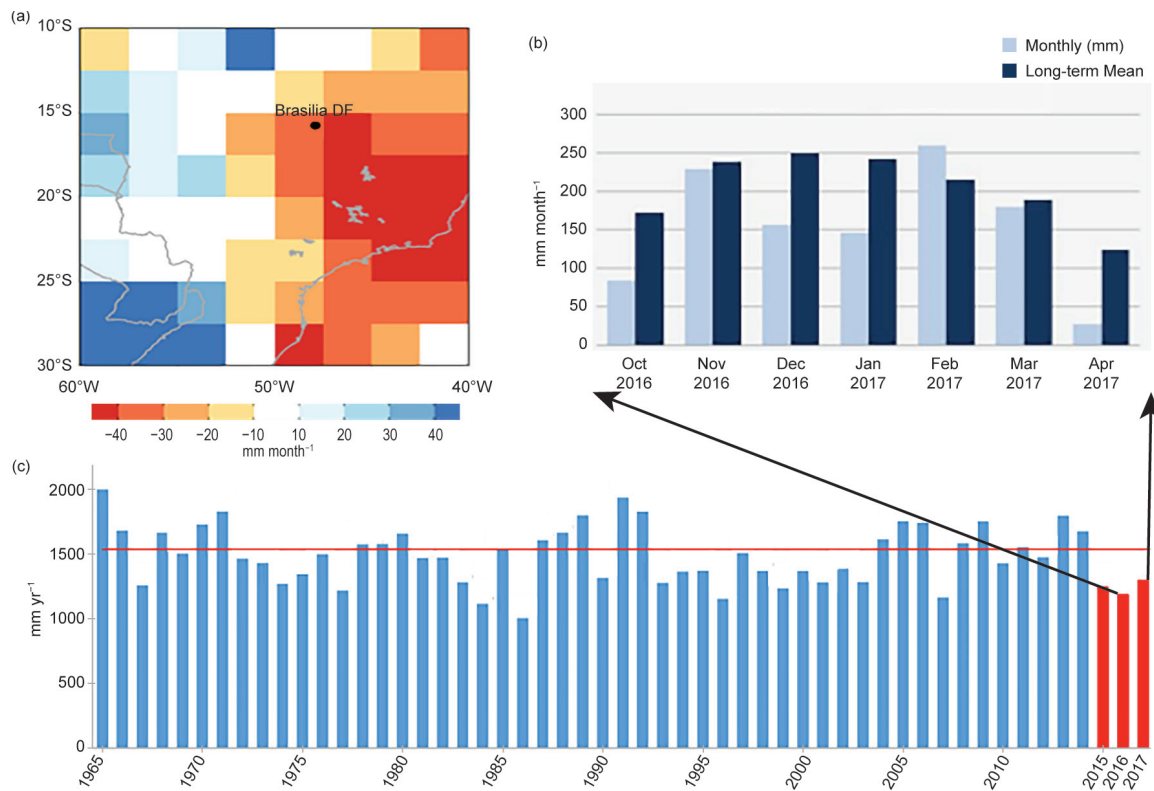


FIG. 7.15. (a) Rainfall anomalies in west-central Brazil during Jan–Apr 2017; the city of Brasilia is marked with a black dot; (b) Monthly rainfall (mm) in Brasilia from Oct 2016 to Apr 2017; 2017 monthly totals are depicted in light blue, while the 1981–2010 normals are in dark blue; (c) Time series of annual rainfall (mm) from 1965 to 2017; normal annual value is depicted with a red line. (Source: GPCP and INMET.)

West-central Brazil, particularly Brasilia (Distrito Federal), has been affected by dry conditions since 2015. The drought conditions, which continued into 2017, were the worst in the last 57 years. In April 2017, Brasilia received only 20% of its normal April precipitation, which is 125 mm; in fact, during the peak of the rainy season (October 2016–April 2017), only February had above-normal monthly rainfall (Fig. 7.15). This prompted a state of emergency and mandatory water restrictions.

The most intense cold episode during austral winter 2017 occurred during 17–19 July. A polar air mass affected the Andes, bringing cooler-than-normal conditions to the western Amazonia regions of Brazil, Peru, and Bolivia. On 17 July, minimum temperatures as low as 10°C were recorded in the Bolivian Amazon and in Puerto Maldonado, Peru (July climatology of 18°C), while on 18 July the western Brazilian Amazon saw temperatures drop to 7.2°C in Campo Verde (located in the state of Mato Grosso; climatology of 21.2°C), 11.3°C in Epiteciolândia (located in the state of Acre; climatology of 19.0°C), and 11.1°C in Guajará-Mirim (located in the state of Rondonia; climatology of 20.0°C). In the city of São

Paulo, the maximum temperature was 8°C (climatology of 11.7°C) on 18 July, and one person died due to exposure to the cold temperatures. From mid-July to mid-August, a cold front in Peru produced temperatures as low as –20°C at 4000 meters above sea level (the record-coldest value is –25°C set on 6 July 1968 at Macusani station in Puno region), and snow fell in the Andes of Peru and Altiplano.

3) SOUTHERN SOUTH AMERICA—J. L. Stella and L. S. Aldeco

This region includes Argentina, Chile, and Uruguay.

(i) Temperature

Above-normal temperatures were observed across southern South America (SSA) during 2017, with annual mean temperatures 0.5°–1.5°C above normal. The national mean temperature anomaly for Argentina and Uruguay was +0.68°C and +1.0°C, respectively, placing 2017 as the warmest year on record since 1961 for both countries. The five warmest years on record for Argentina have all occurred since 2012 (Fig. 7.16). The mean temperature anomaly by decade since the 1960s (Fig. 7.17) shows an increase

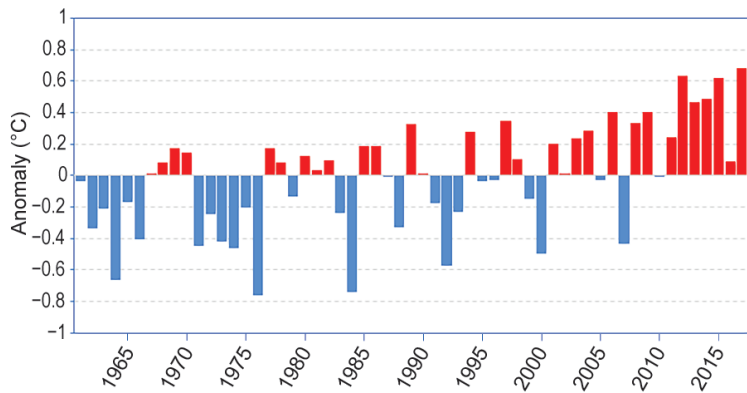


FIG. 7.16. Annual mean temperature anomalies (°C; 1981–2010 base period) for Argentina for 1961–2017. (Source: Argentina’s National Meteorological Service.)

across central and northern Argentina during 2001–2010 and a significant rise across the country as a whole during the decade to date (2011–2017).

Summer (December–February) 2016/17 was particularly warm over most of SSA, with mean temperatures 1°–2°C above normal. Chile had its second warmest summer since 1964. At the end of the season, a heat wave affected a large area in central Argentina. The maximum duration of extreme heat, defined here as minimum and maximum temperatures surpassing the 90th percentile, ranged between five and eight days, and for some locations these conditions extended into the beginning of March, resulting in one of the latest heat waves recorded in that area.

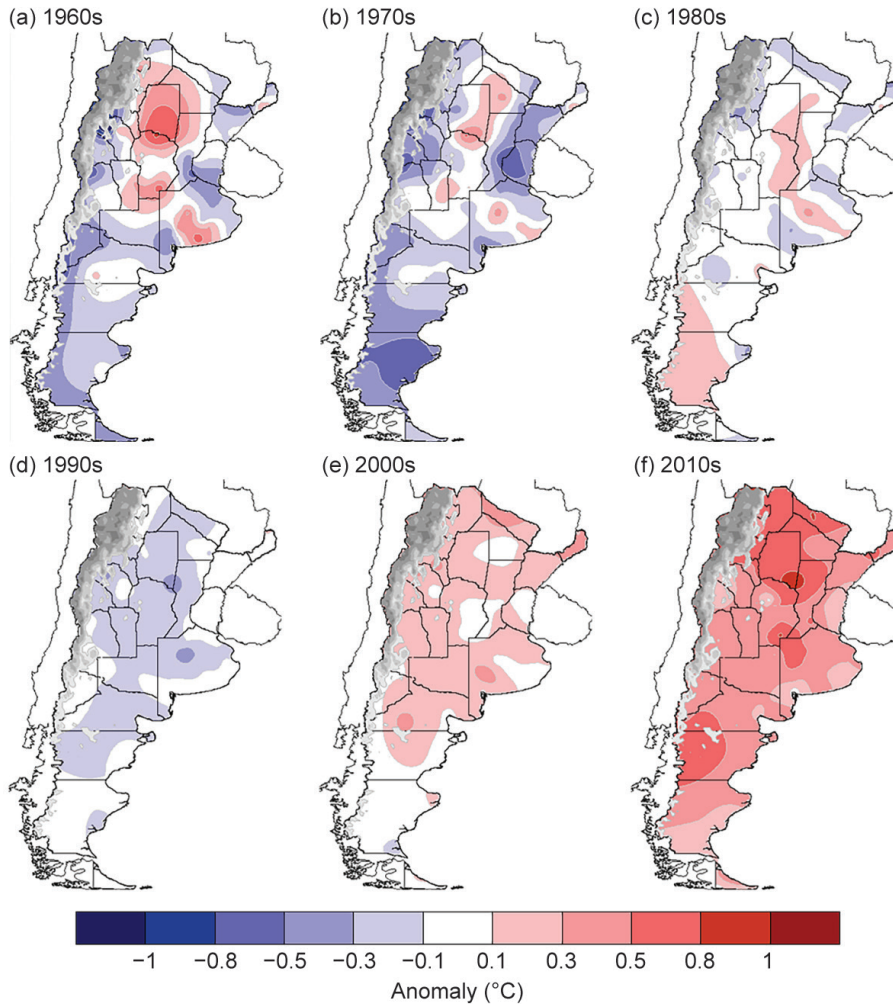


FIG. 7.17. Decadal mean temperature anomalies (°C; 1981–2010 base period) across Argentina from the 1960s through 2017. (Source: Argentina’s National Meteorological Service.)

Below-normal maximum temperatures and above-normal minimum temperatures during austral autumn (March–May) resulted in near-normal mean temperatures across much of SSA ($\pm 0.5^\circ\text{C}$).

Winter (June–August) 2017 was extremely warm over much of the region, with temperatures 1°–3°C above normal across the eastern and northern parts of SSA. This was the warmest winter on record for Uruguay and second warmest for Argentina in their 46-year records. Several individual locations in eastern Argentina reported their warmest winter on record. A new national maximum temperature record was set on 17 June when the temperature soared to 40°C at Tinogasta (northwestern Argentina), marking the first time on record the

temperature reached 40°C between May and July. Meanwhile, a few cold outbreaks during June and July also impacted the region. Bariloche (northwestern Patagonia, Argentina) broke its absolute minimum temperature record when temperatures dropped to -25.4°C on 16 July. The previous record was -21.1°C set on 30 June 1963. These cold spells also caused heavy snowfalls over southern Argentina and Chile and broke several minimum temperature records across Uruguay during June and July.

Spring (September–November) was characterized by below-normal temperatures. The cooling in the Pacific Ocean during spring contributed to the change in temperature pattern across SSA.

(ii) Precipitation

Much of eastern and southern SSA had above-normal annual rainfall during 2017. The most significant precipitation totals were observed in central Argentina, Uruguay, eastern Patagonia, and southern Chile (between 40° and 50°S). Conversely, central Chile and northwestern Patagonia (32°–42°S) had below-normal rainfall during 2017. The estimated annual precipitation anomaly for Argentina was 109.8% of normal, the fourth consecutive year with above-normal rainfall after a long dry period (2003–13). At Isla de Pascua, Chile, 2017 was the second driest year on record since 1950.

The beginning of 2017 was particularly dry in central Argentina and central Chile, causing severe drought that contributed to the development of wildfires in both countries. Meanwhile, northeastern Argentina and Uruguay had above-normal rainfall during summer 2016/17. This pattern intensified and extended to central Argentina during autumn and winter. Intense precipitation affected central and northeastern Argentina and Uruguay, triggering floods in large parts of the region. One of the most extreme precipitation events occurred in Comodoro Rivadavia, a city located in eastern Patagonia (see Notable events and impacts section). Heavy precipitation events also occurred in April 2017, affecting northern, eastern, and southern Uruguay, with several locations recording new daily precipitation records. The copious rainfall triggered floods and caused road interruptions.

During May, intense daily rainfall (>100 mm) affected the Coquimbo region in central Chile; it was considered the most extreme event since the 1950s. La Serena, also in central Chile, received 200% of its normal precipitation for the month.

As La Niña conditions emerged in October, the precipitation pattern across SSA changed abruptly. Most of the SSA region had below-normal rainfall, particularly during October and November, with 50–150 mm below-normal precipitation reported in northern Argentina and 25–50 mm below normal in central Patagonia of Chile and Argentina.

(iii) Notable events and impacts

During January, an extraordinary heat wave affected central Chile and Argentina. The Chilean cities of Antofagasta and Curicó recorded the most prolonged warm periods with extreme high temperatures for 14 and 17 days, respectively. The temperature at Santiago de Chile rose to 37.4°C, the highest value recorded in the 104-year record. The locations of Chillán (41.5°C), Los Angeles (42.2°C), and Curicó (37.3°C) also broke their maximum temperature records. In Argentina, the temperature reached 43.4°C on 27 January at Puerto Madryn, the highest temperature ever recorded so far south (43°S) anywhere in the world.

Drought, combined with high temperatures, triggered devastating forest fires in large areas of central and southern Chile in January. More than 600 000 hectares were burned, with thousands of people affected. Central Argentina had a similar situation with forest fires affecting La Pampa province, leading to more than 1 million hectares burned and cattle and crops losses.

On 30 March, Comodoro Rivadavia reported an impressive daily rainfall amount of 232.4 mm, close to the city's annual normal precipitation total. The heavy rain produced severe flash floods that affected the region. A few days later, the city was impacted once again by heavy rainfall (more than 60 mm in a few hours), leaving most of the city destroyed.

On 15 July, Santiago, Chile's capital, experienced its heaviest snowfall since 1922, with 3–10 cm of snow. Meanwhile, the same synoptic system produced 40 cm of snow over the city of Bariloche, Argentina—its heaviest snowfall in 20 years.

SIDEBAR 7.2: THE 2017 COASTAL EL NIÑO—K. TAKAHASHI, V. ALIAGA-NESTARES, G. AVALOS, M. BOUCHON, A. CASTRO, L. CRUZADO, B. DEWITTE, D. GUTIÉRREZ, W. LAVADO-CASIMIRO, J. MARENGO, A. G. MARTÍNEZ, K. MOSQUERA-VÁSQUEZ, AND N. QUISPE

The original concept of El Niño consisted of anomalously high sea surface temperature and heavy rainfall along the arid northern coast of Peru (Carranza 1891; Carrillo 1893). The concept evolved into the El Niño–Southern Oscillation (ENSO; Bjerknes 1969), although the original El Niño and the Southern Oscillation do not necessarily have the same variability (Deser and Wallace 1987), and the strong El Niño episode in early 1925 coincided with cold-to-neutral ENSO conditions (Takahashi and Martínez 2017). To distinguish the near-coastal El Niño from the warm ENSO phase, Peru operationally defines the “coastal El Niño” based on the seasonal Niño 1+2 SST anomaly (ENFEN 2012; L’Heureux et al. 2017). While recent attention has been brought to the concept of ENSO diversity (e.g., “central Pacific” vs “eastern Pacific” events; Capotondi et al. 2015), the coastal El Niño represents another facet of ENSO that requires further study in terms of its mechanisms and predictability.

A strong coastal El Niño developed off the coast of Peru from January to April 2017 (ENFEN 2017; WMO 2017a,b; Takahashi and Martínez 2017; Ramírez and Briones 2017; Garreaud 2018). The changes were dramatic within the cool coastal upwelling region, as daily SST at Puerto Chicama (7.8°S, 79.1°W) increased abruptly from ~17°C by mid-January to a peak of 26.9°C in early February (ENFEN 2017). The mean maximum/minimum air temperature anomalies along the coast ranged between +1.0°C and +2.3°C across the north, central, and southern regions during February–March.

Convective precipitation is activated in the eastern Pacific when SST exceeds a threshold of ~26–27°C (Takahashi and Dewitte 2016; Jauregui and Takahashi 2017). With SST well in excess of 27°C, the southern ITCZ branch (Huaman and Takahashi 2016; Fig. SB7.2a) was very strong between February and March 2017 and extended into the South American continent

(Fig. SB7.2b). The coastal city of Piura (5.2°S, 80.6°W), located at the core of the ITCZ extension, had a February–March precipitation total of 723 mm, which is nearly seven times its normal amount of 106 mm. The largest precipitation anomalies were observed at low and medium elevations on the western slope of the Andes, triggering several floods and mudslides along the Peruvian coast. Mean January–March 2017 river discharge was around 250% of normal in the Santa (9.01°S, 77.76°W), Rímac (11.77°S, 76.46°W), and Cañete (12.77°S, 75.83°W) River basins.

Impacts along the coast were severe. In the northern regions, a total of 50 927 houses were damaged with close to 1.2 million people affected by flooding, and over 76 000 ha of crops were damaged. As is common with El Niño, this event affected marine resources, primarily the anchovies (Ñiquen and Bouchon 2004; Ñiquen et al. 1999), resulting in decreased fat content and early spawning as a reproductive strategy (IMARPE 2017). The estimated growth of the Peruvian gross domestic product in 2017 was 1.3% lower than expected (BCRP 2017).

The coastal El Niño appears to have been initiated by westerly anomalies in the equatorial far-eastern Pacific in January, the largest for that month since 1981, with a northerly component near the coast (Fig. SB7.3a). At upper levels, the Bolivian high (Lenters and Cook 1996) was located west of its normal position, and a subtropical ridge spread from the Northern Hemisphere, resulting in easterly anomalies and divergence favorable for convection over northwestern Peru (Kousky and Kayano 1994; Vuille et al. 2000). The Madden–Julian oscillation (MJO) had its highest amplitudes in the second half of January and was dominated by the MJO phases 1 to 3, which feature westerly anomalies in this region, according to the Real-time Multivariate MJO index (RMM; Wheeler and Hendon 2004; see Section 4c). The northerly component

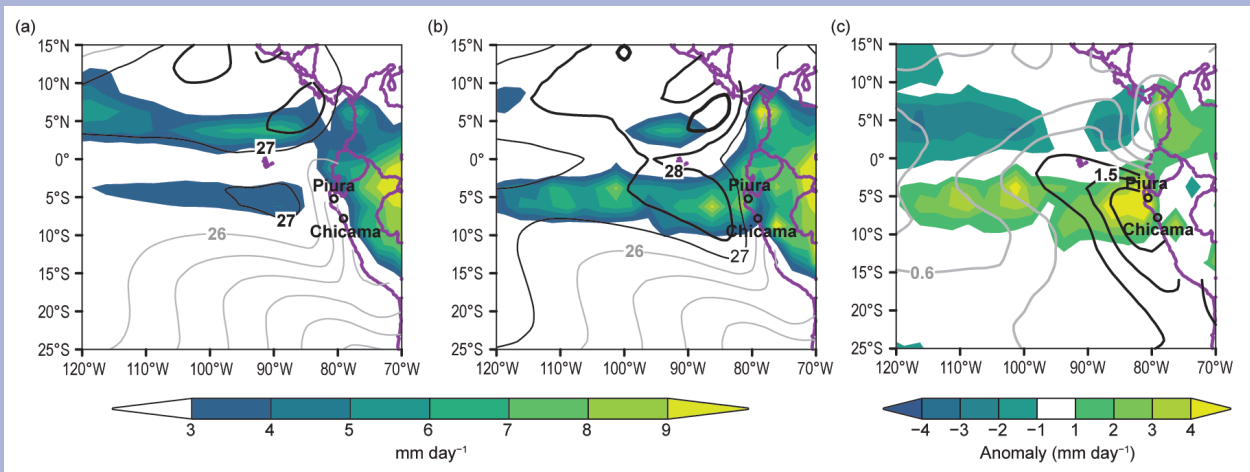


FIG. SB7.2. Feb–Mar SST (contours, interval 1°C) and rainfall (shading, mm day⁻¹): (a) 1981–2010 climatology, (b) 2017 observations, and (c) 2017 anomalies (contour interval: 0.25°C). (Sources: SST: ERSST v5; rainfall: CMAP.)

was probably associated with the negative mean sea level pressure anomalies in the southeast Pacific (Fig. SB7.3a). The latter could have been associated with Rossby-wave teleconnections from the western Pacific (Garreaud 2018), but the SLP anomalies also extended zonally uniformly across the subtropical South Pacific (Fig. SB7.3a), consistent with the negative phase of Antarctic Oscillation (Mo 2000a), while the subtropical anomalies closer to the coast of South America were probably partly a response to preexisting positive SST anomalies in that region.

In early February, rainfall in the southern ITCZ became active, and the subsequent growth and maintenance of the event was consistent with the ocean–atmosphere mechanisms proposed for the 1925 coastal El Niño (Takahashi and Martínez 2017), that is, positive feedback between surface warming to the south of the equator, enhanced southern branch of the ITCZ, and reinforced near-equatorial northerly surface wind anomalies (Figs. SB7.3b,c; e.g., Xie and Philander 1994). The strong coastal ocean warming off northern Peru ($> +2^{\circ}\text{C}$) was limited to a shallow layer of about 30 m until the end of February, consistent with local surface forcing (Garreaud 2018). This, jointly with the smaller regional basin scale, explains the much faster timescale of this event (Takahashi and Martínez 2017). The termination of the event in April (Fig. SB7.3d) was also abrupt, as the insolation-driven seasonal sea surface cooling (Takahashi 2005) deactivated the southern branch of the ITCZ, shutting down the feedback mechanism. We should note that toward the end of March, the subsurface warming off northern Peru became deeper (down to 180 m; ENFEN 2017) and persisted until May, probably associated with local ocean–atmospheric Bjerknes feedback (Takahashi and Martínez 2017; Dewitte and Takahashi 2017), although warm ENSO conditions did not materialize (L’Heureux et al. 2017; also see Section 4b), similar to 1925.

The knowledge of the basic mechanism of the 1925 coastal El Niño guided the official Peruvian forecasts in

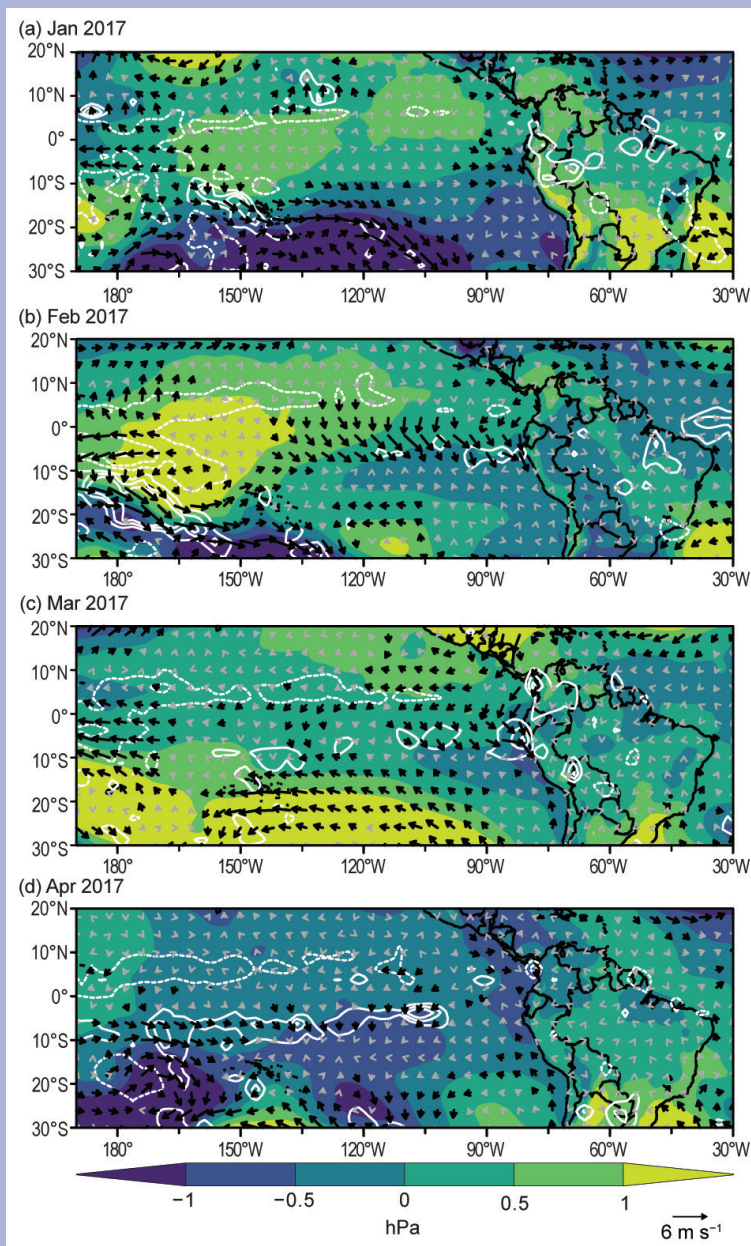


FIG. SB7.3. Mean sea level pressure (shading, hPa), 10-m wind (vectors, m s^{-1} ; $>1 \text{ m s}^{-1}$ in black), and precipitation [contours: 3 mm day^{-1} , solid (dashed) contours represent positive (negative) anomalies. Zero not shown]. (Sources: MSLP and wind: ERA-interim; precipitation: CMAP.)

2017, but only once the event started in late January, since international climate models provided little indication that such an event would occur (ENFEN 2017). Extending the lead time and accuracy of the prediction of coastal El Niño events is a critical challenge for Peru and requires increased understanding and improved models for this region.

e. Africa

In 2017, most of Africa experienced above-normal air temperatures, with slightly lower-than-normal temperatures in a few areas of West and southern Africa (Fig. 7.18). For the continent as a whole (except for a few areas in southern Africa and in the deep Sahara, stretching between Niger and Libya), 2017 was above normal by about 0.3°–1.8°C. Annual mean rainfall was above normal over boreal summer rainfall areas in West, central, and parts of East Africa. Below-normal rainfall was recorded in equatorial and southern Africa between 10° and 20°S (Fig. 7.19).

Extreme events like heavy rainfall and flooding were reported in many parts of the region. These reports include heavy downpours in February and December 2017 in Morocco and during August and September in Nigeria, The Gambia, and Niger. Tropical cyclone events in the Mozambique Channel affected Mozambique and Zimbabwe. An additional tropical cyclone over the southern Indian Ocean affected Réunion Island and Madagascar.

This report was compiled using observational records from the meteorological and hydrological services of Morocco, Egypt, Nigeria, Ethiopia, South

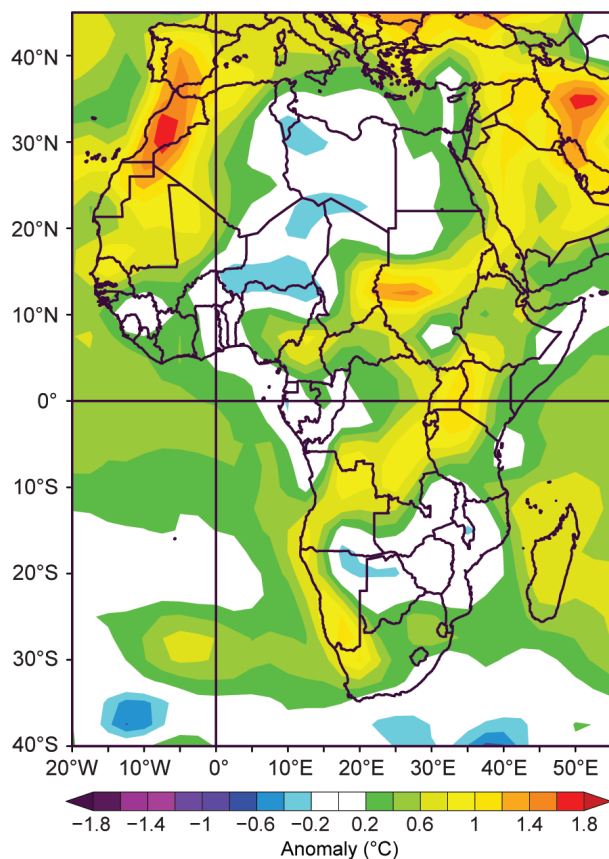


FIG. 7.18. Annual 2017 mean temperature anomalies (°C; 1981–2010 base period) over Africa. (Source: NOAA/NCEP.)

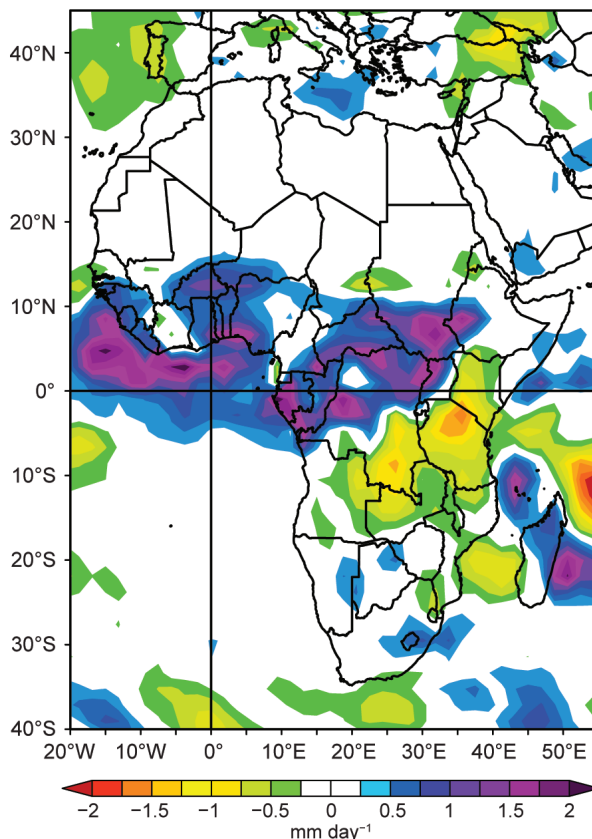


FIG. 7.19. Annual 2017 rainfall anomalies (mm day⁻¹; 1981–2010 base period) over Africa. (Source: NOAA/NCEP.)

Africa and the southern Indian Ocean Island countries of Madagascar, Seychelles, Mayotte (France), La Réunion (France), Mauritius, and Rodrigues (Mauritius). Reanalysis data from NCEP/NCAR and the ECMWF and rainfall from version 2 of Climate Hazards Group Infrared Precipitation with Stations data (CHIRPS) were also used. Precipitation fields from reanalyses are problematic, but unfortunately observations from many African nations are not available. fatalities and flooding hazards are as reported in news outlets. The climatological base period used is 1981–2010.

1) NORTH AFRICA—K. Kabidi, A. Sayouri, M. Elkharrim, and A. E. Mostafa

Countries considered in this section include Morocco, Mauritania, Algeria, Tunisia, Libya, and Egypt.

In 2017, the region was marked by unusually high temperatures, below-normal rainfall, and extreme events including heavy rainfall and flooding that caused loss of life and property damage. In Morocco, extreme events were pronounced during February and December.

(i) Temperature

Temperatures in 2017 were above normal over most of the region. However, January was cooler than normal over most of North Africa (Fig. 7.20a). Minimum temperatures of about 3°C below normal were observed over the mountains and southern parts of Morocco. Mean temperatures of about 2°–3°C below average were also observed over most of Algeria, southern Tunisia, and western parts of Libya in January (Fig. 7.20a). January–February mean temperatures were also below normal over southern parts

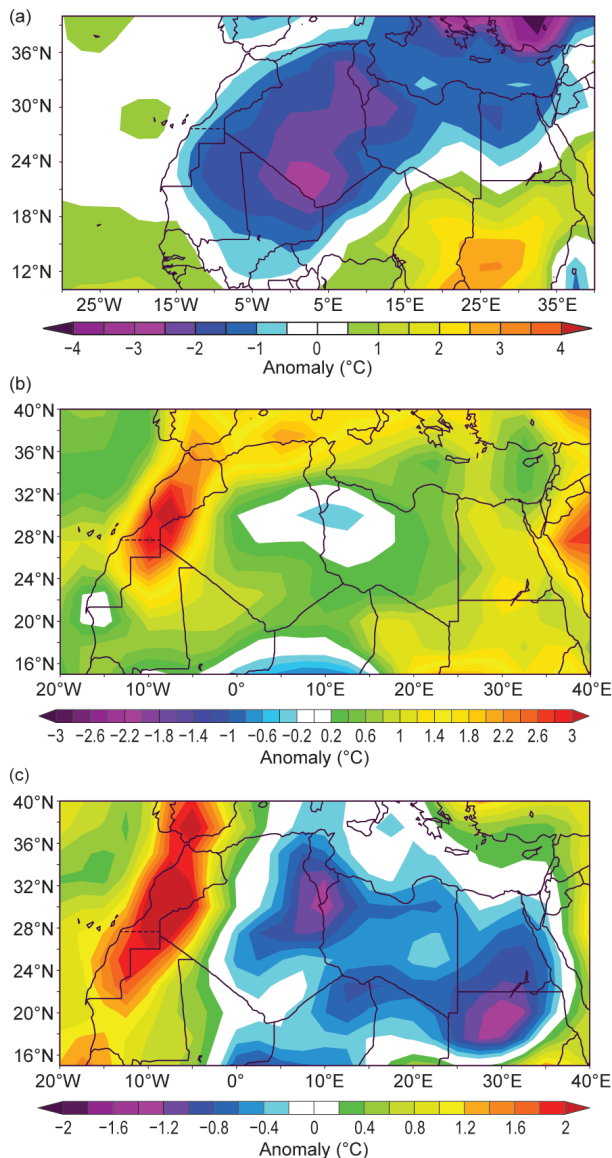


FIG. 7.20. (a) Northern Africa 2017 surface air temperature anomalies (°C; 1981–2010 base period) for Jan. (b) Northern Africa 2017 surface air temperature anomalies (°C; 1981–2010 base period) for Jun–Aug. (c) Northern Africa 2017 surface air temperature anomalies (°C; 1981–2010 base period) for Sep–Nov. (Source: NOAA/NCEP.)

of Morocco, northern and northwestern Mauritania, extreme southern Algeria, and over Libya and Egypt. Extreme minimum air temperatures of 0.2°C at El-Arish (northern Egypt) on 10 January and 1.3°C at Asyut (Upper Egypt) on 10 February were recorded.

Minimum and maximum temperatures over Morocco were among the highest in the period of record starting in 1901. The mean annual temperature anomaly was 0.65°C above normal (exceeding the value recorded in 2016 by +0.2°C), with anomalies of +0.6°C for the annual maximum temperature and +0.7°C for the annual minimum temperature. The largest monthly mean temperature anomalies of about 3.7°C were recorded in May and October in Morocco.

Summer temperatures were above normal over most of the region and up to 3°C above normal over most of Morocco (Fig. 7.20b). Autumn (September–November) temperatures were above normal over Morocco, with anomalies exceeding 2°C over central regions, and in Algeria. Eastern Algeria, southern Tunisia, and most of Libya and Egypt were colder than normal (Fig. 7.20c).

(ii) Precipitation

Annual precipitation over Morocco was 61% of normal. Morocco received 40% less precipitation in 2017 than 2016. Moroccan precipitation was characterized by strong spatial and temporal variability. About 13% of normal precipitation was recorded in the south at Smara (Saharan region), while close to normal rainfall (~89% of normal) was received in the north at Rabat. About half (46%) of the annual precipitation was received in February and December 2017.

January–February precipitation over the region was largely below average due to a prevailing anticyclonic circulation that settled over North Africa’s Atlantic coast and western Europe. However, heavy rainfall was recorded in Morocco on 22–24 February (Fig. 7.21). Heavy rainfall events were observed at many places, including 91 mm in 24 hours at Agadir in southwest Morocco. Above-normal rainfall was observed over northern Algeria in February. Heavy rainfall was also reported from Egypt in January.

The spring season (December–March) was generally characterized by rainfall deficits over most of the region. In Morocco, the seasonal precipitation was 47% of normal. Seasonal totals of 60%–80% of normal were recorded along the northern coastal areas of Algeria. Some eastern and southern Moroccan stations received less than half of their normal precipitation, with some recording zero precipitation. Spring precipitation was below normal, especially in

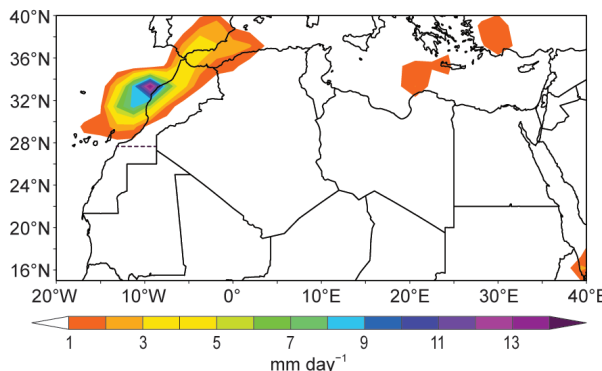


FIG. 7.21. Northern Africa 2017 rainfall rate anomalies (mm day⁻¹; 1981–2010 base period) over 21–24 Feb. (Source: NOAA/NCEP.)

northern and east-central Algeria. In Algeria, Skikda received no precipitation, and Annaba received only 11% of its normal March rainfall. Alexandria received a record rainfall of 50 mm in 24 hours on 21 April, the highest 24-hour rainfall in Egypt during 2017.

Precipitation during summer (June–September) was generally below normal over the entire region; however, convective events in August produced monthly rainfall that was 192% of normal in Morocco. Al Hoceima observed 44.8 mm, an order of magnitude greater than its normal 4 mm. In Algeria, summer rainfall was highly variable, with deficits across the northern part of the country. Western coastal stations observed amounts on the order of 40%–85% of normal. Stations in the plains and inland basins of Algeria received just 10%–40% of normal, while Saïda (in the northwest) received 166% (66% above normal) of normal precipitation. Farther south, at Saharan Atlas stations of Algeria, the seasonal totals varied, from 20%–60% of normal near El Bayadh and Mechria, to 125%–150% of normal at AinSefra and Naâma.

In contrast to summer, precipitation during autumn was 38% of normal in Morocco. However, precipitation for November was above normal over northern Tunisia, leading to flooding on 10–11 November at Gabès, killing 5 people and causing more than 117 evacuations.

(iii) Notable events and impacts

Flooding in both February and December 2017 caused loss of life and damage to property in Morocco. Cold spells, ranging from 0.3° to 7.0°C below normal, were reported in January and December in Morocco. An all-time heavy rainfall of 119.2 mm was recorded on 23 February at Rabat, Morocco.

Extended heat waves occurred over the region during May and June with maximum temperatures

exceeding 40°C. These were associated with eastern continental winds and caused significant forest fires, especially in Morocco and Algeria. About 325 forest fires were reported in Morocco, causing the destruction of about 2056 hectares of forested land.

2) WEST AFRICA—S. Hagos, I. A. Ijampy, F. Sima, S. D. Francis and Z. Feng

In this section, West Africa refers to the region between 17.5°W (eastern Atlantic coast) and ~15°E (the western border of Chad), and from 5°N (near the Guinean coast) to 20°N. It is typically divided into two climatically distinct subregions; the semiarid Sahel region (north of about 12°N) and the relatively wet Coast of Guinea region to the south. The rainy period over the region is associated with the latitudinal movement of the convective zone referred to as the West African monsoon which typically occurs during June through September.

(i) Temperature

The annual mean temperature over western parts of West Africa was higher than average, with much of the region about 0.5°C above normal (Fig. 7.18). During September (Fig. 7.22), much warmer-than-average conditions— ~0.5°C above normal—were reported with record-warm conditions over Ghana, Ivory Coast, Burkina Faso, and southern Nigeria. There was, however, significant regional variability. For example, daily temperatures >40°C were recorded between January and June in parts of Nigeria, especially over its northern states. The highest daily temperatures of April, March, and May were 45.3°, 44.2°, and 44°C, recorded at Maiduguri, Yelwa, and Nguru, respectively. Other cities, such as Sokoto

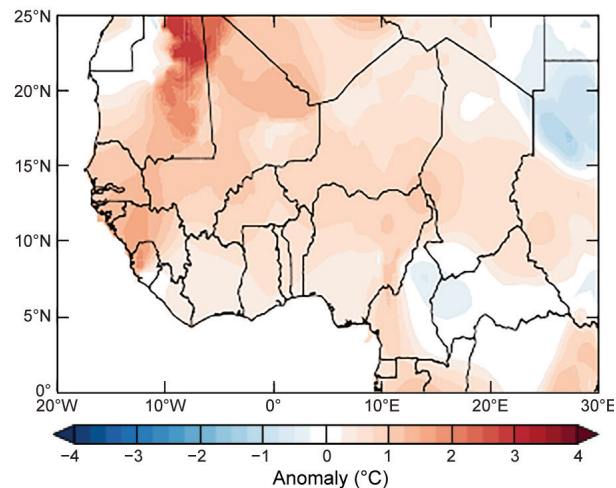


FIG. 7.22. Temperature anomalies (°C; 1981–2010 base period) for West Africa for Sep 2017. (Source: NOAA/NCEP.)

and Yola, also recorded daily high temperatures of 43.0° and 43.5°C, respectively. The Gambia also experienced warmer-than-normal conditions during 2017. The annual mean maximum temperature over the country was 35.6°C, about 4.5°C above normal. Daily maximum temperatures exceeded 40°C in some places, such as the 47.7°C recorded at Kaur, in the Central River region of The Gambia.

(ii) Precipitation

Rainfall totals for June to September (JJAS), during which the West African monsoon provides much of the annual precipitation, are presented in Fig. 7.23. During JJAS, the northern Sahel was wetter, and coastal regions were drier, than normal. This was consistent with above-normal SSTs over the northern tropical Atlantic early in the season. Early-season monsoon precipitation over the Sahel region, particularly northern Nigeria and southern Niger, was observed. Later in the season, the southern and central tropical Atlantic was warmer, and relatively

drier conditions dominated much of the region, with significant regional variability. According to the Nigerian Meteorological Agency, most of the country recorded normal rainfall conditions, while the cities in central and northwestern Nigeria recorded below-normal rainfall. The Gambia experienced early onset and cessation of the rains, but overall seasonal rainfall was near normal. However, the timing of rainfall had an uneven distribution, with prolonged dry spells and flooding, leading to crop failure in some parts of the country. Most of the rain during the 2017 season was in July–September, with the highest amounts of 130.8 mm recorded in August at Jenoi in the lower river region of The Gambia.

(iii) Notable events and impacts

On 6 July, flooding and wind storms occurred at Jarra Bureng and Jasobo, in The Gambia’s Lower River region, destroying hundreds of homes and farms, and affecting 20 000 individuals; wells and latrines were also affected. The event lasted for 4 hours. The event affected 94 households and 857 people across 5 communities. On 12 July, a wind storm at Kerewan, North Bank region, caused one casualty and affected 222 households. A wind storm claimed two lives the same day in The Gambia’s West Coast region.

In Nigeria, heavy rain during August and September caused the Niger and Benue Rivers to overflow, causing flooding in the Benue and Kogi States. In Benue State, it was reported that 100 000 people were displaced by flooding, 12 local governments within the state were affected, and around 4000 homes damaged. No fatalities were reported. Flooding in Kogi State came just days after thousands of people were displaced by floods in Benue. The Kogi flood displaced over 10 000 people. The worst affected area was the state capital, Lokoja, which lies at the confluence of the two rivers. Other affected areas included Ibaji, Igalamela-Odolu, Ajaokuta, Bassa, and Koton-Karfe. A bridge at Tatabu village along Mokwa-Jebba road, in the Kwara State, collapsed after a heavy rainfall. The road is the major link between the northern and southern parts of the country; motorists were advised to use alternative routes. The popular Ahmadu Bello way in Victoria Island, Lagos State, was temporarily closed on 7 September by the Lagos State Police Command due to flooding.

On 27 August, several hours of rainfall caused floods in Churchill Town, Bakoteh, and Ebou town in The Gambia’s west coast region, and Tabanani and Sare Molo in its Central River region. Two lives were lost, more than a thousand homes were damaged, and about 4000 people were displaced.

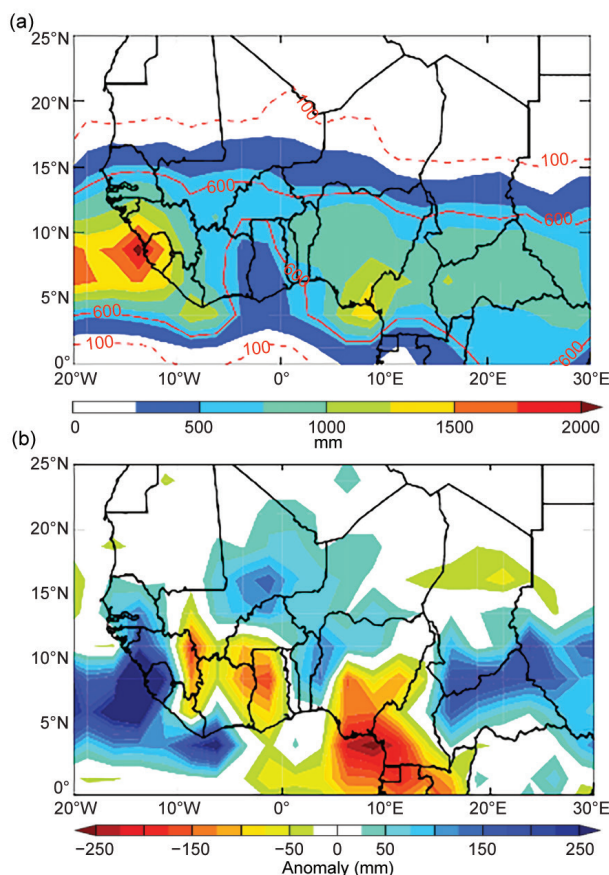


FIG. 7.23. Jun–Sep 2017 precipitation (mm) for West Africa: (a) total accumulation; 100-mm isohets (red dashed line), 600-mm isohyets (red solid line). (b) Departure from 1981–2010 climatology. (Source: NOAA/NCEP.)

On 12 and 29 August, flooding at Kuntaur Niani, in the Central River region, caused significant internal displacements, damage to public and private properties, including a bridge, and submerging of farmlands. There were five fatalities and around 8000 people affected.

In Niger, heavy rain on 26 August caused flooding in the capital city of Niamey and surrounding areas; around 100 mm of rain fell in Niamey. The UN Office for the Coordination of Humanitarian Affairs (UNOCHA) reported that two people had died and four were injured. According to Niger’s government, 219 houses were destroyed and over 1000 people were left homeless in Gabagoura and other villages around Niamey.

3) EASTERN AFRICA— G. Mengistu Tsidu

Eastern Africa, also known as the Greater Horn of Africa (GHA), is a region comprised of South Sudan, Sudan Republic, Ethiopia, Somalia, Eritrea, Kenya, Uganda, Rwanda, Burundi, and Tanzania. Despite its location across the equator, the region has a relatively cool climate due to its generally high altitude. Some parts of the region are also characterized by bimodal seasonal rainfalls. In general, the GHA experienced above-average temperatures in 2017.

(i) Temperature

The December 2016–February 2017 (DJF) mean temperature was below normal to normal over central Kenya, the Ethiopian highlands, eastern Ethiopia, much of northern Somalia, and the northwestern Sudan Republic (Fig. 7.24a). Above-normal anomalies, up to +3°C, were observed over the rest of the GHA. During MAM, the GHA remained warmer than normal, except for the northern Ethiopian highlands, northwestern Sudan Republic, part of central Kenya, north-central and southwestern Tanzania which had normal to below-normal temperatures (Fig.

7.24b). During June–August (JJA), above-normal temperatures covered large parts of GHA, extending to the Ethiopian highlands and northwestern Sudan Republic (Fig. 7.24c). However, South Sudan and western Ethiopia enjoyed near-normal temperatures during this season. During September–November (SON), cold anomalies of up to –2°C prevailed over the northern half of Sudan Republic, southwestern Ethiopia, and adjoining South Sudan and northern Uganda, extending across western Kenya towards northern Tanzania (Fig. 7.24d). The rest of the GHA region experienced above-normal mean temperatures.

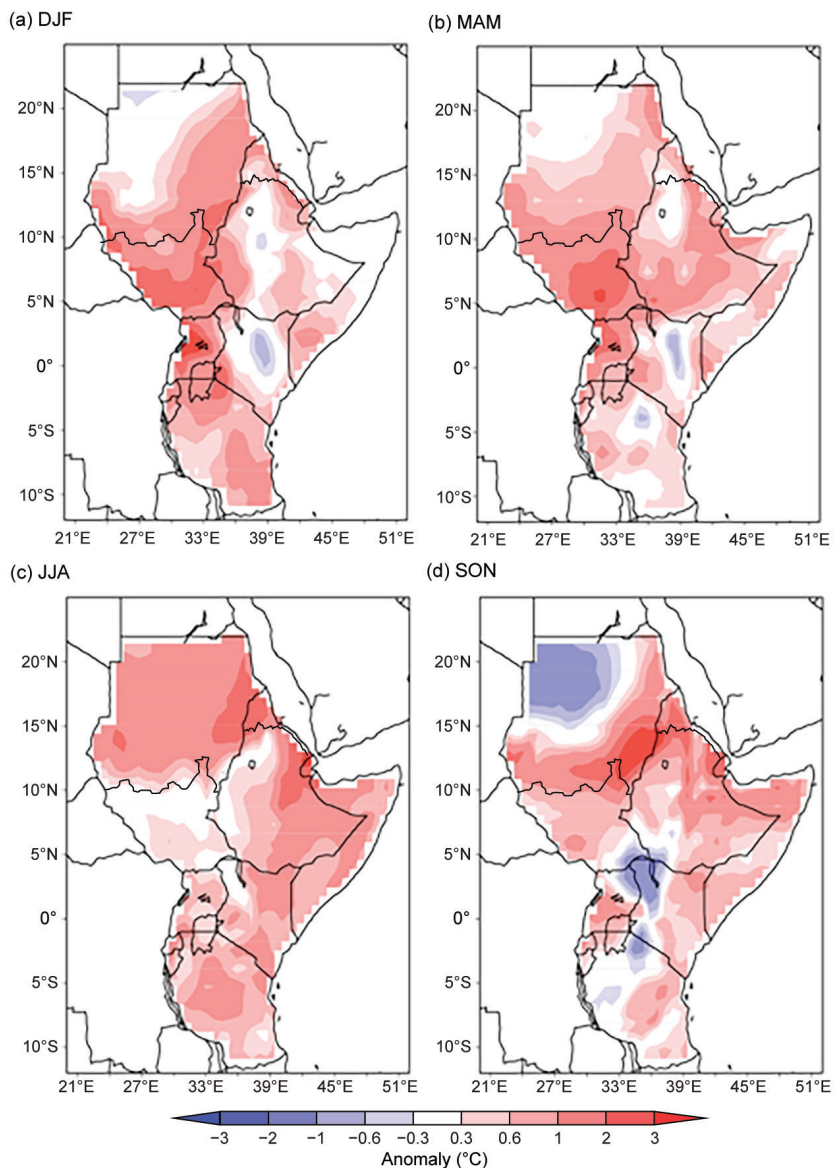


FIG. 7.24. Eastern Africa seasonally averaged mean temperature anomalies (°C; 1981–2010 base period) for (a) DJF 2016/17 and (b) MAM, (c) JJA, and (d) SON 2017 (Source: ERA-Interim.)

(ii) Precipitation

The northern half of Uganda, northwestern and northeastern Kenya, and adjacent western Somalia received normal to above-average rainfall, whereas southern Uganda, most of Kenya, Tanzania, Burundi, and Rwanda received 50%–90% of the base period mean during DJF (Fig. 7.25a). Some isolated pockets in Tanzania and Kenya received less than half of their normal DJF rainfall. Rainfall during MAM was below normal over southern Ethiopia and adjacent southern Somalia, all of Kenya, northern Uganda, and most of Tanzania (Fig. 7.25b). Southeastern Tanzania, in particular areas along the coast, received above-normal rainfall during MAM. Ethiopia, with the exception of

its southeastern lowlands, South Sudan, and southern Sudan Republic receive their main rainfall during JJAS. Normal to above-average rainfall, ranging from 110% to 200% of the seasonal mean, dominated the region in 2017, including unseasonal rain over the southern half of GHA (Fig. 7.25c). Dry conditions prevailed over most of Kenya, central Tanzania, and coastal Somalia during SOND, which is the climatological rainy season in this area (Fig. 7.25d).

(iii) Notable events and impacts

Heavy rainfall recorded in most parts of the region throughout the 2017 rainy seasons caused flooding. For example, eastern Kenya and Tanzania had steady torrential rain in May. As a result, Mombasa recorded 235 mm on 9 May, which led to flash flooding. According to news outlets, at least nine people perished. There were also heavy rains in mid-May, with a number of stations in western and central Ethiopia recording 49 mm and above (e.g., Gore: 59.9 mm; Jimma: 53 mm; Addis Ababa Bole: 49 mm). The subsequent flooding led to a death in the Gambella region of Ethiopia on 18 May. JJAS rainfall was also notably heavy over Sudan and Ethiopia. Resulting floods affected more than 53 000 people in the Gambella and Oromia regions during August and September, according to a UNICEF humanitarian report.

4) SOUTHERN AFRICA — G. Mengistu Tsidu, A. C. Kruger, and C. McBride

Southern Africa comprises the Republic of South Africa, Angola, Botswana, Zimbabwe, Namibia, Malawi, Zambia, Lesotho, Swaziland, and Mozambique. The rainfall assessment is based on rainfall from CHIRPS, and in situ observations from South Africa.

(i) Temperature

Above-normal temperatures prevailed across Angola, northeastern Zimbabwe, western Namibia, western South Africa,

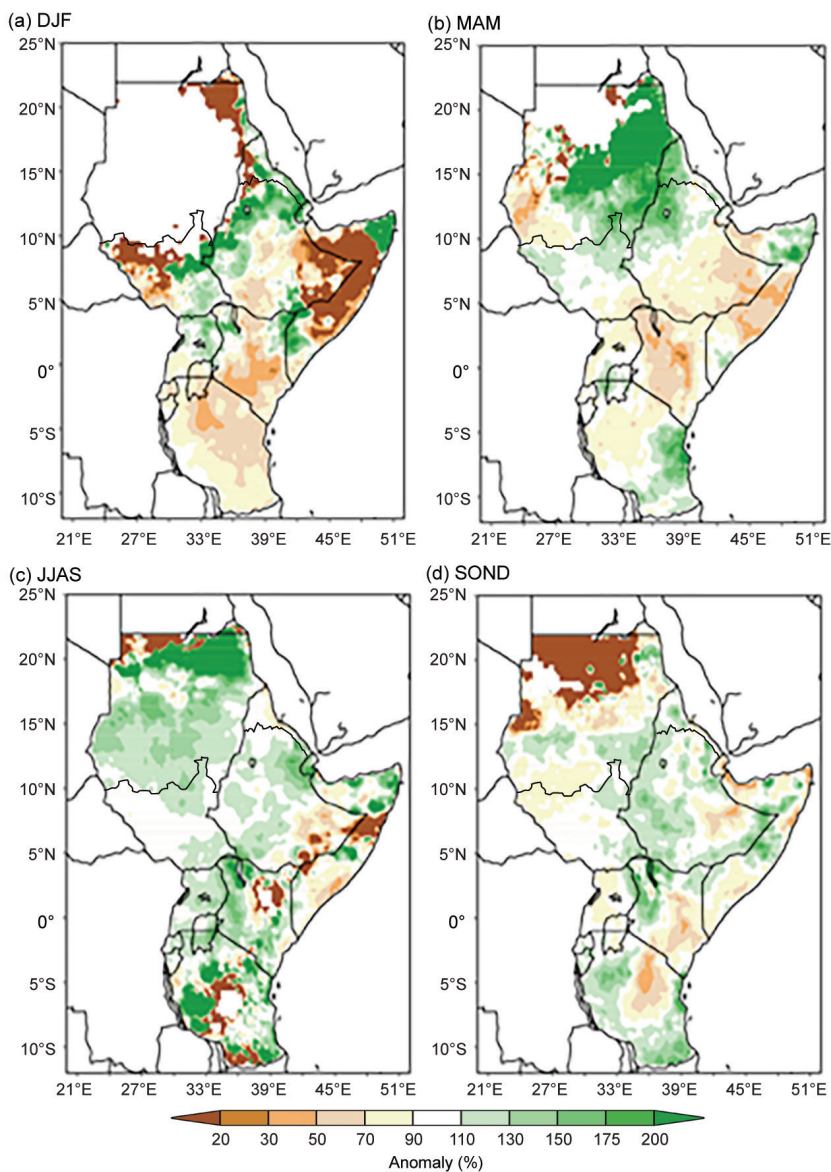


FIG. 7.25. Eastern Africa seasonal total rainfall anomalies (% of normal; 1981–2010 base period) for (a) DJF 2016/17 and (b) MAM, (c) JJAS, and (d) SOND 2017 (Source: CHIRPS.)

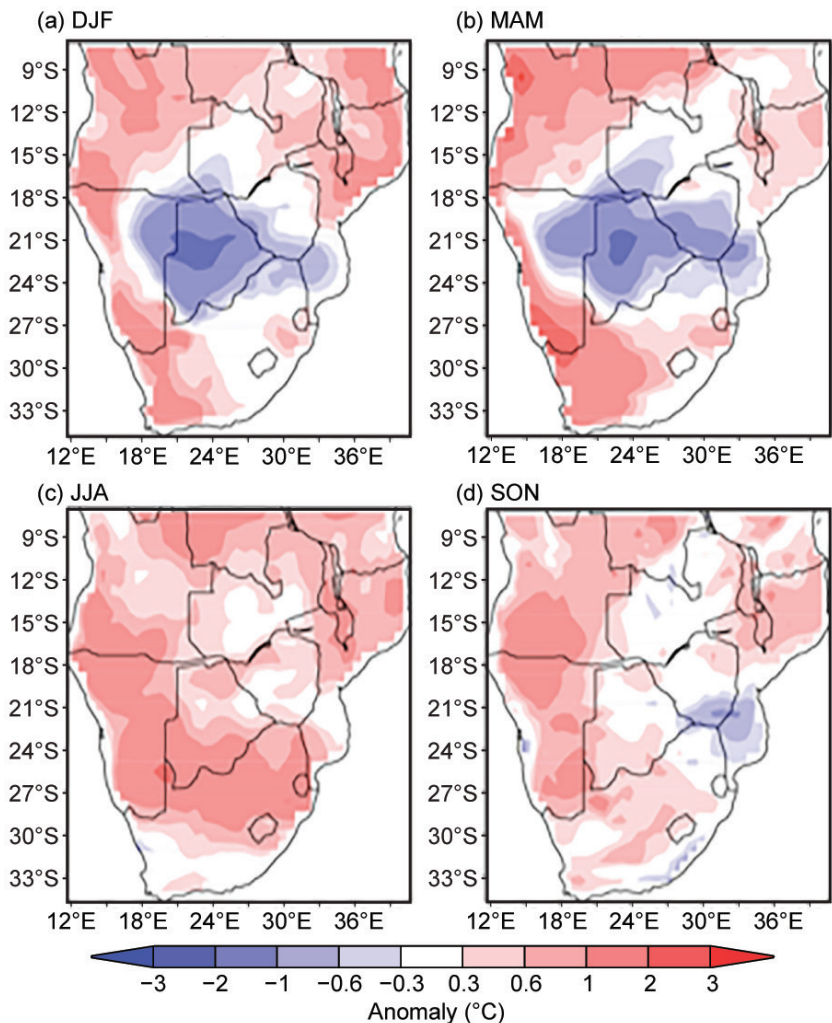


FIG. 7.26. Southern Africa seasonally averaged mean temperature anomalies (°C; 1981–2010 base period) for (a) DJF 2016/17, (b) MAM, (c) JJA, and (d) SON 2017 (Source: ERA-Interim.)

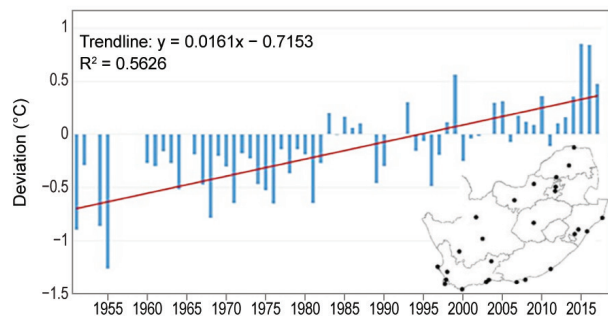


FIG. 7.27. Annual mean temperature anomalies (°C; 1981–2010 base period) of 26 climate stations in South Africa, as indicated on inset map, for 1951–2017. Red line represents the linear trend. (Source: South African Weather Service.)

and Mozambique from December 2016 to February 2017. In contrast, northeastern Namibia, all of Botswana, Southern Zimbabwe, Zambia, southern

Mozambique, and northeastern South Africa remained lower than normal (Fig. 7.26a). Normal to below-normal mean temperatures expanded to include much of Zimbabwe in MAM (Fig. 7.26b). During JJA, warm conditions dominated across the region, with the exceptions of isolated pockets in Botswana, Zimbabwe, Zambia, Mozambique, and southern strips of South Africa, where normal mean temperature conditions were observed (Fig. 7.26c). However, during SON, southern Mozambique and adjoining areas in Zambia experienced temperature anomalies exceeding -1°C , with normal mean temperature prevailing over most of Zimbabwe, Zambia, northern Botswana, northeastern South Africa, and Swaziland. The rest of the region remained moderately warmer than normal (Fig. 7.26d). For the year as a whole, warmer-than-normal conditions throughout 2017 prevailed across the southern part of the region (spatial representation not shown), as evident from the annual mean temperature anomalies of 26 climate stations in South Africa, which averaged 0.48°C above average (Fig. 7.27).

(ii) Precipitation

Above-normal rainfall, exceeding 150% of average, was observed over Botswana and adjoining eastern Namibia, eastern Angola, Zimbabwe, Zambia, western Mozambique, and most of South Africa from December 2016 to February 2017. However, most of Angola, western Namibia, western South Africa, and eastern Mozambique experienced below-normal rainfall (Fig. 7.28a). Wet conditions persisted through MAM only over central parts of the region, namely northern Botswana, northern Namibia, Zambia, Mozambique, and southern Zimbabwe. Below-normal conditions—as low as 20% of normal—prevailed over the rest of the region (Fig. 7.28b). The JJA period is typically dry over the region. Compared to this

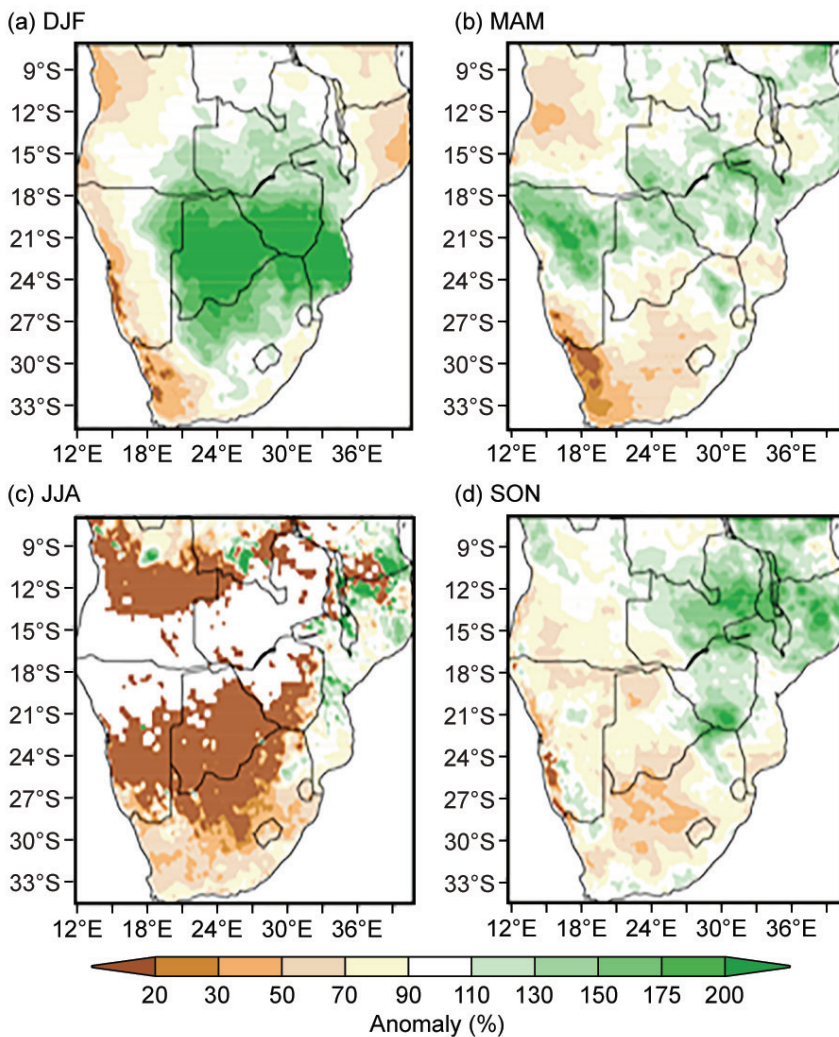


FIG. 7.28. Southern Africa seasonal total rainfall anomalies (% of normal; 1981–2010 base period) for (a) DJF 2016/17 and (b) MAM, (c) JAS, and (d) SON 2017 (Source: CHIRPS.)

baseline, most of Mozambique received above-normal rainfall (Fig. 7.28c), whereas the rest of the region remained drier than normal. The wet conditions in Mozambique in JJA expanded to Zimbabwe, Zambia, and isolated areas in the northeastern part of South Africa by SON (Fig. 7.28d).

Analysis of annual total gauge rainfall over South Africa confirms that large parts of the country received near-normal rainfall. The most notable exception was the region including the largest part of the Western Cape and the western parts of the Northern Cape, which received less than 75% of its normal annual precipitation (figure not shown). The western Northern Cape was especially dry with station averages indicating less than half of normal rainfall, in agreement with the analysis of seasonal rainfall from CHIRPS. 2017 was the driest year over the last three-year period in the southwestern Cape

since at least 1951. A Standardized Precipitation Index (SPI) analysis of South Africa (not shown) indicates that almost the whole Western Cape Province, including the adjacent areas of the northern and eastern Cape Provinces, experienced what can be described as moderate to extreme drought conditions over an extended period of time, (i.e., longer than two years). In addition, an analysis of Cape Town in particular shows that the only other comparable dry period was around 1973/74, with a probability of occurrence lower than 3%.

(iii) Notable events and impacts

Tropical cyclones impacted the region during early February. Cyclone Carlos was active from 3–10 February. On 13 February, Cyclone Dineo formed in the Mozambique Channel and made landfall in southern Mozambique on 15 February. The cyclone subsequently tracked westwards, leaving significant flood-related damage in southern Mozambique and southern Zimbabwe. The impact of Dineo was also felt as far west as Bo-

tsswana, where daily rainfall of 70 mm was observed at Kgomokitswa on 19 February and 136 mm at Lobatse on 20 February. These amounts accounted for 70% and 66%, respectively, of the total February rainfall at each station. As a result, the Gaborone dam filled up due to the intense rains, marking an abrupt end to the multiyear hydrological droughts that have affected the region.

Other notable but localized events during early summer includes stormy weather over South Africa. In October, a cut-off low system moving southeastward from northwestern South Africa triggered large thunderstorms, especially over western Gauteng province, with several tornado sightings. A subsequent statement by the South African Weather Service reported that severe thunderstorms with heavy downpours, strong damaging winds, and large hail hit parts of eastern North-West, Gauteng, eastern Free

State, KwaZulu-Natal, Mpumalanga, and Limpopo provinces on 9 and 10 October. Areas that were most affected were Mogale City, the city of Johannesburg, and Ekurhuleni Metropolitan municipalities. There were two sightings of tornadoes in Ruimsig (adjacent to Roodepoort and Krugersdorp) and Eloff, near Delmas (Mpumalanga), which caused extensive damage to property. Elsewhere in the Free State, a tornado was observed near Bethulie. Golfball- to tennis ball-sized hail was also reported near Krugersdorp. The system moved rapidly east, affecting KwaZulu-Natal from 10 October, with severe urban flooding and high winds resulting in loss of life. In 24 hours, Durban recorded 108 mm of rain, where 65 mm fell in less than an hour. Similarly, Virginia in KwaZulu-Natal received 142 mm of rain, where 89 mm occurred within an hour. Maximum sustained wind speeds of 75 and 78 km h⁻¹ were reported in Durban and King Shaka airport to the north, respectively.

5) WESTERN INDIAN OCEAN ISLAND COUNTRIES—
G. Jumaux, C. L. Rakotoarimalala, M. Belmont, and
K. R. Dhurmea

This region consists of several island countries: Madagascar, Seychelles, Mayotte (France), La Réunion (France), Mauritius, and Rodrigues (Mauritius).

Overall, the 2017 mean temperature for the region was well above normal, while precipitation was mixed across the region. It was the warmest year on record in the Mascarenes archipelago (Réunion, Mauritius, Rodrigues) because of strong SST anomalies in this

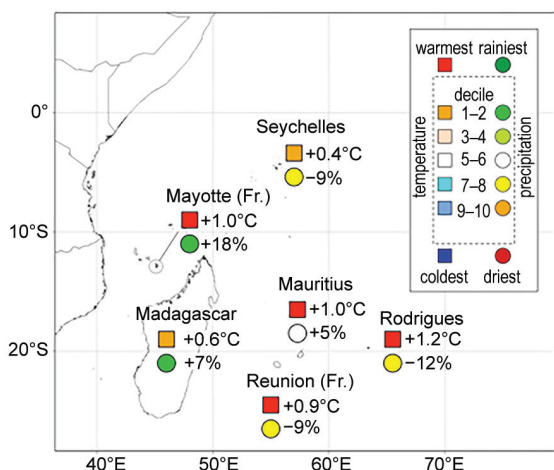


FIG. 7.29. Mean annual temperature anomalies (°C; squares), annual rainfall anomalies (% of average; circles), and their respective deciles for the western Indian Ocean islands countries in 2017. (Sources: Météo France; and Meteorological Services of Madagascar, Seychelles, and Mauritius.)

region. Figure 7.29 shows temperature and rainfall anomalies for selected areas.

(i) Temperature

In Madagascar, the annual mean temperature, based on fifteen stations, in 2017 was 24.1°C; the annual anomaly was +0.6°C. It was the fifth warmest year on record since 1978. June recorded the highest monthly anomaly, around +1.4°C. The highest maximum temperature was observed in Antsohihy on 10 October (37.7°C), and the lowest minimum temperature (2.0°C) was recorded three times in Antsirabe: on 13, 15, and 19 July.

At Seychelles International Airport, monthly mean maximum temperatures were slightly below normal during the first four months of 2017. Above-normal temperatures prevailed from June through November. The annual mean maximum temperature was 30.3°C and ranks as the seventh highest since records began in 1972. (The warmest year on record is 2009 with an annual mean of 30.6°C.) The 2017 extreme daily maximum temperature was 33.7°C on 22 April. Monthly mean daily minimum temperature departures from the long-term means varied from +0.3° to +1.2°C. The extreme daily minimum temperature for 2017 was 21.6°C, recorded on 6 July. Finally, the annual mean temperature was +0.4°C above normal, ranking as the fourth highest since 1972. The highest monthly temperature deviation occurred during October (+1.2°C).

For Mayotte Island, 2017 was the warmest year since records began in 1961, with an annual mean temperature anomaly of +1.0°C at Pamandzi Airport. Temperatures during January and February were slightly above normal. From March to December temperatures were well above the reference base period, often more than +1.2°C from June to November.

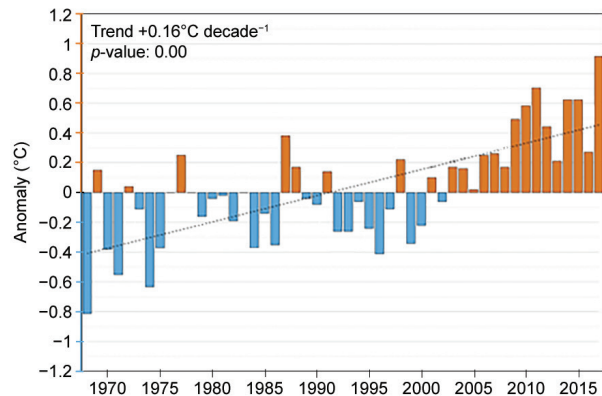


FIG. 7.30. Annual mean temperature anomalies (°C; 1981–2010 base period) for Réunion Island, 1968–2017. (Source: Météo-France.)

For Réunion Island, the annual mean temperature, based on three stations, was +0.9°C above normal in 2017, ranking as the highest since 1968, far exceeding the previous record of +0.7°C in 2011 (Fig. 7.30). Temperatures during January and February, the warmest months of the year climatologically, were slightly above normal. From March to December they were well above the reference base period, often by more than +1.0°C.

Over the island of Mauritius, the annual mean maximum temperature anomaly based on two stations was +0.6°C, and the annual mean minimum temperature anomaly was +1.5°C, indicating a greater departure during nighttime. July and August were among the warmest on record since 1951. The annual mean temperature anomaly over the island was +1.0°C. This makes 2017 the warmest on record since 1951. Similar observations were made at Rodrigues (Pointe Canon) with an annual mean temperature anomaly of +1.2°C.

(ii) Precipitation

For Madagascar, annual precipitation, based on 21 stations, was 107% of normal in 2017. It was the sixth wettest year on record since 1978. Nine months were above normal, with November the relative wettest at 175% of normal for the month. More stations in western Madagascar were below normal than in the eastern part (Fig. 7.31). The highest percent of normal (233%) was recorded at Mananjary and the lowest at Morombe (30%). The highest accumulated precipitation within a 24-hr period in 2017 was 215.4 mm recorded in Sambava on 7 March, the eighth wettest day there since 1961.

For Seychelles, five months recorded higher-than-normal rainfall during 2017. The second half of the year was dominated by persistent negative anomalies that impacted the amount of rain received at the beginning of the rainy season. The outer islands were worst affected during that period. (The rainy season usually starts mid-October and ends mid-April.) The total rainfall amount recorded for the year is 2146.2 mm, which is 91% of the long-term mean, ranking as 18th driest since records began in 1972. The total number of rain days was 195, which is slightly below normal.

For Mayotte Island, the annual rainfall amount based on two stations was 118% of average, ranking eighth wettest since 1961. January, May, and October were drier than normal, whereas February, April, and December were among the rainiest on record.

For Réunion Island, the annual rainfall based on 34 stations was 91% of the long-term mean, ranking 18th driest since 1969. January was the second driest on record, associated with a late rainy season onset in early February. Total precipitation during the rainy season (January–April) was only 76% of average, ranking ninth driest. During May to November, typically the driest months of the year, the rainfall amount was 133% of average, ranking fifth rainiest. At Plaine des Fougères, 215 mm of rain fell in three hours on 29 August, which is very unusual during this season.

The year started very dry both at Mauritius and Rodrigues (Fig. 7.32). Dry conditions persisted over Rodrigues until March. May, usually a dry transition month, was very wet on both islands; it was the seventh wettest on record for both Mauritius and Rodrigues. Heavy rainfall and widespread flooding affected both islands. Winter months (May–October) yielded a positive rainfall anomaly over Mauritius. December 2017 was the second driest in Mauritius since 2010 and second driest in Rodrigues (Pointe Canon) since 2003. The total annual rainfall over Mauritius amounted to

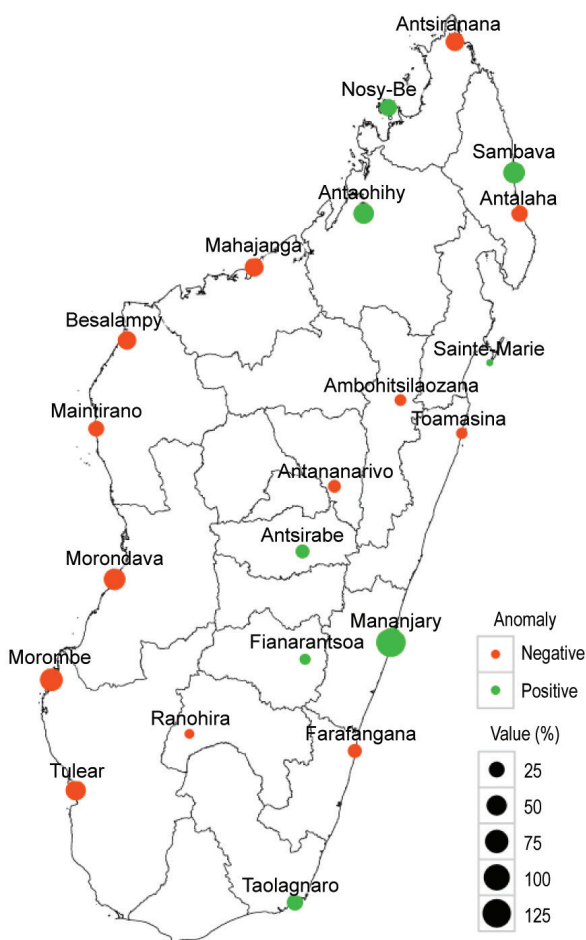


FIG. 7.31. Annual total precipitation anomalies (% of average; 1981–2010 base period) for Madagascar in 2017. (Source: Madagascar Meteorological Services.)

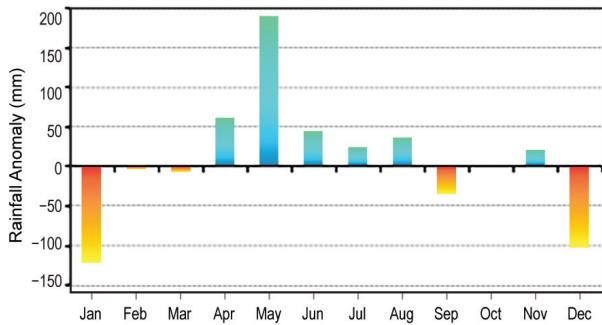


Fig. 7.32. Mean monthly total precipitation anomalies (mm; 1981–2010 base period) over Mauritius in 2017 (Source: Mauritius Meteorological Services.)

2110 mm (105% of average). The total annual rainfall amounted to 968 mm at Rodrigues (88% of average).

(iii) Notable events and impacts

Tropical cyclone Carlos passed 130 km off the western coast of Réunion Island on 7 February. A maximum wind gust of 37 m s^{-1} was recorded at Bellecombe, and 934 mm of rain was recorded at Grand-Ilet within a 72-hr period. The agricultural sector sustained losses up to 4.9 million U.S. dollars.

In Madagascar, March 2017 was marked by Cyclone Enawo which formed in the Indian Ocean. It tracked across the island from 7 to 9 March, producing three-day precipitation totals of 224 mm at Sambava, 210 mm at Antsohihy, 184 mm at Antananarivo, 159 mm at Fianarantsoa, 291 mm at Mananjary, and 178 mm at Taolagnaro which were, respectively, 82%, 86%, 112%, 113%, 81%, and 101% of the normal monthly precipitation for March at each location. Enawo led to 81 fatalities, injured 250 people, and caused significant flooding. Eastern Madagascar was the most affected.

f. Europe and the Middle East—P. Bissolli, M. Demircan, J. J. Kennedy, M. Lakatos, M. McCarthy, C. Morice, S. Pastor Saavedra, M. R. Pons, C. Rodriguez Camino, B. Rösner, S. Sensoy, S. Spillane, K. Trachte, and G. van der Schrier

For this section, 1961–90 is used as the base period for temperature, and 1981–2010 is used as the base period for precipitation, as described in Figs. 7.33–7.37, unless otherwise specified. European countries conform to different standards applied by their individual national weather services, and their specific base periods are noted throughout the subsections as needed. All seasons mentioned in this section refer to the Northern Hemisphere. More detailed information can be found in the Monthly and Annual Bulletin on the Climate in RA VI – European and the Middle East, provided by WMO RA VI Regional

Climate Centre on Climate Monitoring (RCC-CM; www.dwd.de/rcc-cm). Anomaly information has been taken from Figs. 7.34–7.37 when national reports are not available.

1) OVERVIEW

Based on the CRUTEM4 dataset (Jones et al. 2012) dating to 1851, Europe (35° – 75° N, 10° W– 30° E) observed its fifth warmest year on record with an anomaly of $+1.3^{\circ}$ C; its five warmest years have all occurred since 2011 (Fig. 7.33). NOAA data (not shown) also ranks Europe as fifth warmest for 2017.

Local temperature anomalies varied mostly between $+1^{\circ}$ and $+2^{\circ}$ C and were homogeneously distributed across Europe, with local areas in the Ukraine and central Spain above $+2^{\circ}$ C (Fig. 7.34).

While large parts of Europe had near-normal precipitation for the year on average, some regions like northeastern Germany, northern Poland, and western Russia recorded above-normal precipitation totals up to 167%. This contrasted with 60%–80% of normal precipitation on the Iberian Peninsula, in southern France, and Italy. Especially noteworthy is the Middle East, with 20%–60% of normal precipitation (Fig. 7.35).

Winter 2016/17 was exceptionally mild over Scandinavia with temperature anomalies reaching more than $+4^{\circ}$ C, whereas the southern Balkan states, Greece, and Turkey recorded widespread below-average temperature anomalies down to -2° C (Fig. 7.36a). The 500-hPa heights featured above-average heights which allows for an anomalous southwesterly flow of mild marine air masses into northern Europe (dotted in Fig. 7.36a). In particular, January was a cold month over much of central and southeastern Europe. With respect to precipitation, winter in Europe was dry

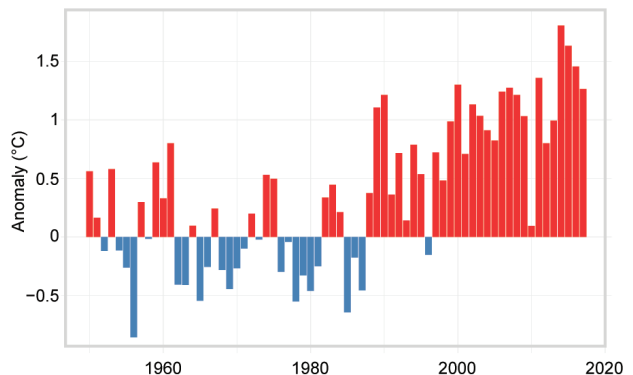


Fig. 7.33. Annual average land surface air temperature anomaly for Europe (35° N– 75° N, 10° W– 30° E) relative to the 1961–90 base period. [Source: CRUTEM4 dataset (Jones et al. 2012.)]

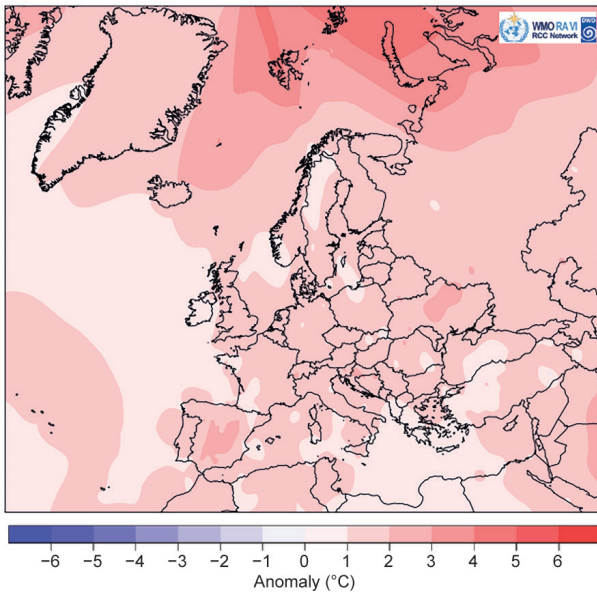


FIG. 7.34. Annual mean air temperature anomalies ($^{\circ}\text{C}$, 1961–90 base period) in 2017. (Source: DWD.)

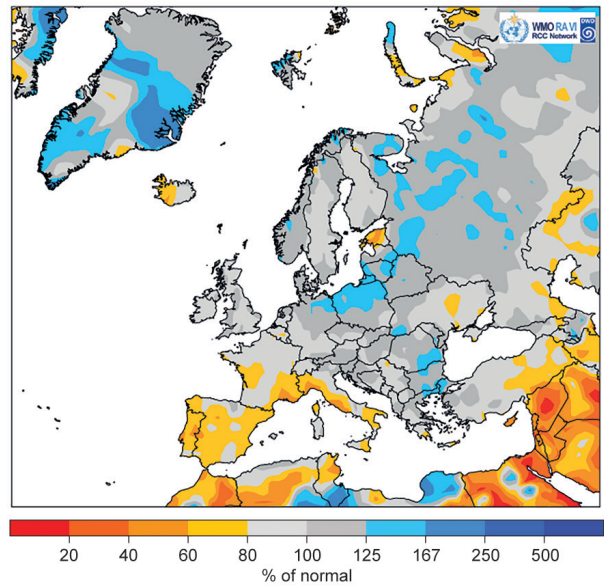


FIG. 7.35. European precipitation totals (% of 1981–2010 average) for 2017. (Source: DWD.)

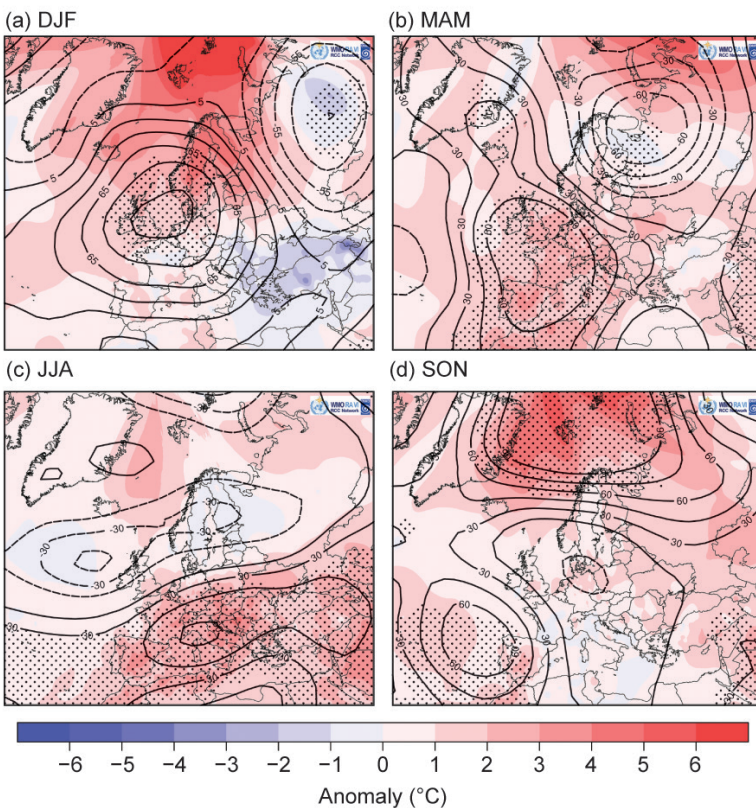


FIG. 7.36. Seasonal anomalies (1961–90 base period) of 500-hPa geopotential height (contour, gpm) and air temperature (shading, $^{\circ}\text{C}$) using data from the NCEP/NCAR reanalysis and DWD, respectively, for (a) DJF 2016/17, (b) MAM 2017, (c) JJA 2017, and (d) SON 2017. Dotted areas indicate regions where 500-hPa geopotential is higher (lower) than the 95th percentile (5th percentile) of the 1961–90 distribution, while hatched areas represent the corresponding thresholds but for air temperature.

with values ranging mostly from 40% to 60% of normal, except for the Norwegian coast, which was wet with some locations exceeding 167% of normal (Fig. 7.37a). This was a consequence of both the strong Icelandic low and Azores high (NAO +1.22), favoring westerly flows inducing a mild and wet winter in northern Europe and dry winter conditions over the more southern parts.

In spring, along with above-average 500-hPa heights situated over central Europe (dotted in Fig. 7.36b), above-normal temperatures were measured all over Europe, up to +4 $^{\circ}\text{C}$ in Spain. However, an unusually warm March was followed by a cold late April, and severe late frosts led to agricultural losses across many European countries. April and May temperatures were well below normal in northwest Russia and northern Scandinavia, contributing to the highest May snow cover extent in this area since 1985. While eastern Europe, except for central Ukraine, showed normal to slightly above-normal spring precipitation totals, most of the Iberian Peninsula, Italy, and the Benelux countries continued to be drier than normal.

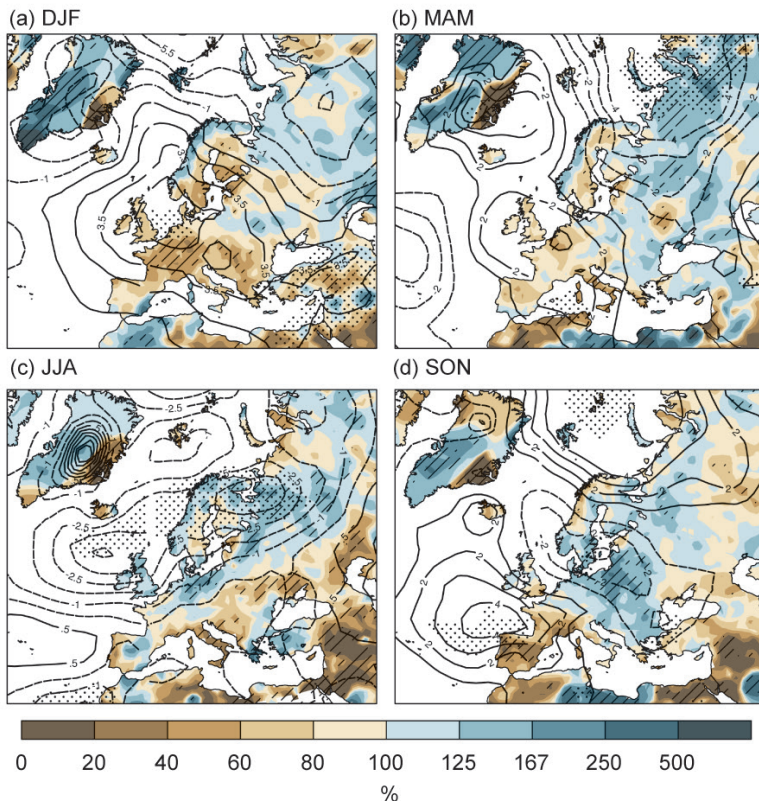


FIG. 7.37. Seasonal anomalies for 2017 (1981–2010 base period) of sea level pressure (hPa) from NCAR/NCEP reanalysis (contours) for (a) DJF 2016/17, (b) MAM 2017, (c) JJA 2017, and (d) SON 2017. Colored shading represents the percentage of seasonal mean precipitation for 2017 compared with the 1981–2010 mean from the monthly Global Precipitation Climatology Centre (Schneider et al. 2015) dataset. Dotted areas indicate regions where SLP is larger (lower) than the 95th percentile (5th percentile) of the 1981–2010 distribution, while hatched areas represent the corresponding thresholds but for precipitation.

With a similar circulation pattern featuring the development of a high pressure bridge during the summer months, temperatures in central Europe continued to be high, with anomalies of up to +5°C measured in Italy and the Balkan states (former Yugoslavia). Characteristically for this blocking pattern situation, summer in Italy and the Balkan states was dry, with precipitation totals as low as 20% of normal while northern Europe, western Russia, Greece, and western Turkey recorded above-average precipitation totals of up to 250% under the influence of the surrounding lows. Italy in particular experienced a massive heat wave with record-breaking temperatures and extreme drought.

During autumn, temperatures in central Europe remained near-normal, while eastern Europe experienced above-normal temperature anomalies of up to +2°C. The Iberian Peninsula was under the influence of above-average 500-hPa height anomalies, which led to temperatures up to +3°C above normal. Due to fre-

quent cyclonic situations, autumn was characterized by some severe storms accompanied by extreme wind velocities and heavy precipitation leading to widespread severe damage to infrastructure and floods in northeastern Germany, Poland, Slovakia, and the Czech Republic. Therefore, eastern Europe received precipitation up to 250% of normal, while on the Iberian Peninsula precipitation totals were mostly well below 60% of the normal.

With temperature anomalies reaching +4°C or more and above-normal precipitation of at least 125%, the year ended very mild and wet for northeastern Europe, while temperature anomalies of around -1°C and below-normal precipitation of locally less than 40% in the Mediterranean region brought a rather cold and dry December.

2) CENTRAL AND WESTERN EUROPE

This region includes Ireland, the United Kingdom (UK), the Netherlands, Belgium, Luxembourg, France, Germany, Switzerland, Austria, Poland, Czech Republic, Slovakia, and Hungary.

(i) Temperature

Overall, western and central Europe were warmer than normal for 2017, with many countries reporting a year ranking among their ten warmest [UK +0.7°C (fifth; since 1910), Switzerland +0.8°C (sixth; since 1864), Austria +0.8°C (eighth; since 1767), France +0.8°C (fifth; since 1900); reference period is 1981–2010 for all four].

Winter 2016/17 was mostly mild or around normal. In February, several storms in southwestern Europe brought warm air masses to central Europe, leading to exceptionally high temperatures, with France reporting its warmest February and several stations in Switzerland observing record-breaking daily maximum temperatures in their more than 100-year measurement series.

This warm episode continued in March, with many new monthly records set in France, Austria, Belgium, and Germany. For the first time in station history (since 1837), a monthly mean temperature of 9.0°C was measured in Graz, 3.7°C above the 1981–2010 normal. In Vienna, the high value of

March monthly means (in 1990) was surpassed by +0.1°C. Similarly, in France, record-high monthly mean temperatures of 10.1°C and 10.9°C were measured at the stations in Dunkerque and Le Mans, respectively. In Germany, at the station Kitzingen, a maximum temperature of 25.6°C was measured on 30 March, a temperature not generally observed so early in the year. At Swiss stations La Chaux-de-Fonds and Meiringen, records of +4.0°C and +4.1°C above their 1981–2010 March normal were reached. After a late-night frost episode in many countries (e.g., Germany, Switzerland, Austria, United Kingdom, the Netherlands) during the second half of April, a low pressure system northwest of Ireland in May led to the advection of warm dry air from Africa, leading to many more daily maximum temperature records in France (35.1°C at station Biscarrosse), the United Kingdom (29.4°C at station Lossiemouth), the Netherlands (33.5°C at station Volkel), and Austria (35.0°C at station Horn).

Summer was characterized by exceptional heat, when high pressure conditions dominated. June was the warmest month since 1901 in the Netherlands (together with 1976) as well as the second warmest month in Austria (251 year series), France (after June 2003), and Switzerland (after June 2003). In Belgium, June 2017 was also one of the warmest, close to the record of June 2003. In August, subtropical warm air reached as far north as Bavaria and Baden-Württemberg (southern Germany), leading to new records in those regions. The station in Emmendingen-Mundigen, Germany, experienced 11 consecutive hot days (daily maximum temperature equal or above 30°C), and the Czech Republic had daily maximum temperatures as high as 38.3°C. In Figari (Corsica, France), a record high temperature of 42.7°C was reached. In July and August, Hungary reported a record 27 days of heat wave conditions and Budapest experienced a record-breaking 34 tropical nights (minimum temperature $\geq 20^\circ\text{C}$; Klein Tank et al. 2009) in the series since 1901.

In autumn, anticyclonic conditions prevailed over western Europe, which on average made western and central Europe slightly warmer than normal (around +1°C) with some exceptions like Austria, where temperature anomalies were below average by 1.5°C in September as well as in France where, although the mean monthly temperature anomaly was +0.9°C, locally daily maximum temperature anomalies (1981–2010 base period) of -5°C were measured. Switzerland reported a September monthly mean anomaly of -1.6°C below its 1981–2010 average. In contrast, autumn in the Netherlands was among its ten warm-

est, with October (+2.6°C anomaly; 1981–2010 base period) fourth warmest since 1901. On 7 November, a station in Freiburg (Germany) recorded 23.2°C, its highest daily maximum temperature for November. The year ended with close to or moderately above-normal temperatures for the United Kingdom and northern France and as much as +2° to +4°C above normal east of Germany, while Switzerland, particularly the south, and the Mediterranean coast of France were colder than normal in December.

(ii) Precipitation

Most of central Europe recorded near- to above-normal precipitation—up to 167% in northeastern Germany and northern Poland; however, France, had slightly below-normal precipitation and even experienced exceptional drought in the region Provence-Alpes-Côte d’Azur, with an average deficit of less than 60% of normal between May and November, the lowest cumulative rainfall since 1959.

In winter 2016/17, central Europe was much drier than normal with 20%–80% of normal precipitation; except for Poland, which had above-normal precipitation of around 125%. Regionally, Switzerland recorded its driest winter for the last 45–55 years. In the mountains in the canton of Ticino, an unprecedented 14 cm average of snow depth was the lowest value since the beginning of measurements.

In spring, western Europe continued to be drier than normal on average, with eastern France, the Benelux countries, and western Germany having a precipitation deficit as low as 40%–60% of normal; conversely, parts of Poland locally received up to 167% of normal. In March, a deep low pressure system over the United Kingdom triggered a foehn storm in the northern Alps, bringing up to 100 mm of precipitation within three days in the southern Alps. Austria and Switzerland reported intense snowfall in late April, with 35 cm accumulation within two days in St. Gallen (Switzerland).

Frequent Atlantic cyclones during the summer brought above-normal precipitation to most of the northern region. Northern Germany and northern Poland received as much as 250% of normal. Often accompanied by thunderstorms, the cyclones brought heavy rainfall that led to flooding and widespread traffic impact. Highest daily total records were broken, for example, at station Berlin-Tegel where 197 mm on 29 June was measured (previous record was below 90 mm). Station Shannon Airport (Ireland) reported its wettest July in its 71 year record with 133.6 mm (203% of normal).

In autumn, southern France, under the influence of above-normal 500-hPa heights centered over the Iberian Peninsula, experienced a rain deficit as low as 20% in the Mediterranean region, while eastern Europe received up to 250% of normal precipitation due to several low pressure systems. At the end of the year, precipitation was distributed unevenly, but with above-normal precipitation for most of central Europe (exceptions are the coast of southern France, eastern Germany, and the border region of Poland and the Czech Republic, which received below-normal precipitation).

(iii) *Notable events and impacts*

A severe storm affected France on 6–7 March, with peak gusts reaching 54 m s^{-1} in Brittany.

On 18–19 May, thunderstorms over Germany (low “Dankmar”), accompanied by hail and heavy rainfall of more than 36.3 mm (Bad Bibra) within 1 hour, led to flooding in several cities.

Local intense rainstorms occurred in France during 29–31 May, with 24-hr totals often exceeding 20 mm: 53.9 mm in Genouillax, 58.9 mm in Muret, 72.1 mm in Castelnau-Magnoac, and 80 mm in Chateauponsac. During the same period, in Switzerland a violent storm with heavy rain and hail the size of golf balls was reported at the station in Thun; the storm brought the highest daily precipitation amount (59.6 mm) there since the start of measurements in 1875.

In summer, severe hailstorms impacted western and central Europe. Perhaps the most remarkable was cyclone Zlatan, which developed over England on 19 July. Moving eastward, it affected the eastern half of France, Switzerland, Austria, Germany, the Czech Republic, and Poland with heavy rain and hail causing damage, especially in Germany (North Rhine-Westphalia, Station Cologne measured 48.8 mm h^{-1} and gusts of 26 m s^{-1}) with closed roads and traffic delays. The airport in Cologne was closed for 90 minutes.

In Austria, between 4 and 6 August, intense precipitation in Lungau (state of Salzburg) and Obersteiermark (state of Styria) led to several landslides, causing an estimated damage of more than 20 million Euros (\$25 million U.S. dollars) to the local road network.

In October, three storms (ex-Hurricane Ophelia, Storm Brian, and Storm Herwart), with extreme wind speeds of 40 m s^{-1} or more, brought much damage to the United Kingdom, Ireland, Germany, the Netherlands, France, Austria, Czech Republic, Poland, and Slovakia, with falling trees killing at least seven people in Germany and three in the UK, as well as road and railway blockings affecting traffic for days during clean

up. During Ophelia, an individual wave height record of 26.1 m was set at the Kinsale gas platform off the Cork coast (Ireland).

Several storms affected central Europe from 17 to 18 November, with wind gusts of more than 48 m s^{-1} , impacting traffic and causing major damage to trees and buildings.

3) THE NORDIC AND THE BALTIC COUNTRIES

This region includes the Nordic countries Iceland, Norway, Denmark, Sweden, and Finland, and the Baltic countries Estonia, Latvia, and Lithuania

(i) *Temperature*

Temperatures across the Nordic and Baltic area in 2017 were mostly higher than normal, between $+1^\circ$ and $+2^\circ\text{C}$. Estonia, Finland, and Denmark had positive anomalies of $+1.5^\circ$, $+1.3^\circ$ and $+1.2^\circ\text{C}$, respectively.

Winter 2016/17 was exceptionally mild due to the influence of above-average 500-hPa heights (Fig. 7.36a), with $+2^\circ\text{C}$ anomalies in the south and up to $+5^\circ\text{C}$ in northern Sweden and Finland. Denmark recorded its fifth and fourth highest daily minimum and maximum temperatures in December, respectively, since 1953. During long-lasting foehn winds in January, a daily mean temperature of 13.8°C was measured at station Sunndalsøra (Norway) on 25 January, which was the highest daily mean temperature ever recorded in January by a weather station in Norway and is a value commonly measured around the beginning of July. During February, 12 stations in Norway observed new daily maximum temperature records as well as extreme anomalies at the Arctic station of Svalbard Lufthavn, with a monthly mean temperature of $+9.3^\circ\text{C}$.

On 26 March, under the influence of southwesterly flows, daily maximum temperatures of 20°C or more were measured at stations Akershus, Oslo, Hedmark, Buskerud, and Telemark in Norway, the first known occurrence of such high temperatures in March. In May, the northeastern part of the North suffered from a cold wave which led to several record below-average anomalies in Latvia (e.g., station Rezekne -4.7°C , Mersrags -6.1°C). Finland was also affected, with anomalies between -1° and -3°C for May across the whole country. Temperatures for Lithuania in May also were slightly below normal, and frost days were even recorded. In contrast, a new record high maximum temperature of 31.8°C was measured at Sigdal - Nedre Eggedal (Buskerud) in Norway on 27 May.

Under the influence of below-average 500-hPa anomalies, summer in the Baltic States on average had slightly below-normal temperatures with anomalies

ranging from -0.5° to -2.5°C in the east of Finland. Lithuania observed an unusually cold July (-1.4°C), while the rest of the summer was closer to average. Overall, the summer was rather cold without any hot spells, which was apparent in the maximum temperatures; for example, Sweden, with a daily maximum temperature of only 28.0°C , had its coolest summer since 1922.

During autumn, temperatures were higher than normal in all Nordic and Baltic countries, with around $+1^{\circ}\text{C}$ anomaly. The entire north was under the influence of above-average 500-hPa height anomalies, which also led to a new record high sea level air pressure of 1044.1 hPa at Lycksele and Åsele in northern Sweden. November and December were especially mild. It was the warmest autumn in Denmark since 1984, with a new maximum temperature record of 17.1°C on 2 November at Kjevik (Kristiansand, Vest-Agder, Norway), as well as at station Yngør Lighthouse (Tvedestrand, Norway) with a reading of 14.4°C . With temperatures up to $+5^{\circ}\text{C}$ above normal in eastern Finland and between $+1^{\circ}\text{C}$ and $+4^{\circ}\text{C}$ for most of the Baltic States, 2017 ended rather warm.

(ii) Precipitation

Except for Iceland and most regions of the northern Baltic States, annual precipitation totals were around normal to above normal. Norway experienced its sixth wettest year since records began in 1900.

During winter 2016/17, all Baltic states and most Nordic countries had a precipitation deficit; only Norway received a surplus of up to 167% of normal, with northern Norway having its wettest winter on record but only the 15th wettest for the country as a whole. This deficit continued in spring, especially in May, with Lithuania observing only 24% of its normal precipitation and Latvia having its sixth driest May, with a nationally-averaged total of 21.4 mm.

Summer in northern parts of the Baltic was drier than normal; however, Lithuania, Denmark, and Norway received above-normal precipitation. Lithuania reported a wet summer, particularly notable for July (almost 150% of normal), due in part to several severe storms with heavy rainfall. Norway, with 130% of normal precipitation, recorded its third wettest summer since 1900.

Prevailing westerlies in autumn brought well above-normal precipitation to the Nordic and southern Baltic states. Lithuania and Latvia each reported a record (since 1961) wet season with up to 176% and 135% of normal precipitation. Latvia, with a seasonal total of 313.5 mm, reported its second wettest autumn in the last 94 years (for some stations even the wet-

test). At the end of 2017, precipitation totals continued to be above normal for almost all of the Nordic and Baltic States.

(iii) Notable events and impacts

On 12 August, widespread thunderstorms left 50 000 households without power in southern Finland.

At the end of September, following heavy precipitation and warmth, major damage was caused by floods and landslides in southeastern and eastern Iceland.

In Lithuania, three microscale extreme heavy rain events were observed in summer. On 12 July, precipitation totals exceeded 80 mm in 12 hours.

Between 22 and 24 November, Storm Ylva caused wind gusts as high as 47.5 m s^{-1} at station Narvik-Fagernesfjellet (Nordland) in Norway. Another storm, “Birk”, brought heavy precipitation to Hordaland and Rogaland counties, with a maximum daily precipitation total of 127.5 mm at Gullfjellet (highest mountain in Bergen, Hordaland) measured on 23 December.

4) IBERIAN PENINSULA

This region includes Spain and Portugal. Anomalies refer to a reference period of 1981–2010 for Spain and 1971–2000 for Portugal.

(i) Temperature

Temperatures for 2017 on the Iberian Peninsula were well above normal, by $+1^{\circ}$ to $+3^{\circ}\text{C}$ in central Spain. Portugal recorded its second warmest year on record with $+1.1^{\circ}\text{C}$ anomaly compared to the 1971–2000 average and a new average annual maximum record temperature of 22.82°C , $+2.32^{\circ}\text{C}$ above normal, since records began in 1931. With an anomaly of $+1.1^{\circ}\text{C}$, Spain recorded its warmest year since its series began in 1965, exceeding the previous record of 2011, 2014, and 2015 by $+0.2^{\circ}\text{C}$. More than thirty individual stations in Spain (almost one-third of all principal stations) surpassed their annual mean temperature records in 2017.

During winter 2016/17, January had below-average anomalies of around -0.5°C . This situation was associated with an inflow of cold air from the north caused by a high pressure system located above the Canaries ranging as far north as Iceland and a low pressure system ranging from Scandinavia to the Mediterranean. Some stations in Portugal measured exceptionally low daily minimum air temperatures and, on 19 January, some even recorded absolute daily minimum records. February, in contrast, was

clearly warmer than average, with anomalies as high as +1.6°C in Spain.

Above-normal 500-hPa height anomalies situated over central Europe led to an extremely warm spring, with anomalies of +1.7°C, making 2017 the warmest spring since 1965 in Spain, exceeding the previous record of 2011 by 0.1°C. In Portugal, April was the fifth and May the third warmest month since the record began in 1931. Additionally, the highest and second highest average maximum temperatures, respectively, since 1931 were measured for each of these months.

The warmth continued into summer, with Spain observing its second hottest since 1965, at +1.6°C above normal, behind only 2003. June was particularly warm, with a monthly anomaly of +3.0°C. During 12–16 July, the highest daily maximum temperatures of that summer were observed: 46.9°C at Córdoba Airport, 45.7°C at Granada Airport, and 45.4°C at Badajoz Airport. Eight stations in the southern half of the peninsula observed their highest maximum absolute temperature of any summer month. With a mean temperature of 22.70°C, summer in Portugal was +1.43°C warmer than the 1971–2000 normal, its ninth warmest summer since 1931.

While the autumn anomaly for Spain was only +0.8°C above normal, October was the warmest since 1965 (+2.6°C). Although it was only the fifth warmest autumn (with respect to mean temperatures) for Portugal since 2000, the average maximum temperature was 24.40°C (+2.93°C above normal), which is the highest value since 1931. With slightly below-average temperature anomalies of –0.4°C in December, the year ended cold for the Iberian Peninsula.

(ii) Precipitation

Overall, the Iberian Peninsula was very dry in 2017 and was characterized by intensive drought. It was the second driest year since the beginning of the series in 1965 for Spain and third driest for Portugal since 1931.

The winter season 2016/17 was drier than normal, with 69% of normal precipitation for Portugal. In Spain, a dry January (23% of normal) was followed by a wetter-than-normal February (136% of normal). Some regions, including the southern half of Galicia, west Castilla-León, south Navarra, and extensive areas of La Rioja, Central System, Pyrenees, Huesca, and Huelva provinces, as well as the eastern Canary Islands, had above-normal rainfall of 175%.

For Spain, spring began with a wet March but the seasonal average showed a precipitation deficit of about 75% of normal for both Spain and Portugal. While summer in Portugal was its seventh driest

since 1931 with an average of 23 mm corresponding to 40% of normal, summer in Spain was slightly wetter than normal (107% of normal). Notably, much of the precipitation can be attributed to storms during which new daily maximum precipitation total records were measured.

Autumn was dominated by above-normal 500-hPa height anomalies centered above the Iberian Peninsula. As a result, both Spain and Portugal recorded below-average precipitation totals, making 2017 the driest autumn on record in Spain and second driest autumn since 1931 for Portugal (only 35% of normal precipitation). September was the driest such month of the last 87 years in mainland Portugal, with an average precipitation of 2 mm (5% of the normal). In many places, no precipitation was measured at all. It was followed by the driest October of the last 20 years in Portugal. By the end of October, 25% of Portugal suffered from severe and 75% from extreme drought. This extended period of drought led to widespread wildfires in Portugal, with new records in the size of area burned. December marked the ninth consecutive month with below-normal precipitation for Portugal.

(iii) Notable events and impacts

A heat wave lasting 17–18 days in the northern and central regions of Portugal and 11–12 days in the remainder of the country occurred between 7 and 24 June.

During summer, high temperatures and severe precipitation deficits in Portugal enhanced extensive wildfires (> 1000 ha), with more than 60 fatalities; the fires were so large they were visible from space.

Due to ex-Hurricane Ophelia, strong winds prevented the extinguishing of fires in Portugal and Spain (9–21 October). At least 41 people were killed in wildfires across the region. Additionally, ashes from the fires were transported as far as the UK, where yellow skies and a red sun were reported, and Switzerland, where ashes were detected at air monitoring sites in Payerne and on Jungfrauoch (3580 m a.s.l.). According to the Portuguese Institute for Nature Conservation and Forests, burned areas exceeded 440 000 ha, a new record. Central regions of mainland Portugal were the most affected by very large fires (> 1000 ha) during several periods: 16–21 June, 16–18 July, 23–26 July, 9–19 August, 23–27 August, 5–9 September, and 12–15 October. During these periods, the associated meteorological conditions were extremely favorable to fire propagation and adverse to fire combat; fire weather index values were higher than the 90th percentile in the majority of the regions.

5) MEDITERRANEAN, ITALY, AND BALKAN STATES

This region includes Italy, Malta, Slovenia, Croatia, Serbia, Montenegro, Bosnia and Herzegovina, Albania, Republic of North Macedonia, Greece, Bulgaria, and Turkey. Balkan States include North Macedonia and Bulgaria unless otherwise specified.

(i) Temperature

The Mediterranean and the Balkan states showed average anomalies of mostly between +1° and +2°C in 2017. Based on station Zagreb-Grič, Croatia had its sixth warmest year in the series from 1862. With an anomaly of +1.2°C, Bulgaria experienced its warmest year on record since 1980.

Winter 2016/17 was dominated by an unusually cold January due to a low pressure system centered over southeastern Europe leading to an inflow of cold air masses from Siberia. In Greece, monthly minimum and maximum temperatures were 3° to 5°C below the 1971–2000 normal. Slovenia reported its coldest January of the last 30 years. In west Bulgaria, minimum daily temperatures were close to the records of the last 50 years, with –26°C in Kyustendil and –27°C in Pernik (–1.2°C below normal for the whole winter). Serbia observed its fourth coldest January since its record began in 1951. Turkey reported a negative January anomaly of –1.5°C below its 1981–2010 normal.

In spring, due to prevailing southerly flows, temperatures in Italy, Greece, and the other countries of the Balkan Peninsula were above normal with anomalies around +1°C. Although anomalies showed only a slightly warmer-than-normal spring, events like the heat wave that occurred between 12 and 13 May in the central and southern parts of Greece led to a new daily maximum temperature record of 40.6°C at the station Argos.

A prolonged anticyclonic situation over the northern Adriatic Sea contributed to a very warm summer for Italy and the Balkan states, with anomalies around +3° to +5°C. Several heat waves contributed to these high anomalies during all three summer months. Some stations in Italy measured new all-time records in early August, for example, 41°C in Pescara. Slovenia reported its second warmest summer, surpassed only by 2003. Serbia also reported its second warmest summer; July and August proved to be extraordinarily warm. Several stations in Serbia observed their third highest August temperature, although on average across the country, it was seventh highest. A record-breaking number of days with temperatures above 38°C and new all-time records for the number of tropical nights were set

at several stations in Serbia. Croatia categorized its summer as extremely warm, with above-average anomalies between +2.7° and +4.5°C. During heat wave events, Bulgaria measured extreme maximum temperatures of 42.5°C in Sandanski and 43.6°C in Ruse. Macedonia experienced unusually long-lasting periods of warm weather, with anomalies exceeding +5°C in mid-June. Turkey set a new all-time high temperature record of 45.4°C in Antalya on 1 July.

Anomalies were up to +2°C in eastern Turkey in autumn. Temperatures mostly fluctuated around normal, and no major extremes were reported. The year ended warmer than normal for the region (except parts of Italy, Malta, southern Greece) due to prevailing southerly flows over southeastern Europe in December.

(ii) Precipitation

Especially for Italy, 2017 was drier than normal. For most Balkan states, precipitation totals were near-normal but often irregularly distributed in both time and space. For example, while overall Serbia was near-normal, the station in Zrenjanin recorded its driest year since its record began in 1925. Similarly, Croatia was slightly wetter than normal for the year but the wider area of the town Split was extremely dry.

Winter 2016/17 was drier than normal, with precipitation of around 60% of normal for the Balkan states and most of Italy. Nevertheless, in January, due to the cold Siberian air masses crossing the warmer Aegean Sea, high amounts of snowfall were observed in Greece and North Macedonia with adverse impacts on transportation. Turkey reported a winter precipitation deficit of 19.5%.

With the exception of Italy and southern Greece, spring was near to slightly wetter than normal overall. In May, several extreme precipitation events were measured during low pressure situations over Greece and Bulgaria. Thunderstorms accompanied by cyclone “Victor” led to flooding and hail that destroyed crops. During 17–18 May, 230 mm of rain was measured at station Sitta in Greece, while 139 mm fell in twelve hours at station Semprona at the end of the month.

Throughout the summer, several cut-off lows were centered south of Greece and supplied Greece and western Turkey with well above-normal precipitation (up to 250% of the seasonal normal), including heavy rainfall and hailstorms, sometimes leading to flooding; conversely, Italy and the Balkan states, under the influence of high pressure, experienced a drier-than-normal season. The summer for the Emilia-Romagna region in northern Italy was its

third hottest since 1961; warm temperatures, combined with dryness, aggravated drought conditions. At the end of August, the drought in Italy reached its maximum intensity. Serbia reported a dry to very dry summer, and Malta had its driest July since 1951 (56% of normal precipitation). Autumn in the Balkan states was wetter than normal, especially in Bulgaria with precipitation up to 167% of normal. In October, Bulgaria's average precipitation was 2.5–3 times the normal. Conversely, Italy and most of Turkey suffered from precipitation deficits and drought. The year ended drier than normal for southern Turkey and southern Italy, while most of the Balkan states received above-normal precipitation.

(iii) Notable events and impacts

In Bulgaria, for the first time in the past 60 years, the coastal waters of the Black Sea were frozen—an occurrence observed only three times since the beginning of the 20th century.

On 21–22 April, a severe frost event in Slovenia caused catastrophic damage to crops.

In Greece, extensive and long-lasting snowfall during several days in January caused severe traffic problems, trapping hundreds of vehicles, disturbing public transport in Thessaloniki, and suspending flights. After serious power failures, the Aegean islands of Skopelos, Alonnisos, and Evia declared a state of emergency.

A severe hailstorm during 7–9 May caused heavy damage in the agricultural areas in northern Greece. At the beginning of June, Bulgaria was hit by a series of severe thunderstorms accompanied by heavy rainfall and hail causing floods and damage to crops. Further local storms with hail were reported in Slovenia and Italy with hourly precipitation totals reaching as high as 46.5 mm in Salsomaggiore (Italy). At station Vojsko in Slovenia, on 6 June, a new 24-hr daily precipitation record of 200 mm was set. Two intense hailstorms were registered on 7 and 14 June in North of Macedonia.

On 3 July, northwestern and north-central Bulgaria reported severe convective storms accompanied by strong winds and extreme hail, with stones measuring up to 8 cm diameter in Mezdra and Levski.

During the first half of July, an intense heat wave hit Croatia, drying out the plant cover, which led to the outbreak of a wildfire on 17 July near Split. Approximately 4300 ha of forest, brush, olive groves, and vineyards were burned. With a 40-km long fire front at its maximum, it was one of the biggest wildfires in Croatian history.

Turkey recorded a severe hailstorm on 27 July, with hailstones up to 9 cm in diameter observed in Istanbul.

In Naples, Italy, a heavy thunderstorm on 5 September brought hail up to 11.5 cm in diameter and weights up to 350 g, injuring several people and animals, as well as causing damage to vehicles, houses, trees, and crops.

The slow-moving cyclone “Quasimodo”, approaching Italy from the Ligurian Sea, reached the city of Livorno on 9 September, with heavy precipitation causing flooding and damage, along with six fatalities. After passing over Toscana and the city of Pisa, the cyclone reached the Balkans. The Adriatic coast and the islands of the Adriatic Sea received more than 500 mm precipitation, causing floods in Croatia that damaged houses and cars. A total of 135 million Euros (around 160 million US dollars) in damages in the aftermath of the flood was estimated just for the Croatian county Zadar.

Very heavy precipitation on 1 December led to extensive flooding and landslides in Greece. Between 8 and 12 December, an exceptional meteorological event occurred in Italy with intense rain at some locations (more than 300 mm in 48 hours). At Cabanne, Genoa province (Italy), an overall total of 507.0 mm was measured. Strong winds as high as 49.5 m s^{-1} were measured at Loiano.

6) EASTERN EUROPE

This region includes the European part of Russia, Belarus, Ukraine, Moldova, and Romania.

(i) Temperature

For most of European Russia and Belarus, 2017 was warmer than average, with anomalies of $+1.45^\circ$ and $+1.7^\circ\text{C}$, respectively. Moldova and Romania recorded slightly lower positive anomalies of $+1.2^\circ\text{C}$ (normal 1961–1990) and $+0.7^\circ\text{C}$ (normal 1981–2010), respectively. Ukraine reported its third hottest year since the beginning of observations in 1961 with an anomaly of $+1.8^\circ\text{C}$.

The winter season 2016/17 on average was warm for European Russia, Belarus, and Ukraine. Anomalies were below average only in January, when a cold spell in the Volga region dropped temperatures to as low as -40°C and several absolute minimum temperatures were exceeded in the cities of Arkhangelsk, Kotlas, Naryan-Mar, Kirov, and Tver. Similarly, Romania and Moldova reported severe cold during this time, with the latter measuring temperatures of 8° – 10°C below normal. Winter in Moldova, overall,

was slightly colder than normal, with an anomaly of -0.6°C (1961–90 normal) for the season.

At the beginning of spring, under the influence of a cyclone located over northwest Europe, new high temperature records in Moscow and St. Petersburg, as well as abnormal warmth at the Arctic coast, were reported. During the second half of March, temperature records in Smolensk, Tambov, Cheboksary, and other Russian cities were measured and, overall, the seasonal weather was climatologically ahead by a month. A nation-wide heat wave hit Romania in March, with a monthly temperature $+3.4^{\circ}\text{C}$ above its 1961–2010 normal. At the station in Baisoara, the absolute monthly maximum temperature for March was exceeded. Moldova also reported an abnormally warm March. Then, in late April a wintry spell resulted in additional—this time minimum—temperature records in the area, as low as -15°C in Smolensk (Russia). The season ended with a cold May, which brought additional minimum temperature records. Nevertheless, overall, spring was warmer than normal for Moldova, Belarus, and the Ukraine. With a monthly mean air temperature of 10.9°C , Moscow (Russia) experienced its coldest May of the 21st century.

Even with a late frost event on 4 June (temperatures down to -1°C) in the Ukraine, overall, summer for the Ukraine, Moldova, and Romania was warmer than normal, with widespread anomalies up to $+2^{\circ}\text{C}$ above normal. In contrast, the northern part of European Russia was colder than average; a new daily low temperature record of 7.8°C was set in Moscow on 15 June, with observations dating to 1949.

Autumn was warmer than normal for Russia, Ukraine, Belarus, and Moldova, while temperatures in Romania were near-normal. During the second half of September and November, anomalies of up to $+2^{\circ}\text{C}$ were observed, while the rest of the season mostly remained close to normal. The year ended with an exceptionally warm December—especially notable in European Russia where anomalies exceeded $+6^{\circ}\text{C}$; anomalies for Belarus, Ukraine, and Moldova, ranging between $+3^{\circ}$ and $+5^{\circ}\text{C}$, were also quite high, and only the southern part of Romania showed anomalies below $+3^{\circ}\text{C}$.

(ii) Precipitation

Precipitation totals were near- to slightly above normal in eastern Europe with the exception of Ukraine, which reported precipitation 60%–70% of normal in the south and central regions and near-normal for the rest of the country. Russia and Belarus on average had slightly above-average totals of 115%

and 121%, respectively. Nevertheless, it was the second wettest year on record for European Russia.

During winter 2016/17, only Romania, Moldova, and isolated spots in Russia showed below-average precipitation of around 60% of normal; the rest of the area was near-normal or slightly above.

Spring was rather wet for Moldova, where some places during April observed values of 85–128 mm, corresponding to 230%–350% of normal precipitation, for the first time in the period of record dating back at least 80 years. Most areas of Russia also reported a precipitation surplus (of up to 167% and locally even more) while Belarus was near-normal. The exception to the wet spring was the central region of Ukraine where deficits of 60% of normal were measured.

During summer, this deficit extended over all of Ukraine, with 60% of the agricultural area affected by drought. Belarus reported a dry June but, overall, summer precipitation was near- or slightly above normal. Most regions of European Russia, other than the south, which received 3%–25% of normal monthly precipitation in August, had near-normal precipitation or even a surplus (up to 167% in the northwest). After heavy rain events accompanied by hail and strong winds caused major damage in June and July, Moldova experienced a precipitation deficit in August where locally severe drought was reported.

With prevailing anticyclonic conditions in September, autumn began with a large precipitation deficit (mostly below 60% of normal) for the south of European Russia as well as for eastern Ukraine. October was the wettest month of the year for the eastern countries (Moldova, Belarus, and Romania). At the end of the season, only eastern Ukraine, southern parts of European Russia, and the Ural region suffered from precipitation deficits. December was wet throughout eastern Europe.

(iii) Notable events and impacts

On 20 April, the Kirov region (Russia) reported exceptionally heavy snowfalls and freezing rain, leading to power failures due to damage to transmission lines for 44 settlements and to extensive damage to forests and agriculture.

In April, Moldova reported extreme weather conditions, with rain, snow, and sleet depositing on wires and trees, as well as strong wind and frost with disastrous consequences for the country's economy. Likewise, reports were made in the Ukraine of unusually high numbers of frost days that damaged fruits, vegetables, and other crops.

A severe thunderstorm (“Falk”) hit Moscow (Russia) and the surrounding area on 30 May. For the first time since the beginning of instrumental observations in Moscow for more than 100 years, wind gusts of 30 m s^{-1} were recorded, resulting in structural damage to buildings. Also in Moscow, 11 people were killed and 70 injured on 29 July during a storm where wind gusts reached 29 m s^{-1} .

Heavy precipitation of 100–120 mm within a 24-hr period in the region of Bucharest (Romania) caused flooding in July.

7) MIDDLE EAST

This region includes Israel, Cyprus, Jordan, Lebanon, Syria, West Kazakhstan, Armenia, Georgia, and Azerbaijan.

(i) Temperature

In the Middle East, temperatures in 2017 were above normal by $+1^\circ$ to $+2^\circ\text{C}$. Israel reported its fourth warmest year among the last 67 years.

The year began on a cold note, however. Winter 2016/17 temperatures on average were below normal. January and February showed negative anomalies down to -2°C for some regions in Georgia, Armenia, Israel, and Jordan. Israel reported its coolest February daily minimum temperatures since 1999.

Spring had slightly above-normal temperatures, with anomalies around $+1^\circ\text{C}$. In May, unusually high temperatures above 40°C were measured in Israel as a result of Sharav (heat wave) events, which brought warm sandy air from the Sinai Peninsula.

The Middle East experienced a hot summer, with anomalies of up to 4°C above normal. Multiple heat waves in July were responsible for extreme temperatures in Cyprus, Jordan, and Israel, which tied with 2012 as the warmest July in Israel since the beginning of records, with average daily temperatures $+2^\circ$ to $+2.5^\circ\text{C}$ above normal.

On average, autumn also was warmer than normal, between $+1^\circ$ and $+2^\circ\text{C}$. The year ended with well above-normal temperatures in December, with some stations in Israel ranking as high as second warmest since the beginning of measurements.

(ii) Precipitation

With regard to precipitation in the Middle East, 2017 was characterized by widespread deficits of 20%–40% of normal and even less for some regions. Israel reported its third lowest annual precipitation total; only 1959 and 1999 had less rainfall. Regionally, it was the driest year on record in the coastal plain of Israel.

During winter 2016/17, precipitation was unevenly distributed, but, except for most parts of the South Caucasus which received slightly above-normal precipitation, totals were below normal, with extreme deficits in some regions. Northeast Israel reported less than 15% of its normal monthly average in February, which was the driest February since 1958 for this area.

Spring continued to be dry, with totals between 20% and 70% of normal for Cyprus, Jordan, Lebanon, and Israel. Georgia and some parts of Azerbaijan and western Armenia received above-normal precipitation. Summer was extremely dry, with no precipitation at all for widespread regions in Lebanon, northern Syria, and Israel.

While autumn was also dry for the region around the Mediterranean, locally heavy precipitation events provided surpluses of up to 250% of the monthly normal (e.g., the Karmel Region in Israel), sometimes resulting in flooding. Georgia received near-normal precipitation amounts, with Armenia and Azerbaijan above normal (up to 167%).

The year ended dry for the Middle East countries on the Mediterranean and near-normal for Georgia, Armenia, and Azerbaijan.

(iii) Notable events and impacts

Three men died after being swept away by strong easterly winds of $14\text{--}18 \text{ m s}^{-1}$ accompanied by gusts of $22\text{--}25 \text{ m s}^{-1}$ in northern Israel on 12 April. One day later, at the station Neot Smadar in the southern Negev, heavy rainfall of 27 mm, of which 10 mm fell within only 5 minutes, was measured, resulting in flooding and the closing of two main routes to Eilat.

On 18 May, severe sandstorms were advected to southern Israel from the Sinai Peninsula, where they were created by downdraft winds related to well-developed clouds. These Haboob-type sandstorms are uncommon in Israel. As a result, the Eilat Airport was closed for several hours.

On 16 October, a heavy rainfall event in Nahariyya (northwest coast of Israel) brought more than 70 mm of precipitation within two hours. During the morning hours of 30 October more than 50 mm within one hour were measured in Haifa. Both events were followed by flooding and subsequent road closures.

g. Asia

Throughout this section the base periods used vary by region. The current standard is the 1981–2010 average for both temperature and precipitation, but earlier base periods are still in use in several countries. All seasons mentioned in this section refer to those of the Northern Hemisphere, with winter

referring to December 2016–February 2017, unless otherwise noted.

1) OVERVIEW—T. Li, Z. Zhu, P. Zhang, T. C. Lee, Y. Mochizuki, S.-E. Lee, L. Oyunjargal, and B. Timbal

Annual mean surface air temperatures during (January–December) 2017 were above normal across most of Asia and much above normal (anomalies >1.5°C) in Siberia (Fig. 7.38). Annual precipitation amounts were above normal from western China to northeastern India, from the western part of the Indochina Peninsula to the central part of the Malay Peninsula, in the Maritime Continent, and from the western part of eastern Siberia to western Siberia, and they were below normal in the eastern part of eastern Siberia, from the Korean Peninsula across northeastern China to Mongolia, and in central Asia (Fig. 7.39).

Though annual mean temperature anomalies were virtually all positive, they evolved quite differently season by season (Fig. 7.40). In winter (Fig. 7.40a), negative temperature anomalies appeared over western Siberia, associated with a large-scale tropospheric barotropic negative geopotential height anomaly (Figs. 7.41a and 7.42a). In spring, cold anomalies appeared over southwestern China and the Indochina Peninsula (Fig. 7.40c), corresponding to positive rainfall anomalies in the region (Fig. 7.40d). In summer, negative temperature anomalies dominated over the northern part of central to eastern Siberia. Autumn was marked by negative temperature anomalies from central Siberia to Japan. Seasonal precipitation amounts were persistently above normal in the western part of the Tibetan Plateau from winter to summer and in Southeast Asia throughout the year, but they were below normal in northeastern China and Korean Peninsula from spring to autumn.

In winter, enhanced convection appeared over the Maritime Continent and the South China Sea (Fig. 7.41a); to its north, positive anomalies of 500-hPa geopotential height and 850-hPa temperature (Fig. 7.42a) were observed over East Asia. In spring, anticyclonic circulation anomalies straddled the equator over the western Pacific in the lower troposphere (Fig. 7.41b). In summer, convective activity was suppressed to the east of the Philippines, and the western North Pacific subtropical high was shifted westward (Fig. 7.41c). In autumn, anticyclonic (cyclonic) circulation anomalies straddled the equatorial western Pacific (Indian) Ocean in the lower troposphere (Fig. 7.41d).

In terms of the summer monsoon in 2017, East Asian summer monsoon rainfall was weaker than normal, while Indian summer monsoon rainfall was near normal. Intraseasonal variability of convective activity was clearly evident in the monsoon regions.

2) RUSSIA—O. N. Bulygina, N. N. Korshunova, M. Yu. Bardin, and S. G. Davletshin

This review for Russia and its individual regions, along with estimates of abnormal climate features, are obtained from hydrometeorological observations taken at the Roshydromet Observation Network. Unless otherwise noted, anomalies are relative to a 1961–90 period, and national rankings reflect an 82-year (1936–2017) period of record.

(i) Temperature

The year 2017 in Russia was warm: the mean annual national air temperature was 2.02°C above normal (Fig. 7.43). This is the fourth highest such temperature on record. Positive annual mean air temperature anomalies were observed in all regions of Russia. The largest anomalies occurred over Asian Russia (east of the Urals, approximately 60°E); the annual tem-

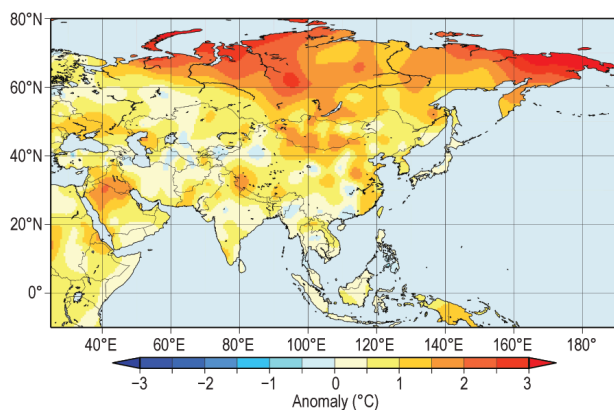


FIG. 7.38. Annual mean surface temperature anomalies (°C; 1981–2010 base period) over Asia in 2017. (Source: Japan Meteorological Agency.)

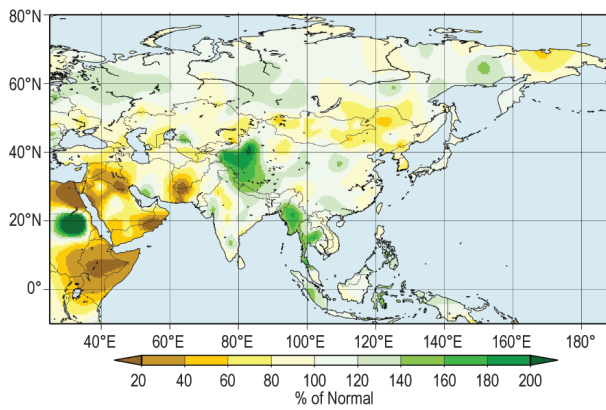


FIG. 7.39. Annual precipitation (% of normal; 1981–2010 base period) over Asia in 2017. (Source: Japan Meteorological Agency.)

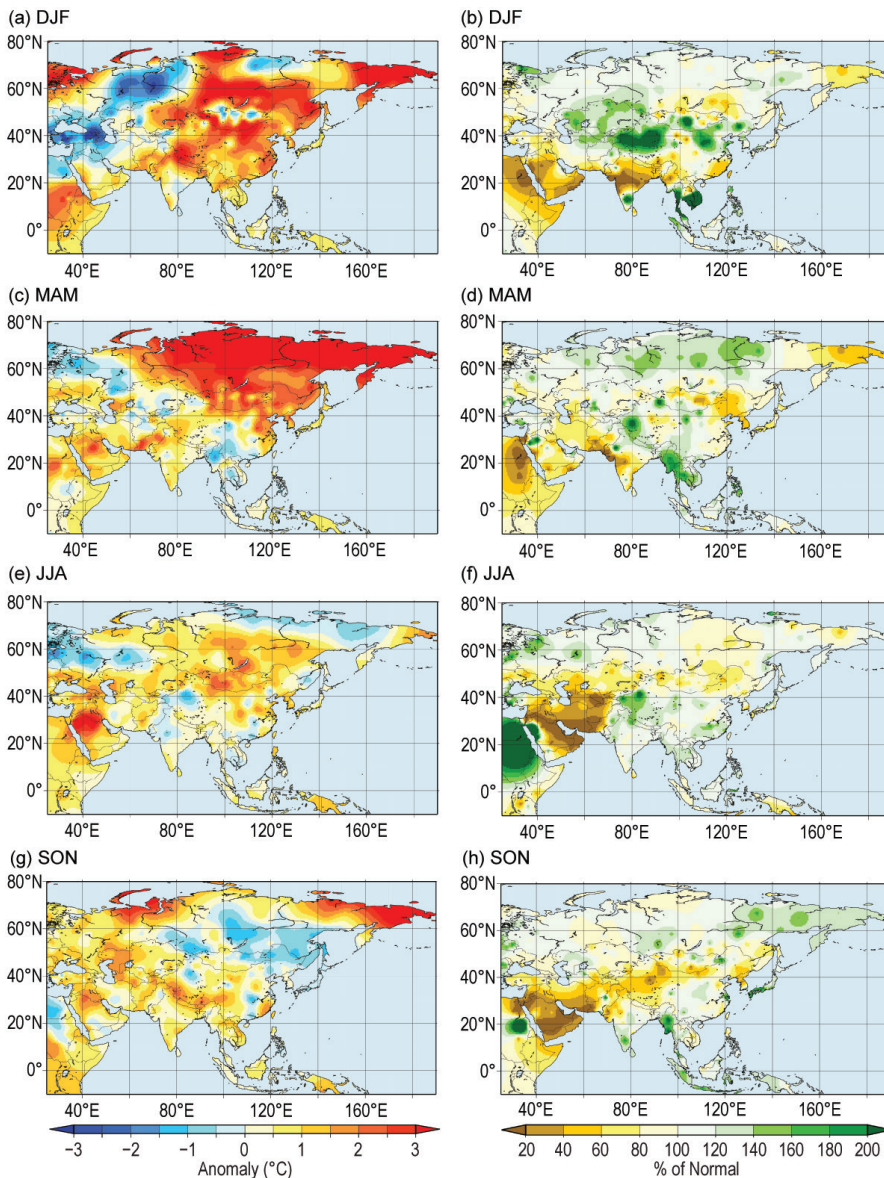


FIG. 7.40. Seasonal mean surface temperature anomalies ($^{\circ}\text{C}$, left column) and seasonal precipitation (% of normal, right column) over Asia in 2017 for (a), (b) winter; (c), (d) spring; (e), (f) summer; and (g), (h) autumn. All relative to 1981–2010. (Source: Japan Meteorological Agency)

perature averaged over this region was 2.27°C above normal, the highest such value on record.

For Russia as a whole, winter was moderately warm, with the mean winter temperature 2.05°C above normal (14th warmest on record).

Spring 2017 was warm, with an average seasonal mean air temperature anomaly of $+2.82^{\circ}\text{C}$; it was the fourth warmest spring since 1936. However, the temperature averaged over Asian Russia was record-breaking at 3.69°C above normal, while European Russia was only slightly warmer than normal ($+0.65^{\circ}\text{C}$ anomaly; the 27th warmest value of the record) with an unusually cold May, especially compared to recent

cal maximum daily temperature was recorded in Tiksi. European Russia was cooler than its Asian counterpart ($+4.14^{\circ}\text{C}$ anomaly; third highest), but extremes above the 95th percentile were observed at most stations in the central and northeastern parts of this region.

Summer 2017 was warm in Asian Russia, with a seasonal air temperature anomaly of $+1.37^{\circ}\text{C}$, the sixth highest since 1936. In European Russia summer was much colder (only $+0.46^{\circ}\text{C}$, rank 39th, which is close to the median value in the series) but not unusual, even against the background of the last two decades. June was the coldest summer month,

decades. March was exceptionally warm (see Fig. 7.44), ranked warmest on record, both for Asian Russia ($+6.79^{\circ}\text{C}$ anomaly) and the whole of Russia ($+6.03^{\circ}\text{C}$ anomaly). Monthly temperature extremes exceeding the 95th percentile were observed at virtually all stations in Asian Russia north of 60°N . North Atlantic cyclones brought warm, wet air in the northern regions as far east as Yakutia. Monthly March anomalies in Yamal-Nenets and Taymyrsky Dolgano-Nenetsky Autonomous Districts exceeded 13°C . At many stations monthly temperatures exceeded previous records. In Tiksi, Nar'jan-Mar, above-normal daily temperatures were observed almost throughout the entire month, with even minimum daily temperatures above the normal daily maximum (Fig. 7.44). On 21 March a daily minimum temperature above the climatological

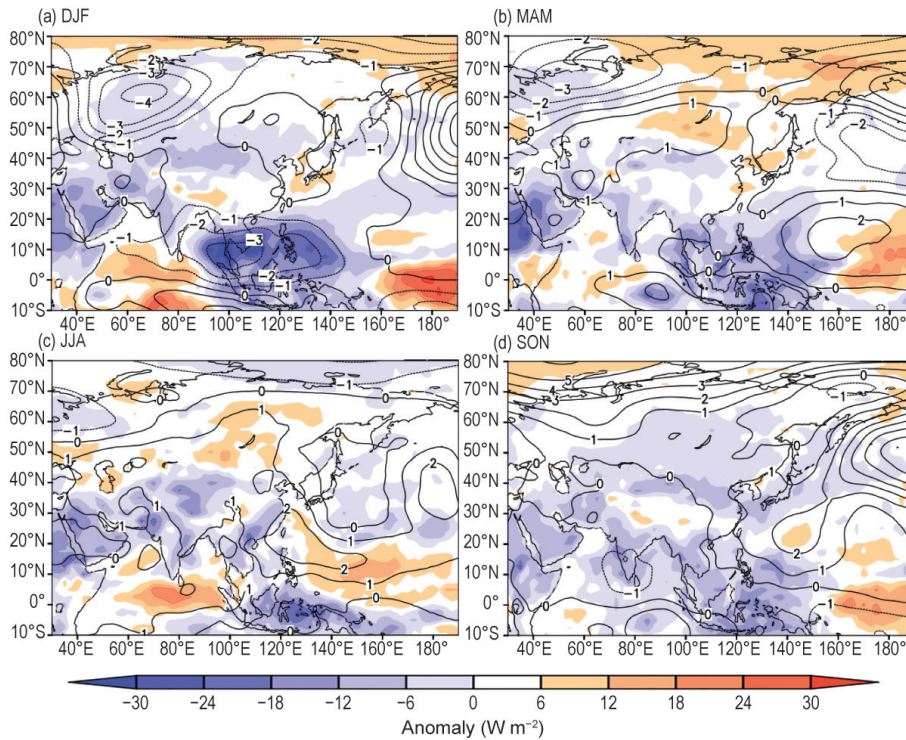


FIG. 7.41. Seasonal mean anomalies of 850-hPa stream function (contour, $1 \times 10^6 \text{ m}^2 \text{ s}^{-1}$) using data from the JRA-55 reanalysis and OLR (shading, W m^{-2}) using data originally provided by NOAA in 2017 for (a) winter, (b) spring, (c) summer, and (d) autumn. Base period: 1981–2010. (Source: Japan Meteorological Agency.)

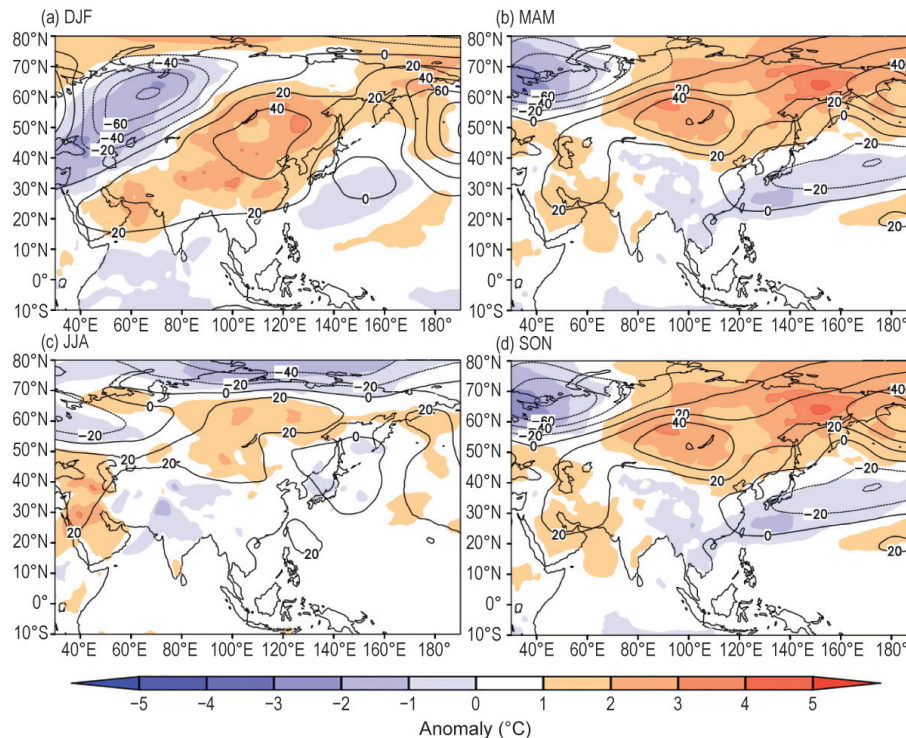


FIG. 7.42. Seasonal mean anomalies of 500-hPa geopotential height (contour, gpm) and 850-hPa temperature (shading, $^{\circ}\text{C}$) in 2017 for (a) winter, (b) spring, (c) summer, and (d) autumn, using data from the JRA-55 reanalysis. Base period: 1981–2010. (Source: Japan Meteorological Agency.)

especially in European Russia, where it ranked as the eighth coldest June on record, with an anomaly of -1.44°C . In contrast, August was exceptionally warm, with the second highest anomaly on record of $+1.61^{\circ}\text{C}$ over Asian Russia and the fourth highest ($+1.81^{\circ}\text{C}$) for Russia as a whole.

Autumn was temperate across Russia, with a seasonal anomaly of $+1.12^{\circ}\text{C}$. December 2017 was very warm in European Russia, with an anomaly of $+4.81^{\circ}\text{C}$ (third warmest). Combined with warmth in Asian Russia ($+2.35^{\circ}\text{C}$), Russia as a whole was 3.05°C warmer than average, the eighth warmest December on record. The location of the Siberian anticyclone remained stable throughout the month. This enabled advection of warm subtropical air along its western periphery and the formation of large positive temperature anomalies in European Russia and western Siberia. The largest anomalies ($> +10^{\circ}\text{C}$) were observed in the Yamal-Nenets Autonomous District. A large anomaly observed in the northern Yakutia and Chukotka persisted from November through the end of the year. At many stations monthly temperatures in December exceeded the 95th percentile. On 24, 25, and 27 December temperatures

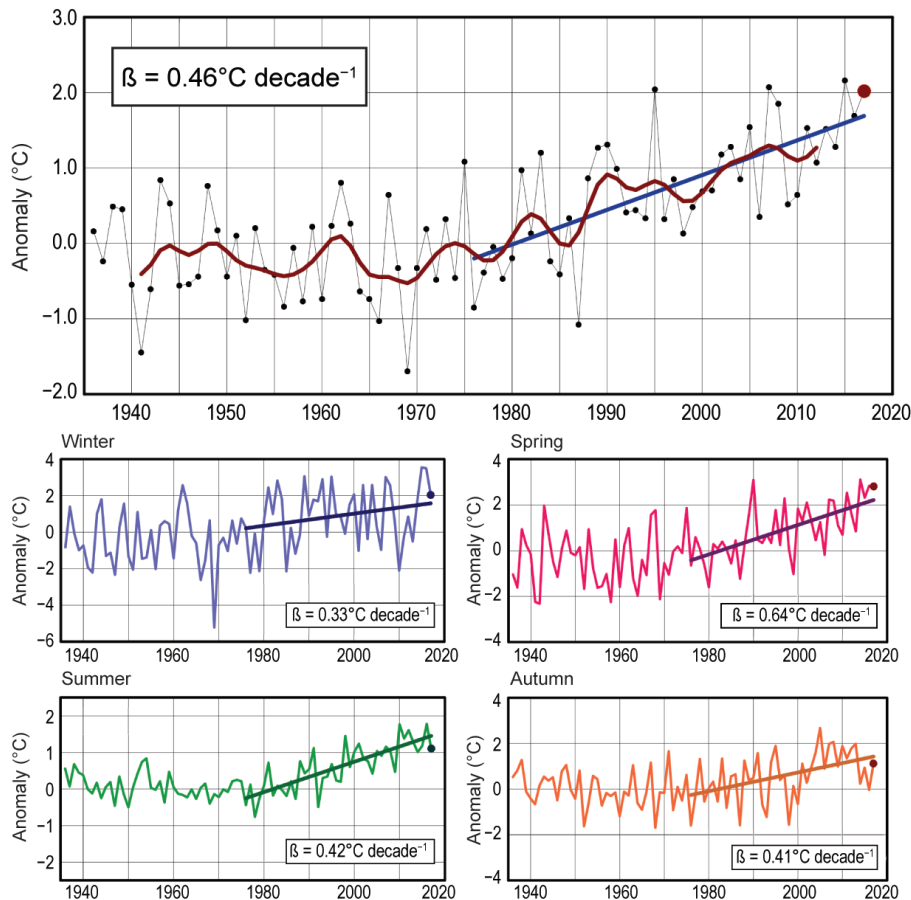


FIG. 7.43. Mean annual and seasonal temperature anomalies (°C; base period 1961–90) averaged over Russia, 1936–2017. The smoothed annual mean time series (11-point binomial filter) is shown as a red bold line. Linear trend β (°C decade⁻¹) is calculated for the period 1976–2017.

above the previous daily maximum were recorded at Mys Uelen, and the December mean temperature there exceeded -5°C for the first time on record.

(ii) Precipitation

In 2017, Russia as a whole received above-normal precipitation, 111% of its 1961–90 normal. This is the second wettest year on record, after 2013, which had 112% of normal precipitation (Fig. 7.45). European Russia was relatively wetter (115%, second wettest) than Asian Russia (109%, fifth wettest).

Winter precipitation was 110% of normal, which ranks 15th wettest. Spring in Russia had 119% of normal precipitation, which ranks fourth wettest. The wettest months of 2017 were April in European Russia (137% of normal) and May in the Asian part (125% of normal).

Although summer precipitation in Russia as a whole was near normal (107%), European Russia received much-above-normal precipitation in June and July (135% and 129% respectively, both ranked

second), while August was drier (87% of normal). Autumn precipitation for the whole of Russia was moderate (108%), with a dry October in the Asian part (87%).

Precipitation in December 2017 was much above normal with 124% of normal precipitation, the third wettest on record. This was especially so in European Russia (128%, tied for second wettest).

(iii) Notable events and impacts

On 8–9 March, an extremely severe snowstorm raged in the eastern Chukotka Autonomous Area, with wind gusts attaining 36 m s^{-1} and visibility as low as 0.5 m. Schools were closed; traffic and local flights stopped.

On 28 April, strong winds (25 m s^{-1}) in the Eravninsk region of Buryatia increased the number

of wild fires. These burned 21 buildings (including 17 homes). Property damage was estimated to exceed 7.5 million rubles (\$130 000 U.S. dollars).

On 3 May, severe forest fires were recorded in the Irkutsk Region and the Krasnoyarsk Territory resulting in the introduction of a federal emergency regime. In the Krasnoyarsk Territory alone, the fire destroyed about 130 houses, leaving more than 500 people homeless. In the Strelka settlement, where the Yenisei and Angara rivers merge, streets were burnt away. Two citizens of Kansk were killed.

On 29 May, a squall wind event in Moscow, with gusts as strong as 29 m s^{-1} , caused the largest number of victims on record for such an event: officially, 11 people were killed. According to the TASS Agency, referring to a source in emergency services, 105 people were admitted to hospitals. Within just a few minutes, the winds felled thousands of trees, damaged many cars and the roofs of 30 houses, and stopped the operation of above-ground subway and commuter trains.

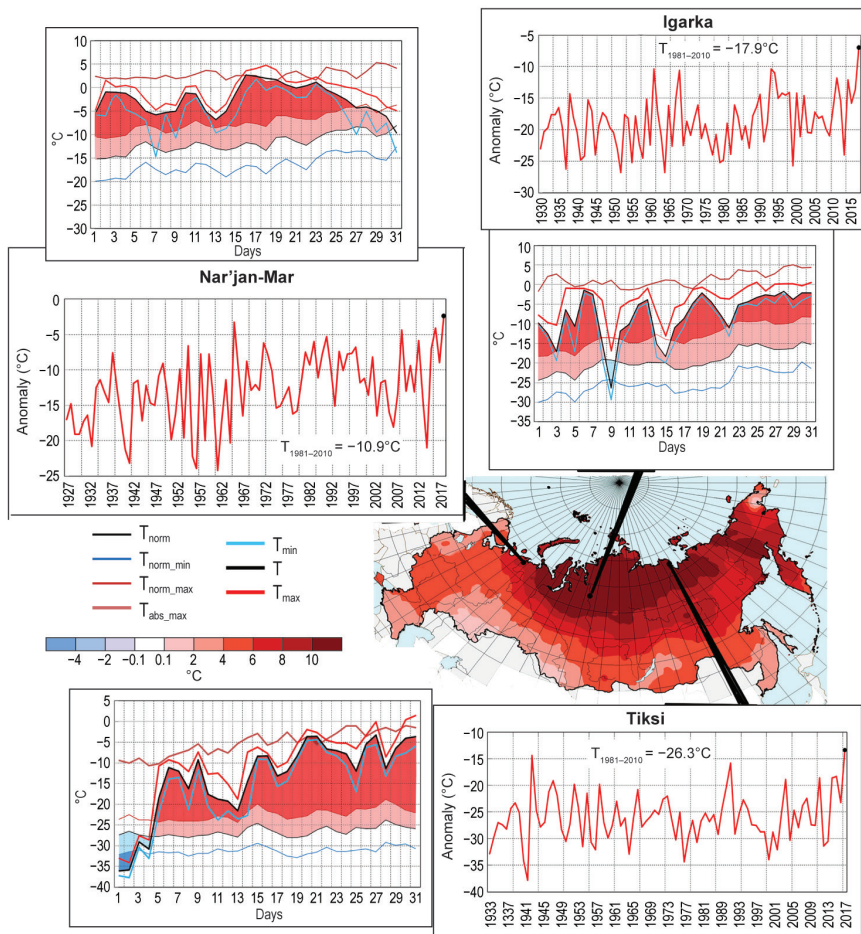


FIG. 7.44. Air temperature anomalies ($^{\circ}\text{C}$, shaded) in Mar 2017. Insets show the series of mean monthly (from the beginning of the record to 2017) and mean daily air temperatures ($^{\circ}\text{C}$) in Mar 2017 at meteorological stations Igarka, Tiksi, Nar'jan-Mar. Plots of daily temperature show observed daily mean (black curve), minimum (blue) and maximum (red) temperatures along with their climatological normals and absolute maximum temperature; the area between daily mean values above normal and the normal daily mean curve is shaded pink, and where values are above normal daily maximum the shading is red.

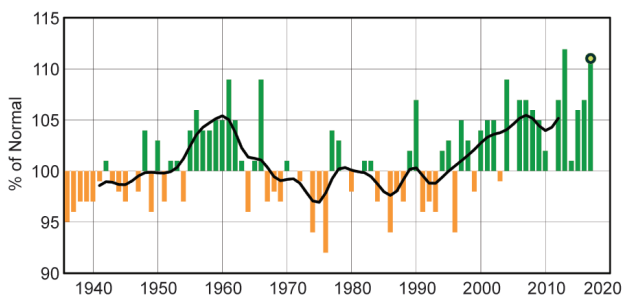


FIG. 7.45. Annual precipitation (% of normal; 1961–90 base period) averaged over Russia for 1936–2017. The smoothed time series (11-point binomial filter) is shown as a bold line.

On 30 June–1 July, a heavy thundershower (65 mm), accompanied by hail as large as 3–8 cm, and strong winds occurred in Moscow. Railroad beds in the Moscow Central Circle and motor roads were inundated, 1200 trees fell, and the roofs of nearly 100 houses and nearly 100 cars were damaged. Two people were killed.

Heavy rains (50–250 mm) in the southwestern Maritime Territory on 6–7 August caused flooding in Ussuriisk on 7–8 August. Parked cars were submerged, ground floors of houses were inundated, and bus services and commuter trains were canceled. On 20–21 August, heavy rain (113 mm) in Krasnoyarsk lasted for more than 24 hours, flooding 40 homes and 43 road sections. In addition, 67 power transforming substations were inundated and cut off from personnel.

On 1 September, in the upper reaches of the Adyl-Su River in the North Caucasus a dam failure occurred, resulting in a water discharge of 400 000 m³ that transformed into a mud flow downstream. A 325-mm gas pipeline was damaged, and a federal highway was blocked. Three people were killed.

3) EAST AND SOUTHEAST ASIA—P. Zhang, T. C. Lee, Y. Mochizuki, S.-E. Lee, L. Oyunjargal, and B. Timbal

Countries considered in this section include: China, Hong Kong (China), Japan, Korea, Mongolia, and Singapore. Unless otherwise noted, anomalies refer to a normal period of 1981–2010.

(i) Temperature

Annual mean temperatures across East and South-east Asia are visible in Fig. 7.38. The annual mean air temperature in 2017 for China was 0.84°C above normal (9.55°C)—the third warmest year since records began in 1951, behind 2015 and 2007. All seasons were warm throughout the year, especially winter, with the highest anomaly in the historical record of 2.0°C above normal. Hong Kong had an annual mean temperature of 23.9°C, 0.6°C above normal and the third highest since records began in 1884.

Annual mean temperatures were near normal in many regions of Japan and were significantly above normal in the Okinawa/Amami region. The 2017 annual average temperature over South Korea was 13.1°C, which is 0.6°C above normal, making 2017 the seventh warmest year since national records began in 1973. The annual mean temperature over Mongolia for 2017 was 1.9°C, 1.4°C above normal, which is the second highest annual value since 1961. The highest anomaly for Mongolia was April, with a mean temperature anomaly of 2.9°C above normal, representing the third warmest April since 1961. The lowest anomaly for Mongolia occurred in October when the mean temperature anomaly was 1.1°C, −0.3°C below normal.

In South Korea, May temperatures have significantly increased since the start of the record in 1973. The temperature averaged over South Korea in May 2017 was 18.7°C, 1.5°C above normal. This marks the fourth consecutive year of a new record high May temperature.

After two successive record warm years in 2015 and 2016, the mean annual temperature of Singapore (27.7°C) returned closer to the long-term climatological average. This was 0.2°C warmer than normal and tied as the 12th warmest year on record since 1929; however, it is Singapore's warmest year on record not influenced by an El Niño event.

(ii) Precipitation

Figure 7.39 shows 2017 annual precipitation as a percentage of normal over East Asia. The annual mean precipitation in China was 641.3 mm, 101.8% of normal. Seasonal precipitation was 93% of normal in winter and 108% of normal in summer. Spring and autumn were near normal. Regionally, annual total precipitation was above normal in northwest China (115% of normal), South China (105%), the middle and lower reaches of the Yangtze River (104%), north China (104%), and near normal in southwest China, but below normal in northeast China (90%). The annual total precipitation over river basins was

above normal in the Yellow River (111%), the Yangtze River (105%), the Pearl River (105%), and the Huaihe River (104%) but below normal in the Liaohe (84%), Songhua River (95%), and Haihe River basins (98%). The annual total rainfall in Hong Kong was 2572.1 mm (107% of normal).

In Japan, annual precipitation amounts were above normal on the Sea of Japan side of northern and eastern Japan, and on the Pacific side of western Japan, and they were below normal in Japan's Okinawa/Amami region. Annual total precipitation over South Korea was 967.7 mm, 74% of normal (1307.7 mm), and the fifth lowest total since 1973. Annual precipitation over Mongolia was 173.4 mm, 86.3% of normal. Although annual total precipitation was near normal, the majority of the growing season, especially May, June, and July, were dry (57.1%–66.1%), causing drought conditions over 75% of the whole territory. Relative to normal, March was the wettest month (225%) while July was the driest (57.1%). January precipitation was near normal, with snow cover extent covering more than 70% of the total area. At the end of the year, snow covered almost 50% of the area and snow depth was 6–45 cm which caused difficulties for livestock pasturing.

In Singapore, there was a mixture of above- and below-normal rainfall for the individual months in 2017. Overall, the annual total rainfall was approximately 94% of the normal of 2165.9 mm.

In 2017, the overall activity of the East Asian summer monsoon was near normal with some area to area differences in the region. Intraseasonal variability of the East Asian summer monsoon was clearly seen during the season. For example, convective activity over and around the Philippines was enhanced from late June to mid-July and was suppressed from late July to mid-August.

(iii) Notable events and impacts

Eight typhoons landed in China, the same number as 2016, and near the average of 7.2. However, the impact period was longer than normal, with the first typhoon, Merbok, landing in Shenzhen, Guangdong, on 12 June, 13 days earlier than normal, and the last typhoon, Khanun, landing in Zhanjiang, Guangdong, on 16 October, 10 days later than normal. Typhoon impacts varied strongly by time and region. For instance, Typhoons Nesat and Haitang landed successively on the coast of Fuqing city in Fujian Province during 30–31 July, and four typhoons hit the Grand Bay Area of Guangdong–Hong Kong–Macao in June, July, August, and October. As Tropical Cyclone Hato headed toward Hong Kong, the subsidence effect

ahead of its circulation brought oppressive heat to the territory on 22 August as the temperature at the Hong Kong Observatory soared to an all-time high of 36.6°C. Stormy weather with hurricane-force winds battered the city during the passage of Hato on the following morning. With Hato's approach coinciding with the astronomical high tide, its storm surge resulted in serious sea water flooding and damage in many low-lying areas in Hong Kong.

In 2017, meteorological disasters caused by rainstorms and floods in China were prominent and brought major losses, especially in southern China. Rainstorms occurred often and frequently in succession. Eleven days of persistent heavy rainfall occurred over southern China from 22 June to 2 July, associated with a rain belt across the provinces of Hunan, Jiangxi, Guizhou, and Guangxi, where local accumulations exceeded 500 mm. During summer, the high temperature events hit China earlier in northern areas but were more intense in southern areas, which resulted in a record number of days with high temperatures (daily maximum temperature $\geq 35^\circ\text{C}$) since the beginning of the record in 1961. On 21 July, the maximum temperature at Xujiahui, in central Shanghai, was 40.9°C, setting a record for its 145-year period of observation (since 1873). In the west during mid-July, 53 high temperatures were recorded, which tied or broke records in counties (or cities) in Xinjiang, Gansu, Inner Mongolia, Shaanxi (44.7°C in Xunyang), Ningxia, and Shanxi.

South Korea experienced above-normal temperatures and slightly below-normal rainfall during summer. The summer mean temperature over South Korea was 24.5°C, which was +0.9°C above normal. In particular, extreme temperatures were observed from late-June through late-July. During this period, South Korea was strongly influenced by the western North Pacific subtropical high that extended more to the northwest compared to its normal position brought hot, moist air by the southwesterlies along its flank. The summer rainfall (609.7 mm) over South Korea was 84% of normal (723.2 mm). The ratios of monthly rainfall amount to the normal value in June, July, and August were 38%, 103%, and 88%, respectively. The 2017 Changma (early summer rainy period) started on 24 June and ended on 29 July. The Changma rainfall total was below normal (291.7 mm; normal: 356.1mm). The 2017 Changma was notable for the following: 1) onset and retreat were later than normal; 2) heavy rainfall events were concentrated on the central part of the Korean Peninsula; and 3) large spatial differences of rainfall between the southern and central regions of South Korea were observed.

In northern Japan, on 5–6 July, record-breaking heavy rain associated with the active Baiu front fell in Kyushu region, with 129.5 mm h⁻¹ and 545.5 mm (24-h)⁻¹ observed at Asakura in Fukuoka prefecture. The heavy rain caused serious damage, including landslides and river overflows. In Okinawa/Amami, monthly mean temperatures were record high in August (+1.4°C above normal) and record-tying (since 1946) high in September (+1.3°C above normal) due to a stronger-than-normal subtropical high over south of Japan. In western Japan, the monthly precipitation total was record high, at 333% of normal for October.

In Mongolia, a total of 76 extreme weather events were observed, including episodes of heavy snow and flash flooding. Together, these events caused about \$1.9 million (U.S. dollars) in economic loss.

4) SOUTH ASIA—A. K. Srivastava, J. V. Revadekar, and M. Rajeevan

Countries in this section include: Bangladesh, India, Pakistan, and Sri Lanka. Climate anomalies are relative to the 1981–2010 normal.

(i) Temperature

In general, South Asia witnessed significantly above-normal temperatures in 2017. The annual mean land surface air temperature averaged over India was 0.50°C above the 1981–2010 average, ranking 2017 as the fourth warmest year on record since nationwide records commenced in 1901 (Fig. 7.46). India's seasonal mean temperatures were above normal for all four seasons. The country-averaged seasonal mean temperatures during the post monsoon season (October–December, with an anomaly of +0.67°C, the third highest since 1901) and the winter season (Janu-

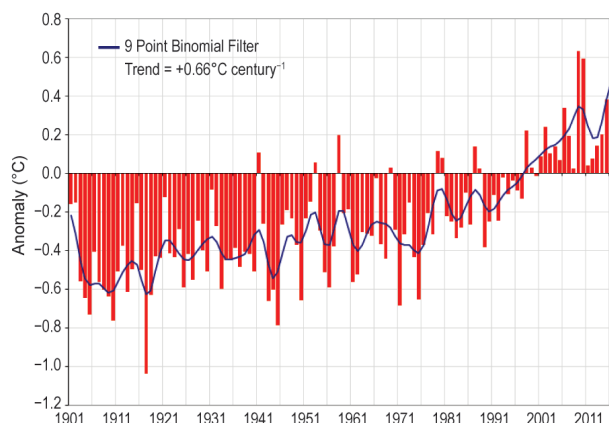


FIG. 7.46. Annual mean temperature anomalies (°C; 1981–2010 base period) averaged over India for 1901–2017. The smoothed time series (9-point binomial filter) is shown as a continuous blue line.

ary–February, anomaly $+0.61^{\circ}\text{C}$, fourth highest ever since 1901) mainly accounted for the above-normal temperature for the year.

(ii) Precipitation

The summer monsoon season (June–September) typically contributes about 75% of annual precipitation over South Asia. The summer monsoon set in over Kerala (southern parts of peninsular India) on 30 May, 2 days prior to its climatological normal date (1 June) and covered the entire country on 19 July (4 days later than its normal date, 15 July).

For India, the long-term average (LTA) value of the summer monsoon rainfall, calculated using all data from 1951 to 2000, is 890 mm. The standard deviation of Indian summer monsoon rainfall (ISMR) is around 10% of the LTA value. However, over smaller regions natural variability of the monsoon is large (standard deviation around 19%). In view of the above, an ISMR exceeding 110% of the LTA in a year is termed as excess rainfall, while an ISMR that is less than 90% of the LTA in a year is termed as deficient rainfall.

During 2017, the ISMR averaged over the country as a whole was 95% of its LTA and was characterized by significant spatial and temporal variability (Fig. 7.47). The homogeneous region of South Peninsula received

normal rainfall (100% of LTA). The homogeneous regions of central India and east-northeast India received 94% and 96% of LTA of the seasonal rainfall, respectively. Northwest India received below-normal rainfall (90% of monsoon season LTA). On monthly scales, rainfall for the country as a whole was normal during June (104% of its LTA value) and July (102%). It was below normal during August (87%) and September (88%). During the monsoon season, out of 36 meteorological subdivisions, five subdivisions (West Rajasthan; Saurashtra & Kutch; Nagaland, Manipur, Mizoram & Tripura; Rayalaseema; and Tamil Nadu & Pondicherry) received excess rainfall, 25 received normal rainfall, and the remaining six subdivisions (four subdivisions from the northwest region and two subdivisions from central India) received deficient rainfall. Figure 7.48 shows the standardized rainfall anomaly over the core monsoon region on a daily scale during the season. There was significant intraseasonal rainfall variability with marked active and break spells.

During the winter season (January–February), season, rainfall over the country was normal (95% of LTA); it was normal (98% of LTA) during the pre-monsoon season (March–May), while it was below normal during the post-monsoon season (October–

December, 89% of LTA). The northeast monsoon (NEM) normally sets in over southern peninsular India during October and over Sri Lanka in late November. The NEM contributes 30% to 50% of the annual rainfall over southern peninsular India and Sri Lanka as a whole. The 2017 NEM set in over southern peninsular India on 27 October, and the seasonal rainfall over south peninsular India was below normal (86% of LTA value). Moderate La Niña conditions prevailed during the season, which could be one of the reasons for the below-normal performance of the NEM.

Pakistan, at the western edge of the pluvial region of the south Asian monsoon, receives 60%–70%

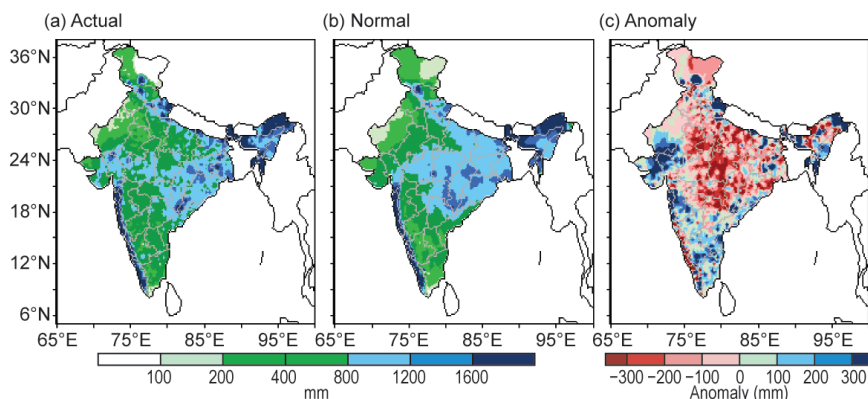


FIG. 7.47. Spatial distribution of monsoon seasonal (Jun–Sep) rainfall over India in 2017. (a) Actual, (b) normal, and (c) anomalies are in mm.

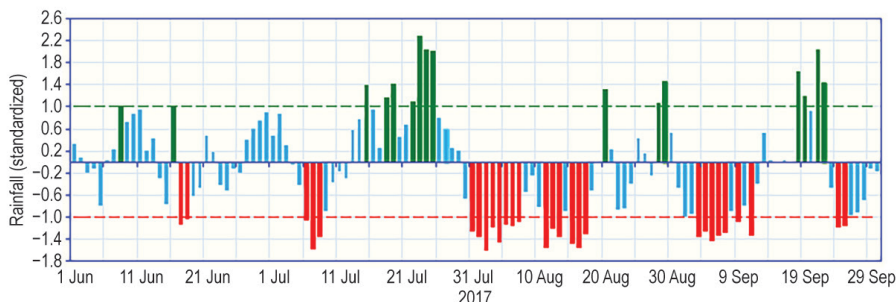


FIG. 7.48. Daily standardized rainfall time series averaged over the core monsoon zone of India (1 Jun–30 Sep 2017).

of its annual rainfall during the summer monsoon season (July–September). The summer monsoon sets in over northeastern parts of Pakistan around 1 July with a standard deviation of five days. In 2017, summer monsoon rainfall over Pakistan was below normal (77.5% of its LTA value). Pakistan observed below-normal rains during all three months from July to September (79.6%, 74.3%, and 82.7% of its LTA values). Rainfall was below normal in all the provinces of Pakistan. Southern parts of Pakistan (especially the southwest) received largely deficient rainfall. Other areas, including central Pakistan, received normal rainfall during the monsoon season. Bangladesh received normal rainfall during the 2017 summer monsoon season.

Sri Lanka received normal rainfall during its summer monsoon season (May–September). Northeast monsoon rainfall activity over the island nation, during October–December 2017, was also normal.

(iii) Notable events and impacts

During 2017, three cyclonic storms (one each in April, May, and November) formed over the north Indian Ocean. The first storm, Maarutha, formed over the east central Bay of Bengal on 15 April. However, it moved northeastward away from the Indian region and crossed the Myanmar coast on 16 April. Though

the system did not cause significant weather over the mainland of India, it caused light to moderate rain over the Andaman and Nicobar islands during its formative stage.

The second severe storm, Mora, formed over the Bay of Bengal during 28–31 May. It made landfall over the Bangladesh coast on 30 May and dissipated over the northeastern parts of the country on 31 May. This system caused moderate to heavy rain over many parts of the northeastern region of India after making landfall.

The last severe storm, Ockhi, (29 November–5 December) formed over south Bay of Bengal and moved to the Arabian Sea. The storm, while moving across southern parts of India, caused severe damages in Kerala, Tamil Nadu, and Lakshadweep. The storm also claimed the lives of many fishermen (18 from Tamil Nadu and 74 from Kerala). Ockhi ultimately recurved and moved towards the south Gujarat coast.

Heavy rain and flood-related incidents during the monsoon season claimed around 800 lives from different parts of India (see Table 7.2 for 24-hr rainfall records over India). Around 150 people reportedly died in the state of Assam from 13 June to 11 September in two spells of floods. More than a hundred people were reported dead in Uttar Pradesh due to heavy rain and floods of the Ghaghara, Gomati, and Rapti

TABLE 7.2. Record rainfall (24hr) during the 2017 monsoon season in India.

S. No.	Station	Rainfall During Past 24 Hrs. (mm)	Date	Previous record (mm)	Date of record	Year of record
			Jun 2017			
1	Karnal	140.4	28	80	30	1994
2	Baderwah	56	30	55.8	2	2004
3	Katra	147.9	30	90.2	30	2000
			Jul 2017			
1	Ranchi AP	205.8	26	178.8	23	1958
2	Bhagalpur	173.6	2	154.6	27	2009
3	Raisen	208.9	28	188.4	22	1973
4	Jagdapur	191.4	19	180.8	7	1934
			Aug 2017			
1	Jalpaiguri	295.2	12	264.2	10	1987
2	Osmanabad	151.0	20	149.8	22	2010
3	Adirampattinam	128.4	9	97.9	29	2007
4	Thanjavur	110	10	105	30	2016
5	Thanjavur	105	30	99.0	7	1982
			Sep 2017			
1	Harnai	373.6	19	308.6	23	1949
2	Pamban	113.5	9	108.5	27	1901
3	Tuticorin	63	1	58.3	6	1979
4	Uthagamandalam	81.6	3	65.3	29	1951
5	Mysore	137	27	129.3	11	1940

Rivers during 4–10 September. About 120 deaths were reported from the western industrial state Gujarat during the month of July and 107 from Bihar during 13–23 August. On 13 August, 46 deaths were reported due to massive landslides at Kotrupi on the Mandi-Pathankot National Highway near Jogindernagar in Himachal Pradesh (India). Similarly, 15 people died in Papum Pare, Arunachal Pradesh on 11 July due to a landslide.

Heat wave conditions prevailed mainly over peninsular parts of India during the second fortnight of May, which claimed the lives of about 100 people in the state of Telangana. However, the loss of lives in 2017 was much less than in the previous years due to timely heat wave warnings and heat wave action plans initiated by government. In April 2017, Larkana, a city in the southern province of Sindh of Pakistan, experienced a record maximum temperature of 51.0°C on 20 April. On 28 May, Turbat, in western Pakistan, recorded a temperature of 53.5°C, tying the all-time highest temperature recorded in Moen Jo Daro, Pakistan, on 26 May 2010.

In August, Bangladesh suffered one of its worst floods in the past four decades, which affected approximately one-third of the country, primarily in the northern, northeastern, and central regions. Rangpur district in the northeast experienced a month's worth of rain—360 mm—in just two days (11–12 August). Around 140 deaths from the floods were reported, over fifty thousand people were displaced, and approximately six million were affected.

Fifteen districts of Sri Lanka were affected by severe floods during the last ten days of May. Parts of Sri Lanka received 300–500 mm of heavy monsoon rain in a 24-hour period around 25 May, resulting in widespread flooding. The highest recorded rainfall was 533 mm in Kukuleganga. Galle, a coastal city, received 223 mm and Ratnapura experienced 453 mm of rainfall during 27–30 May, leading to severe inland flooding. Around 150 people were killed and around 450 000 were affected.

5) SOUTHWEST ASIA—M. Khoshkam and A. Kazemi

This subsection covers only Iran. Turkey is incorporated in the Europe subsection, 7f. Climate anomalies are relative to a 1996–2015 base period.

(i) Temperature

In general, the year was warmer than average for Iran. The mean annual air temperature was 0.5°–1.5°C above the 20-year average. Spring and autumn temperatures were above average for the entire country, while the winter and summer seasons

experienced regional patterns of above- and below-average temperatures. There is a sharp contrast between the pattern of temperature anomalies in winter and summer. Northwestern Iran experienced a colder-than-average winter season but a warmer-than-average summer season.

(ii) Precipitation

In 2017, Iran was drier than normal for the year as a whole, receiving 205 mm precipitation, with totals of 117.4, 53.1, 6.2, and 28.4 mm for winter, spring, summer, and autumn, respectively. The country experienced drier-than-normal conditions in spring, summer, and autumn. The only relatively wet season was winter; however, several provinces, especially in southwestern, northwestern, and parts of central Iran, observed precipitation deficits of up to 50% of normal during winter. The winter seasonal rainfall largely occurred during the second half of the season. MODIS snow data indicate that snow coverage over the country was greatest in February and declined in March. Snow coverage was observed in December 2017, the first month of winter 2017/18.

According to spatial analysis of the standardized precipitation index (SPI), areas with mild to severe drought conditions were encountered especially in the northwest, west, and southwest in winter, the northwest, east, and northeast in the spring, and the northwest and northern parts in the summer. The SPI is a tool that was developed primarily for defining and monitoring drought. Mathematically, it is based on the cumulative probability of a given rainfall event occurring at a station. According to this indicator, most regions of the country were in mild to very severe drought during autumn. The central and eastern areas were in extreme drought conditions during autumn.

(iii) Notable events and impacts

A maximum temperature of 53.7°C was observed in Ahvaz in summer. In spring, an extreme warm temperature of 51.7°C was recorded in Sistan and Balochestan. While the entire country experienced dry conditions during 2017, an extreme rainfall event, with 264 mm in 24 hours, was observed in summer at Station Lahijan. Table 7.3 lists measured extreme events in each season over Iran. The frequency and duration of dust storms in 2017 became higher in some parts of the country, especially in the southwest and southeast during winter and spring.

TABLE 7.3. Measured values of 2017 record temperatures and 24-hr precipitation in Iran. Location includes station (province).

Season	Minimum temperature (°C)	Maximum temperature (°C)	Maximum 24-hr precipitation (mm)
Winter	-30 Hezar Kanian (Kordestan)	37 Rask (Sistan and Balochestan)	164.6 Jem (Bushehr)
Spring	-8.6 Zarineh Obatoo (Kordestan)	51.7 Rask (Sistan and Balochestan)	99.7 Ghir Kazeroun (Fars)
Summer	0.8 Ardebil (Ardebil)	53.7 Ahvaz (Khozestan)	264 Lahijan (Gilan)
Autumn	45.2 Abadan (Khozestan)	-20.2 Khayerabad (Zanjan)	200.1 Ramsar (Gilan)

SIDEBAR 7.3: ABNORMAL WEST CHINA AUTUMN RAINFALL IN 2017 AND PERSISTENCE OF THE PACIFIC–JAPAN PATTERN IN AUGUST 2017—Z. ZHU, T. LI, AND H. TOGAWA

Climatologically, a precipitation peak over West China (27°–35°N, 105°–114°E) during September and October is referred to as West China Autumn Rainfall (WCAR). It is the final stage of the rainy season in mainland China. WCAR can have severe impacts on agricultural production—including the harvesting and sowing of winter crops—and reservoir levels. Due to the fragile ecological environment of West China, above-normal WCAR often results in landslides and debris flows, which threaten lives and economic development in the region.

WCAR in 2017 was 170% of normal (Fig. SB7.4a), the second highest total since records began in 1979 (Fig. SB7.4b). The event greatly affected 6 million people over seven Chinese provinces. Over 480 000 hectares of crops were damaged, and the total economic loss was over \$20 billion (U.S. dollars).

In the lower troposphere during September and October 2017, an anticyclonic anomaly at 850 hPa covered a large domain of southern China, with southwesterly anomalies at its western flank. Another anticyclonic anomaly (high pressure system) existed to the north of the anticyclonic anomaly. These two south–north anticyclonic anomalies led to a horizontal trough over West China. The southwesterly anomalies in the southern portions of the trough transported

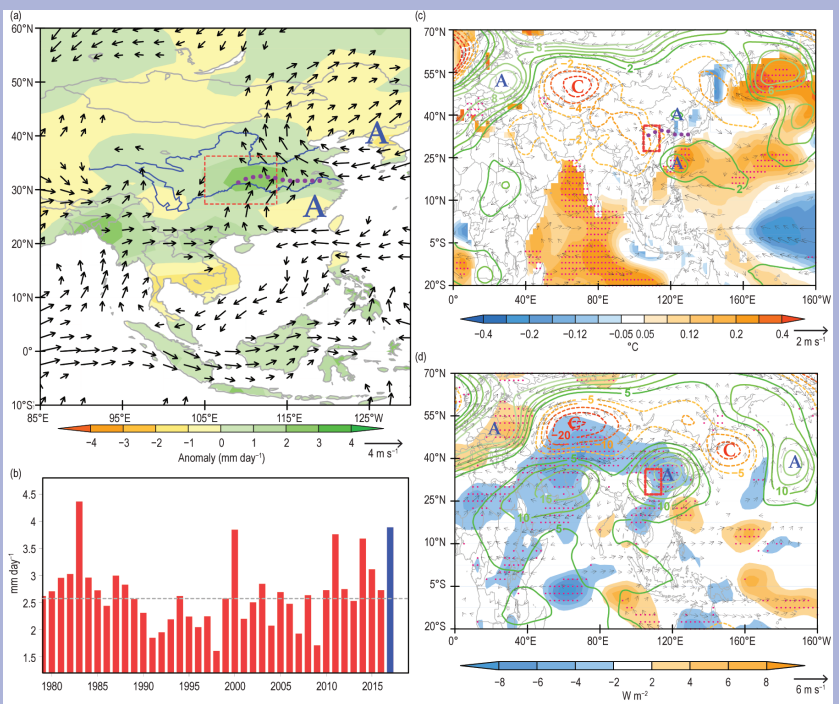


FIG. SB7.4. (a) Precipitation (shading; mm day^{-1}) and 850-hPa wind (vector; m s^{-1}) anomalies in Sep and Oct 2017. Only winds with speeds $>1 \text{ m s}^{-1}$ are shown. (b) Year-to-year time series of the WCAR (red bars; mm day^{-1}). 2017 is blue bar. Gray dashed line is the 1981–2010 climatological mean. (c) Wind (vectors; m s^{-1}), geopotential height (contours; gpm) at 850-hPa, and SST ($^{\circ}\text{C}$) fields regressed onto the WCAR index. (d) as in (c) but for 200-hPa wind, geopotential height, and OLR (W m^{-2}) fields. Only winds significant at the 95% confidence level are shown, and the SST and OLR significant at 95% confidence level are marked by red dots. “A” and “C” denotes the anticyclonic (cyclonic) anomaly. Red box indicates the key region of WCAR, dashed purple line marks the horizontal trough.

into West China while the horizontal trough kept the moisture stationary in the region, resulting in enhanced WCAR.

into West China while the horizontal trough kept the moisture stationary in the region, resulting in enhanced WCAR.

CONT. SIDEBAR 7.3: ABNORMAL WEST CHINA AUTUMN RAINFALL IN 2017 AND PERSISTENCE OF THE PACIFIC–JAPAN PATTERN IN AUGUST 2017—Z. ZHU, T. LI, AND H. TOGAWA

The unusualness of the rainy season was the result of the combination of various atmospheric patterns. Typically, the enhanced WCAR is associated with positive tropical Indian Ocean SST anomalies (Fig. SB7.4c). Positive tropical Indian Ocean SST anomalies could induce a Kelvin wave response in terms of easterly anomalies in the lower troposphere. The Kelvin wave easterlies generated anticyclonic shear and resulted in anticyclonic anomalies over the western North Pacific, leading to anomalous moisture transport as seen in the 2017 event. Divergence at 200 hPa (Fig. SB7.4d) was predominant over West China and appeared to be part of the circumglobal wave train over midlatitudes. Divergence aloft and convergence (associated with the horizontal trough) at lower levels over the region provided a favorable dynamical condition to the enhanced rainfall in the region.

From early to mid-August, convective activity was particularly inactive over and around the Philippines. During the same period, the North Pacific subtropical high (NPSH) did not extend to mainland Japan as usual but shifted southward from its normal position, corresponding to the Pacific–Japan (PJ) pattern (Nitta 1987; Kosaka and Nakamura 2010; Fig. SB7.5a), with suppressed convective activity over and around the Philippines. Furthermore, the Tibetan high in the upper troposphere extended southward to cover Okinawa/Amami. Meanwhile, the Okhotsk high, which brought cool wet northeasterly flows to the Pacific side of northern and eastern Japan, had persisted since late July. The persistence of the Okhotsk high was presumed to be mainly due to blocking-high development over the Sea of Okhotsk, in association with the meandering westerly jet stream over northern Eurasia (Fig. SB7.5b).

Corresponding to the PJ pattern with suppressed convective activity over and around the Philippines, this anomalous atmospheric circulation in the lower troposphere brought longer-than-normal sunshine durations, adiabatic heating associated with stronger-than-normal subsidence, and westerly warm air inflow over Okinawa/Amami. These factors contributed to significantly warm conditions over Okinawa/Amami, and monthly mean temperature over Okinawa/Amami in August 2017 was the highest on record for August since 1946. A southward extension of the Tibetan high presumably contributed to the warm condition over the area. At the same time, the low-level anticyclonic circulation anomalies brought considerable moisture to the middle and lower Yangtze River basin where above-normal precipitation was observed. Meanwhile, due to both the Okhotsk high and the PJ pattern, the Pacific side of northern and eastern Japan experienced significantly below-normal sunshine duration.

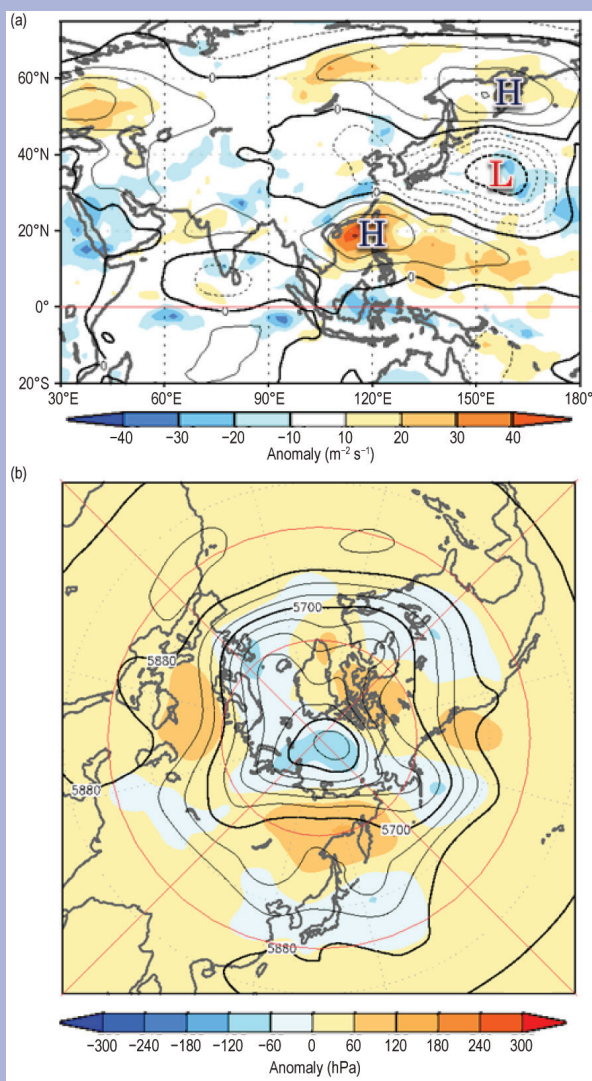


FIG. SB7.5. (a) Stream function anomalies at 850-hPa (contours) and OLR anomalies ($\text{m}^2 \text{s}^{-1}$; color shadings) averaged over 1–20 Aug 2017. Thick and thin contours are intervals of 10×10^6 and $2.5 \times 10^6 \text{ m}^2 \text{s}^{-1}$, respectively. For the NH, solid and dashed lines indicate anticyclonic and cyclonic circulation anomalies, respectively. For the SH, vice versa. (b) 500-hPa height anomaly in the NH averaged over 1–20 Aug 2017. Contours show 500-hPa height at intervals of 60 m. Shading indicates anomalies. Base period is 1981–2010.

The condition of enhanced NPSH over the south of Japan persisted from August to October. It is considered to have been caused by active convection over the Maritime Continent due to positive SST anomalies in the western tropical Pacific, which were related to the development of weak La Niña conditions in the eastern equatorial Pacific (see Fig. 3.2).

h. Oceania

1) OVERVIEW—C. Ganter

The climate of Oceania experienced a neutral ENSO state for most of 2017, which then transitioned to weak La Niña conditions late in the year. The Indian Ocean dipole (IOD) was neutral during its typical active period (May–November), while several countries were influenced by a positive southern annular mode during the austral winter. Persistent strong stationary high pressure systems in the Tasman Sea during November and December contributed to warmer weather across southeast Australia and New Zealand, and they also warmed surface waters of the Tasman Sea, causing a notable marine heatwave which persisted into 2018 (see Sidebar 7.4).

2) NORTHWEST PACIFIC AND MICRONESIA—M. A. Lander and C. P. Guard

This assessment covers the area from the international dateline west to 130°E, between the equator and 20°N. It includes the U.S.-affiliated Islands of Micronesia but excludes the western islands of Kiribati and nearby northeastern islands of Indonesia. Temperature and precipitation anomalies in this section are relative to a 1981–2010 period.

Weather conditions across Micronesia during 2017 were mostly unremarkable. Annual rainfall was near to above average at most locations, and tropical cyclone activity was much lower than average. The western North Pacific summer monsoon system was displaced to the west and north of Micronesia, accompanying a similar westward and northward displacement of the basin's tropical cyclones. These patterns of rainfall, wind, and typhoon distribution were typical for an ongoing La Niña. The regional oceanic response to La Niña climate conditions (e.g., increased trade wind strength) was sustained higher-than-average mean sea level.

(i) Temperature

Temperatures across Micronesia in 2017 were mostly above average. The warmth was persistent, with above-average readings occurring during most or all the months of the year. Only Yap Island and Pohnpei Island reported moderate negative temperature departures for any of the time periods summarized in Table 7.4. Saipan reported extraordinary warmth with daytime highs 3.42°C above average during the second half of the year. The reason for Saipan's excessive warmth (with many records set for highest daily maximum and highest minimum temperatures) is uncertain. The 6-month minimum

and maximum temperatures for selected locations across Micronesia are summarized in Table 7.4.

(ii) Precipitation

Annual rainfall totals during 2017 were mostly higher than average throughout Micronesia, with below-average seasonal and annual rainfall amounts restricted to the northern Mariana Islands (Rota, Tinian, and Saipan), a few of the northern atolls of Chuuk State, and the northern atolls of the Republic of the Marshall Islands (RMI). The 6-month and annual rainfall values for selected locations across Micronesia are summarized in Table 7.4.

(iii) Notable events and impacts

Late in December 2016, and again in October 2017, a landfalling waterspout caused damage on an atoll of Micronesia. In the former case, a large and intense waterspout swept across Falalop (one of the islets of the Ulithi Atoll). Eyewitnesses described a surge of high wind that blasted across the islet, filling the air with lofted debris that appeared to be rotating.

The Ulithi waterspout/tornado occurred in association with deep convection in a near-core rainband of Tropical Storm Nock-ten. As reported in the 23 January 2017 issue of the *Khaselehli Press*:

“On December 22, 2016, a water spout turned tornado ripped through the island, tearing apart over 20 newly repaired homes and cook houses along its path. “It sounded like a jet was flying low over the island. Luckily, we had been warned that Typhoon Nock-ten could be headed in our direction so we were prepared for a potential disaster. If we hadn't received warning about Nock-ten, this tornado would have claimed lives on Falalop,” said local resident Jon Rumal Jr.” ...

It was not officially verified that this event was a tornado, but eyewitness accounts are convincing.

The next incident of a landfalling waterspout occurred on 14 October when waterspouts were observed at Nomwin Atoll in the Hall Islands of Chuuk State. One of the waterspouts went ashore on Nomwin where “it was strong enough to topple banana trees, and weak infrastructure houses were down and damaged” as reported to the Chuuk Weather Service Office. A boat was found capsized in Nomwin waters on 15 October. It is thought by islanders that the boat was capsized by a waterspout. The Nomwin incident of waterspout formation occurred in association with a large area of heavy convective showers comprising the monsoon

TABLE 7.4. Temperature (°C) and rainfall (mm) anomalies for selected Micronesia locations during 2017. Average (AVG) values are for the 1981–2010 base period. Latitudes and longitudes are approximate. “Kapinga” stands for Kapingamarangi Atoll in Pohnpei State, Federated States of Micronesia. Shading of the boxes indicates: red for above-average temperature and blue for below average; green for above-average rainfall and yellow for below average.

Location	Max Temp Min Temp		Rainfall (mm)							
	Jan–Jun	Jul–Dec	Jan–Jun	Jan–Jun	Jan–Jun	Jul–Dec	Jul–Dec	Jul–Dec	Jan–Dec	Jan–Dec
	°C	°C	AVG	2017	%	AVG	2017	%	2017	%
Saipan, 15°N, 146°E	+2.63 +1.60	+3.42 +2.61	449.1	534.2	118.9	1322.8	861.3	65.1	1395.5	78.8
Guam, 13°N, 145°E	+0.70 +0.82	+0.80 +0.64	691.6	900.9	130.3	1788.4	1561.6	87.5	2462.5	99.4
Yap, 9°N, 138°E	-0.70 +0.08	-0.43 +0.01	1169.7	1548.4	132.4	1902.0	1985.0	104.4	3533.4	115.0
Palau, 7°N, 134°E	+0.77 +0.18	+0.97 +0.20	1717.6	2037.8	118.6	2032.5	2452.4	120.7	4490.2	119.7
Chuuk, 7°N, 152°E	+0.51 +1.28	+1.10 +1.31	1584.2	1544.3	97.6	1833.1	1923.8	104.9	3468.1	101.5
Pohnpel, 7°N, 158°E	-0.54 +1.81	-0.54 +1.92	2266.4	2613.7	115.3	2336.5	2231.1	95.5	4844.8	105.3
Kapinga, 1°N, 155°E	—	—	1750.8	2406.9	137.5	1510.5	1855.0	122.8	4261.9	130.7
Kosrae, 5°N, 163°E	+0.09 +2.03	-0.04 +2.39	2567.9	3062.5	119.3	2342.9	2782.1	118.7	5844.5	119.0
Majuro, 7°N, 171°E	+0.07 +0.81	+0.09 +0.65	1368.3	1739.1	127.1	1868.2	2414.3	129.2	4153.4	128.3
Kwajalein, 9°N, 168°E	+0.98 +0.53	+0.65 +0.65	801.4	891.8	112.1	1579.1	1503.6	95.2	2395.5	100.9

depression that would become Tropical Storm Lan two days later.

The sea level across Micronesia exhibits large fluctuations related to ENSO. During the 2015 El Niño, the sea level dramatically fell across the region. During 2016, with the demise of El Niño, the sea level began a dramatic climb to become 6–8 cm above average by the end of the year. The sea level remained well above average throughout Micronesia for all of 2017, as La Niña became established in the second half of the year. Interannual variations of sea level across Micronesia are almost entirely a result of forcing by the Pacific trade wind system (blue line in Fig. 7.49). Fortunately, due to a general lack of high surf and swell, the high sea levels

in 2017 only resulted in mostly nuisance inundations at times of unusually high astronomical tides. However, two incidents of moderate inundation (both related to brief episodes of high wind and waves) occurred on the lagoon side of Majuro and on the northeast coast of Kosrae.

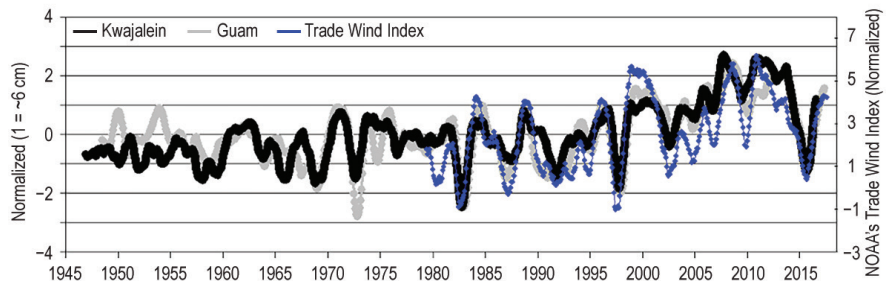


Fig. 7.49. Time series of sea level at Guam (gray line) and Kwajalein (black line) since 1945. Blue line is a time series of NOAA’s trade wind index for the region. Note the rapid rise in all times series at the end of the 1990s through the mid-2000s coinciding with La Niña, and also the sharp minima during strong El Niño events (e.g., 1983, 1997, and 2015). There is a sharp rise of sea level in 2016 that remained high during 2017. A 12-month moving average has been applied to the raw monthly values of each time series.

Low rainfall from late 2016 through September 2017 resulted in drought emergencies in most of the atolls in the northern RMI. Loss of potable water sources required the emergency shipment of bottled water, reverse osmosis systems, emergency food supplies, and public health and hygiene assistance. During this period the Guam Weather Forecast Office issued 18 bi-monthly specially tailored drought information statements for the RMI Government and U.S. State Department relief agencies.

3) SOUTHWEST PACIFIC—A. Peltier

Countries considered in this section include: American Samoa, the Cook Islands, Fiji, French Polynesia, Kiribati, Nauru, New Caledonia, Niue, Papua New Guinea (PNG), Samoa, the Solomon Islands, Tokelau, Tonga, Tuvalu, Vanuatu, and Wallis and Futuna. Air temperature and precipitation anomalies are relative to a 1981–2010 period unless otherwise indicated.

(i) Temperature

The southwest Pacific experienced warmer-than-average conditions throughout most of 2017. The only exceptions were islands close to the equator such as Nauru and Kiribati, where near or below-average temperatures were observed, as ENSO-neutral conditions prevailed for most of the year (Fig. 7.50).

The year started with exceptionally warm conditions across the region. In January, monthly anomalies exceeded two standard deviations over a wide area east of the dateline encompassing Tuvalu, Tonga, Wallis and Futuna, Samoa, American Samoa, and the Cook Islands. This resulted in the second highest monthly anomaly of $+0.96^{\circ}\text{C}$, behind the record set in December 1998 ($+0.99^{\circ}\text{C}$) for the temperature anomaly averaged over the southwest Pacific area $25^{\circ}\text{--}10^{\circ}\text{S}$ and $156^{\circ}\text{E--}226^{\circ}\text{E}$ (Fig. 7.51).

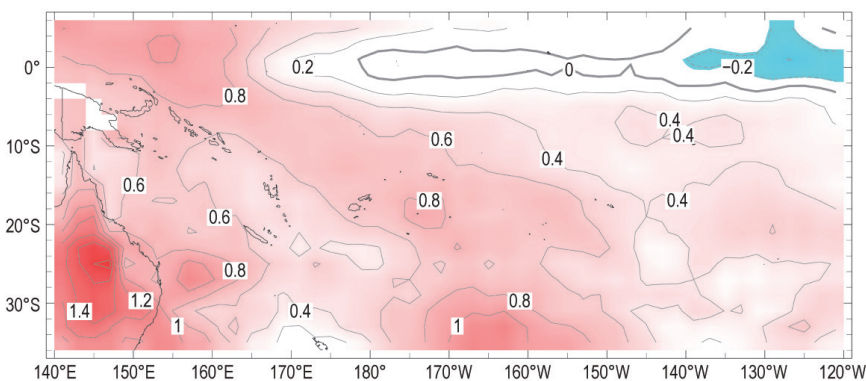


FIG. 7.50. Annual average surface air temperature anomalies ($^{\circ}\text{C}$, 1981–2010 base period; Source: NOAA NCEP CPC CAMS.)

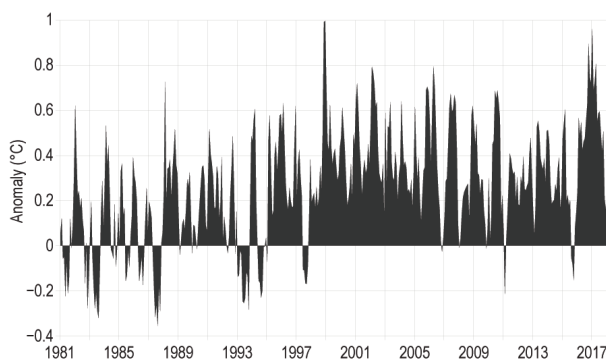


FIG. 7.51. Monthly average surface air temperature anomalies ($^{\circ}\text{C}$, 1981–2010 base period) for the entire southwest Pacific area ($25^{\circ}\text{--}10^{\circ}\text{S}$ and $156^{\circ}\text{--}226^{\circ}\text{E}$) from 1981–2017. (Source: NOAA NCEP CPC CAMS.)

Apart from the equatorial area, which was average to below average, the region experienced relatively large positive temperature anomalies until April. While steadily declining in magnitude, temperature anomalies remained positive until the end of the austral winter. In October, surface temperature anomalies leaned toward negative values over French Polynesia and the Cook Islands. By the end of December, near to below-average temperatures covered most of the Pacific island countries east of the dateline.

(ii) Precipitation

In Nauru and the Kiribati Gilbert Islands, which are located near the equator west of the dateline, drier-than-average conditions prevailed during the first half of 2017, as cloudiness was reduced in both the intertropical convergence zone and the northwestern sector of the southern Pacific convergence zone (SPCZ). After two months of respite in July and August with above-average precipitation, relatively dry weather conditions resumed during the last four months of the year with ENSO trending towards La Niña.

Precipitation totals for 2017 were as low as 50% of average in Nauru and the Gilbert Islands. These dry conditions in 2017 were an extension of a drought event that began during the second half of 2016.

Farther south, the transition from a neutral ENSO state to a weak La Niña resulted in a rainfall pattern close to normal across most of the South Pacific from January to October. Yet, two notable

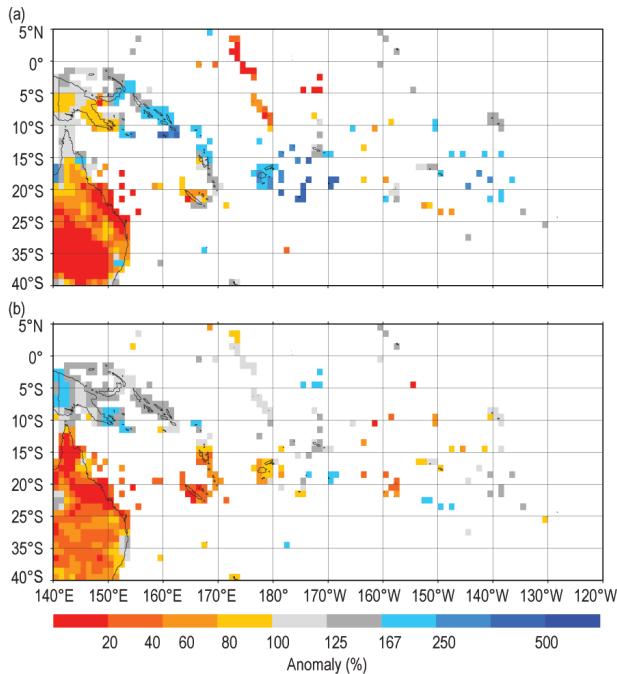


FIG. 7.52. Precipitation anomalies (% of normal wrt 1951–2000): (a) Feb 2017, (b) Jun–Aug 2017. (Source: GPCP Monitoring Product version 5.)

periods stood out. The first of these saw the SPCZ become remarkably enhanced in early February in response to an active Madden–Julian oscillation (MJO) phase over the western equatorial Pacific. This resulted in well above-average February rainfall over many Pacific nations (Fig. 7.52a): the Solomon Islands (170% of average), Fiji (160%), Wallis and Futuna (190%), Tonga (250%), and Niue (350%). The second notable period saw relatively dry conditions prevail between June and September west of the dateline, resulting in precipitation as low as 60% of average in Fiji, 40% in Vanuatu, and 30% in New Caledonia for the austral winter season (Fig. 7.52b). As oceanic indicators leaned towards La Niña in the tropical Pacific, cloudiness patterns across the region also showed a clear La Niña signal. In November and December, the SPCZ was slightly enhanced and displaced towards the southwest. This resulted in above-average rainfall across the Solomon Islands, Vanuatu, Fiji, Tonga, and Niue.

(iii) Notable events and impacts

On 7 February, a trough over the Solomon Islands and a slow-moving tropical low pressure system located in the Coral Sea caused heavy rain in and around Honiara, the capital city, situated on the northwestern coast of Guadalcanal. The rainfall total for that day was 208 mm, the sixth highest since records began in 1949 (Source: Global Historical Climate Network - Daily). The heavy downpour triggered flash flooding

in the city. Major roads were submerged and flooding was reported in the main hospital and in many residences. All of the Guadalcanal plains were covered with water, and farmers who supply vegetables to Honiara lost around 70%–80% of their production.

New Caledonia experienced its driest winter on record. Cold fronts that usually bring precipitation to the island passed farther south than usual from mid-June to mid-July as a consequence of a positive southern annular mode. While the southern annular mode returned to neutral by August and frontal systems returned to their near-average position, most frontal systems rapidly dissipated while approaching New Caledonia. In Noumea, the capital city, the winter precipitation total was 33% of normal, the lowest on record (since 1951). Spring (SON) is usually the driest season in New Caledonia, and 2017 was no exception. The rain showers in early December ended the longest sequence of daily rainfall totaling 5 mm or less: 139 days for Noumea. As a result, New Caledonia experienced agricultural and hydrological droughts in the second half of 2017. The main consequences were restrictions on drinking water and fires that destroyed vast areas of vegetation, including primary forests, despite a territory-wide fire ban.

4) AUSTRALIA—S. Tobin and S. J. Jacobs

The base period for this section is 1981–2010. Nationwide monthly average temperatures are based on the ACORN-SAT dataset (Trewin 2013), which extends to 1911. The rainfall and daily temperatures are based on the AWAP dataset (Jones et al. 2009), which extends to 1910.

(i) Temperature

The 2017 annual mean temperature for Australia was 0.64°C above the 1981–2010 average, its third warmest year on record. The decade ending 2017 was 0.30°C higher than average and the warmest 10-year period in Australian records.

Australian mean maximum temperatures (Fig. 7.53) were 0.97°C above average, the second highest on record. Mean minimum temperatures (Fig. 7.54) were 0.31°C above average, the 11th highest on record.

Annual mean temperatures were above average for almost all of Australia and record high for much of the southern half of Queensland, northwestern New South Wales, and an area on the central coast of New South Wales between Sydney and Port Macquarie.

Maxima were above average for nearly all of Australia and in the highest 10% of observations for nearly all of eastern Australia, South Australia, and most of the Northern Territory. Maxima were the highest on

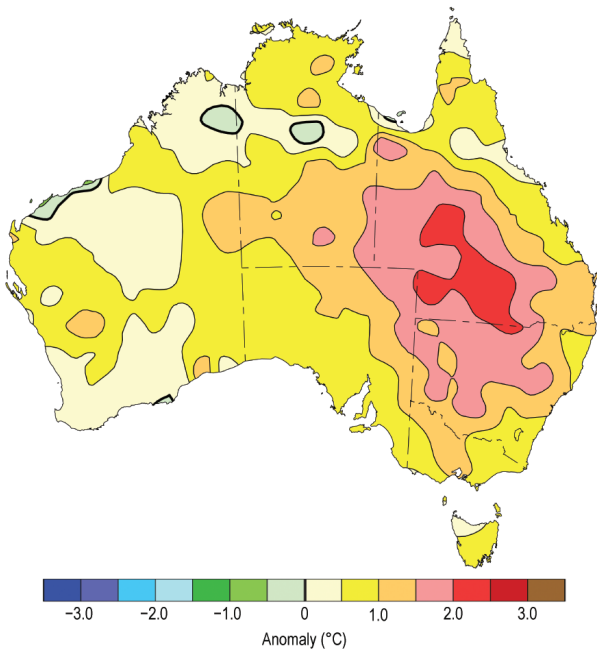


FIG. 7.53. Maximum temperature anomalies (°C) for Australia, averaged over 2017, relative to a 1981–2010 base period. (Source: Australia Bureau of Meteorology.)

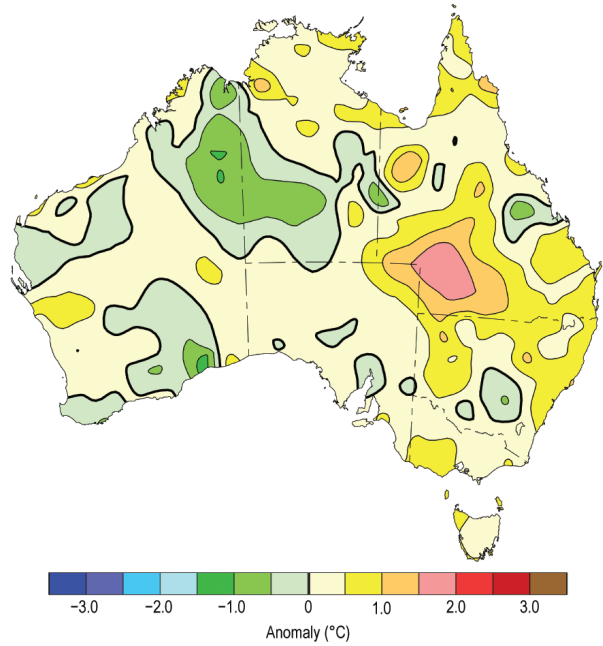


FIG. 7.54. Minimum temperature anomalies (°C) for Australia, averaged over 2017, relative to a 1981–2010 base period. (Source: Australia Bureau of Meteorology.)

record for much of the southern half of Queensland and some parts of northern New South Wales.

Minima were in the highest 10% of observations for much of Queensland, northern and eastern New South Wales, southwest Victoria, parts of coastal South Australia, western Tasmania, and parts of the Top End in the Northern Territory. Minima were highest on record for an area of southwest Queensland. Minima were above average for much of the rest of Australia but cooler than average for an area of inland northwestern Australia spanning the border between Western Australia and the Northern Territory.

Persistent warmth was featured throughout 2017. Daytime temperatures were especially warm, with monthly mean maxima ranking among the ten warmest on record for March, each month from May to September, and December.

January to March was much warmer than average for eastern Australia, while above-average rainfall kept days cooler than average in the northwest. Clear skies associated with a persistent strong high pressure ridge across the country contributed to warm, sunny days and cooler-than-average nights during late autumn and winter. June nights were much cooler than average for much of the southern mainland. Southeast Australia experienced cooler-than-average nights for a longer period, extending into September.

In contrast, daytime temperatures during July were particularly warm, with maxima highest on record for much of northern Australia. Exceptional warmth was present during September–December, largely associated with blocking highs over the Tasman Sea and particularly affecting eastern Australia (see Notable events and impacts and Sidebar 7.4).

These prolonged warm spells on land also affected the surrounding oceans. For the Tasman Sea region, October, November, and December were each warmest on record for their respective months. This occurred without a southward extension of the warm East Australian Current and in the absence of El Niño—both of which contributed to exceptional sea surface temperatures (SSTs) in the region during the first half of 2016.

Annual SSTs for the Australian region were the eighth highest on record, based on ERSSTv5 data. Above-average annual SSTs have been observed each year from 1995 to 2017 (inclusive), with a range of negative effects on the marine environment. Prolonged high SSTs led to significant coral bleaching on the Great Barrier Reef during early 2017, following record bleaching during summer 2015/16. This is the first time mass bleaching events have occurred in consecutive years and in the absence of El Niño (see Sidebar 3.1 for more details).

(ii) Precipitation

2017 was a year of contrasts for rainfall, with a wet start, a dry middle, and a wet end. Averaged across Australia, rainfall for 2017 was 504 mm, 4% above the 1981–2010 average, the 30th wettest in the 118-year record. Annual rainfall was above average for the southeast, interior, and far north of Western Australia, for most of the Northern Territory, and for the west of South Australia. Large parts of Western Australia had annual rainfall in the highest 10% of their records (Fig. 7.55). Rainfall was below average for most of inland Queensland, most of New South Wales, eastern to central Victoria, all of Tasmania, and pockets of the west coast of Western Australia.

January and February rainfall was above average across the western half of Australia, while February rainfall was below average for large parts of eastern Australia.

In March, heavy rainfall events in New South Wales and Victoria, and Severe Tropical Cyclone Debbie in Queensland and northern New South Wales, brought above-average monthly rainfall along the east coast.

From April to September rainfall was generally below average, particularly over southeastern Australia. A positive southern annular mode (SAM) and strong subtropical ridge contributed to below-average winter rainfall by shifting the belt of westerly winds southward, resulting in fewer rain-bearing low

pressure systems and cold fronts crossing southern Australia. A climate change signal has been identified in the observed increase in the strength of the subtropical ridge and reduction of cool season rainfall in southern Australia over recent decades (Timbal and Drosowsky 2012).

June was the second driest on record nationally, and the driest on record for southeastern Australia as a whole (land area south of 33°S, and east of 135°E), while September was the driest on record for the Murray–Darling Basin.

October rainfall was above average for much of Australia, with flooding on the east coast of Queensland around Bundaberg and Tully. For Queensland, it was the third wettest October on record. November rainfall was generally average to above average, and while December was drier than average for Queensland and the Northern Territory, heavy rainfall events in southeast Australia and Tropical Cyclone Hilda in Western Australia resulted in above-average monthly rainfall across large areas.

The main natural climate drivers for Australia—ENSO and the IOD—were in a neutral phase for most of the year. However, cooler-than-average waters to Australia’s west and warmer-than-average waters to the east of Africa to the south of the IOD regions created a strong temperature gradient across the Indian Ocean during the year, exerting a drying influence on Australia.

(iii) Notable events and impacts

Exceptional warmth affected large parts of eastern Australia from late December 2016 into February 2017. Records were set in southeastern Australia and southern Queensland for consecutive warm days or nights, or for total number of warm days or nights during January. Five separate locations in Queensland broke previous state records for hottest February day on the 12th.

The McArthur Forest Fire Danger Index (FFDI) reached catastrophic levels across much of New South Wales on 12 February. A fire in the Warrumbungle Shire destroyed most of the small township of Uarby.

Slow-moving tropical lows brought heavy rain over much of northern and western Australia between late January and early February. Cumulative rainfall resulted in flooding in the Kimberley and in parts of southwest Western Australia, the latter of which typically has low summer rainfall.

Flooding affected large areas of the east coast during March, resulting from thunderstorms in New South Wales around mid-month, thunderstorms in Victoria on 20 and 21 March, and Severe Tropical

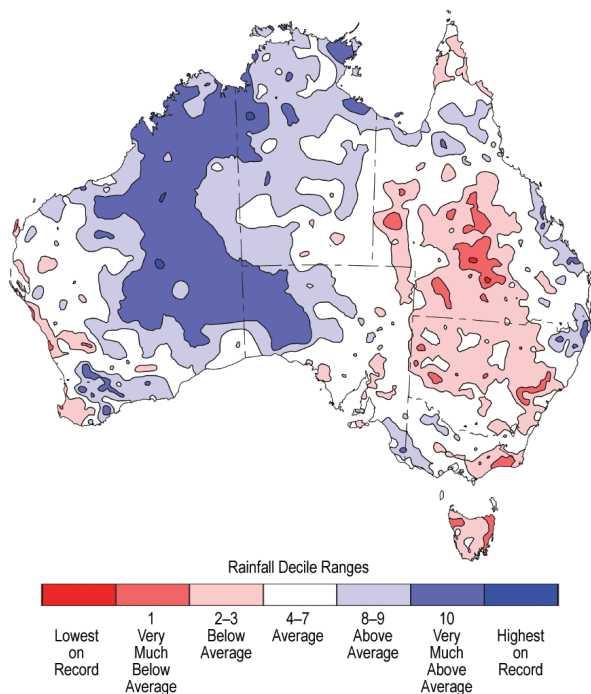


FIG. 7.55. Rainfall deciles for Australia for 2017, based on the 1900–2017 distribution. (Source: Australia Bureau of Meteorology.)

Cyclone Debbie at the end of the month. Debbie caused flooding and widespread wind damage in Queensland and northeastern New South Wales, with flooding continuing into April in some rivers.

An exceptional period of warm weather during the last week of September saw many records for high temperatures or early season warmth set in eastern Australia (see Sidebar 7.4).

In early October, heavy rainfall associated with surface and upper-level troughs affected southeastern Queensland and northeastern New South Wales, with flooding around Bundaberg. Further heavy rain midmonth affected the same region, as well as areas of Queensland's tropical coast, with flooding around Tully.

After a cool and frosty start to November an extended period of very warm weather affected Victoria and Tasmania, driven by long-lived blocking highs over the Tasman Sea during both November and December (see also Sidebar 7.4). November monthly mean temperatures were the highest on record for Tasmania and second highest for Victoria. Warmth was more widespread in December, affecting all states and the Northern Territory. These high pressure systems also contributed to record high sea surface temperatures for Bass Strait and the Tasman Sea as clear skies allowed more solar radiation absorption, and light winds limited mixing of surface waters.

An influx of tropical moisture between 1 and 3 December brought two to three times the monthly average rainfall to parts of northern Victoria and southern New South Wales. Flooding resulted in central to northeastern Victoria, with some flash flooding around Melbourne.

For further detail on these and other significant events please see Monthly Weather Reviews, Special Climate Statements, and the Annual Climate Statement—all available from www.bom.gov.au/climate/current/.

5) NEW ZEALAND—B. E. Noll

In the following discussion, the base period is 1981–2010, unless otherwise noted. The nationwide average temperature is based upon the National Institute of Water and Atmospheric Research (NIWA) seven-station temperature series that began in 1909 (see www.niwa.co.nz/our-science/climate/information-and-resources/nz-temp-record/seven-station-series-temperature-data). All statistics are based on data available as of 9 January 2018.

(i) Temperature

According to NIWA's seven-station temperature series, 2017 was New Zealand's fifth warmest year since records began in 1909. The nationwide average temperature for 2017 was 13.15°C, 0.54°C above the annual average. Annual mean temperatures were near average (within 0.5°C of the annual average) or above average (0.51°–1.20°C above the annual average) throughout the country (Fig. 7.56a). Only January observed a below-average nationwide temperature (0.7°C below average). The three months in 2017 with the largest national temperature anomalies were December (+2.4°C), August (+1.3°C), and November (+1.1°C). These marked New Zealand's second warmest December, third warmest August, and sixth warmest November on record. The warmth seen in November and December were likely influenced by synoptic patterns which also contributed to the exceptional warmth also experienced across southeast

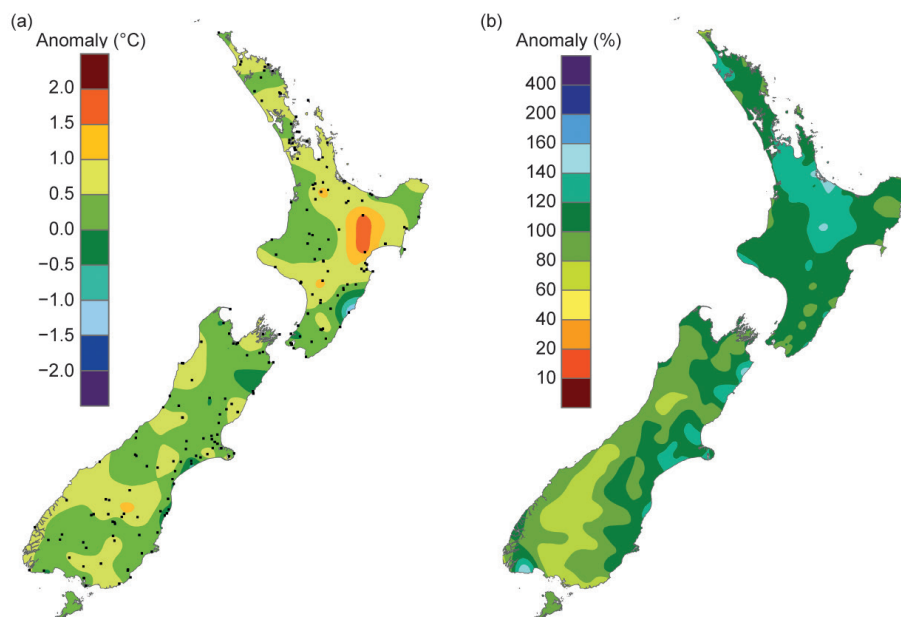


FIG. 7.56. 2017 annual (a) mean temperature anomaly (°C) and (b) total rainfall (%), relative to 1981–2010. (Source: NIWA.)

Australia and the Tasman Sea (see Sidebar 7.4). The highest recorded air temperature for 2017 was 35.5°C, at Wairoa (Hawke's Bay) and Ashburton (Canterbury) on 6 February (see Fig. 7.57 for localities). The lowest recorded air temperature for 2017 (excluding high altitude alpine sites) was -14.6°C, observed at Lake Tekapo (Canterbury) on 29 July.

(ii) Precipitation

Annual rainfall totals for 2017 were above average (120%–149% of the annual average) in Auckland, Waikato, Bay of Plenty, coastal Canterbury, and north coastal Otago (Fig. 7.56b). On the other hand, rainfall was below average (50%–79% of the annual average) across much of Southland and interior Otago. Elsewhere, 2017 annual rainfall totals were near average (within 20% of the annual average). Five locations observed near-record high annual rainfall totals while three locations observed record or near-record low rainfall totals.

Of the regularly reporting rainfall gauges, the wettest location in 2017 was Cropp River, in the Hokitika River catchment (West Coast, South Island, 975 m above sea level), with an annual rainfall total of 8662 mm (76% of the long-term average). The driest of the regularly reporting rainfall sites in 2017 was Clyde (Central Otago), which recorded 278 mm of rainfall (67% of the long-term average). Milford Sound (Southland) experienced the highest one-day rainfall total in 2017: 309 mm on 31 January.

(iii) Notable events and impacts

Figure 7.57 provides a schematic of notable events. By the end of 2017, parts of eleven of New Zealand's sixteen geographical regions had experienced meteorological drought following a dry November and December. These regions included Northland, Auck-

land, Waikato, Taranaki, Manawatu-Whanganui, Wellington-Wairarapa, Hawke's Bay, Marlborough, Tasman, the West Coast, and Southland. In December, the Ministry for Primary Industries classified the drought as a medium-scale adverse event in Taranaki, western parts of the Manawatu-Whanganui region, and around Wellington. The drought conditions occurred following a wet start to the year, which featured significant rain impacts, especially across the North Island. These included two ex-tropical cyclones (Cook and Debbie), which affected the country during April, following a heavy rainstorm between 7 and 12 March. The impact from ex-Tropical Cyclone Debbie (4 April) led to several one-day rainfall records for the month of April across the Bay of Plenty, which contributed to severe flooding in parts of the region, and was particularly notable for the town of Edgecumbe.

Oamaru (Otago) had its second wettest year on record (813 mm of rain). On 21 July, 161 mm of rain fell, leading to flooding and making it the wettest day in the town since records began in 1950; thereafter, Oamaru recorded just 163 mm during the remainder of the year (August–December 2017).

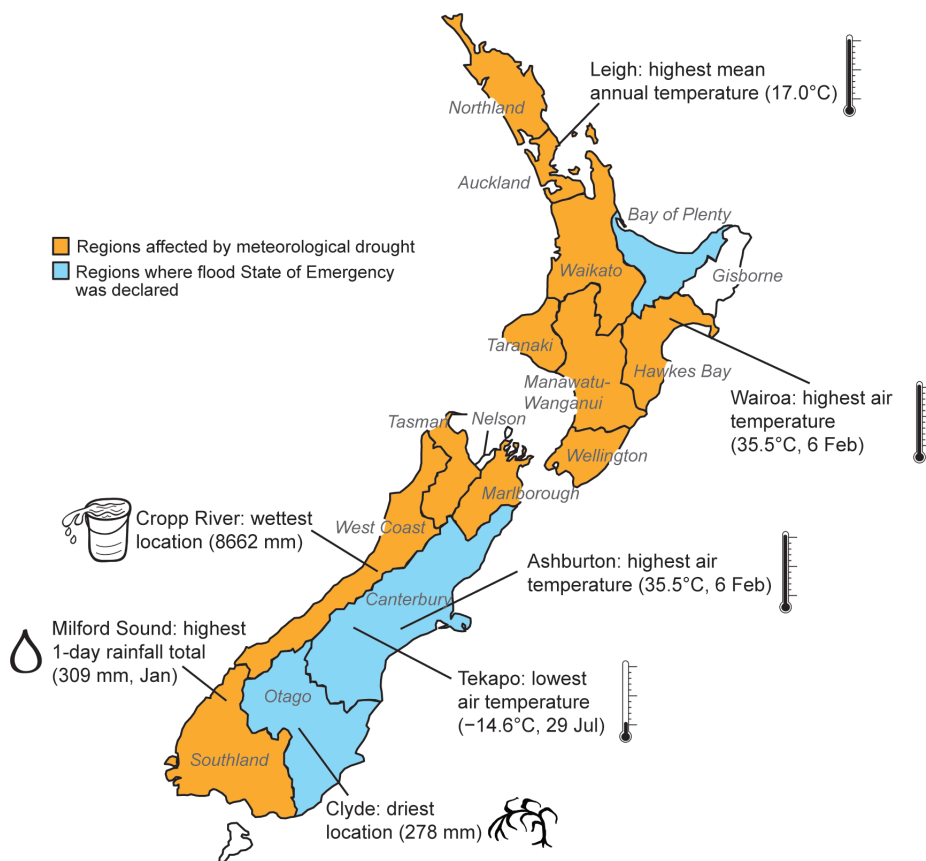


FIG. 7.57. Notable weather events and climate extremes for New Zealand in 2017. (Source: NIWA.)

SIDEBAR 7.4: **SUMMER ARRIVES EARLY IN AUSTRALIA AS THE AUSTRAL SPRING BREAKS RECORDS**—S. TOBIN AND S. J. JACOBS

Two significant heat events occurred during the Australian spring of 2017. The first event in September broke temperature records across eastern Australia while the second broke duration records in Victoria and Tasmania.

A high pressure system moved over New South Wales on 20 September. As a result, large parts of eastern and northern Australia had sunny, cloud-free days. With low rainfall through September and below-average soil moisture, these sunny days led to rapid heating of the land surface and overlying air in Central Australia, Queensland, and New South Wales.

By 22 September, the high pressure system became slow moving over the northern Tasman Sea while a low pressure system developed to the south of Australia. The two weather systems directed hot, dry air from the desert interior into eastern Australia, causing unprecedented hot September weather. The 22nd was Australia's warmest September day since national area-averaged analyses commenced in 1911, although the highest local temperatures were observed on the 23rd. Maximum temperatures were more than 12°C above the 1981–2010 average across much of the mainland southeast on the 23rd (Fig. SB7.6). A number of sites in New South Wales reached 40°C, the first such occurrences in the state during September, while in Victoria, Mildura set a state record for September reaching 37.7°C.

A new high pressure system crossed the southeast into the Tasman Sea between the 26th and 27th, bringing renewed heat to eastern Australia. During this period some New South Wales sites broke the records they had set only days earlier, while in Queensland, Birdsville reached 42.8°C on the 27th, setting a new state record for September. By 29 September more than 20% of Australia (by area) had recorded its hottest September day on record.

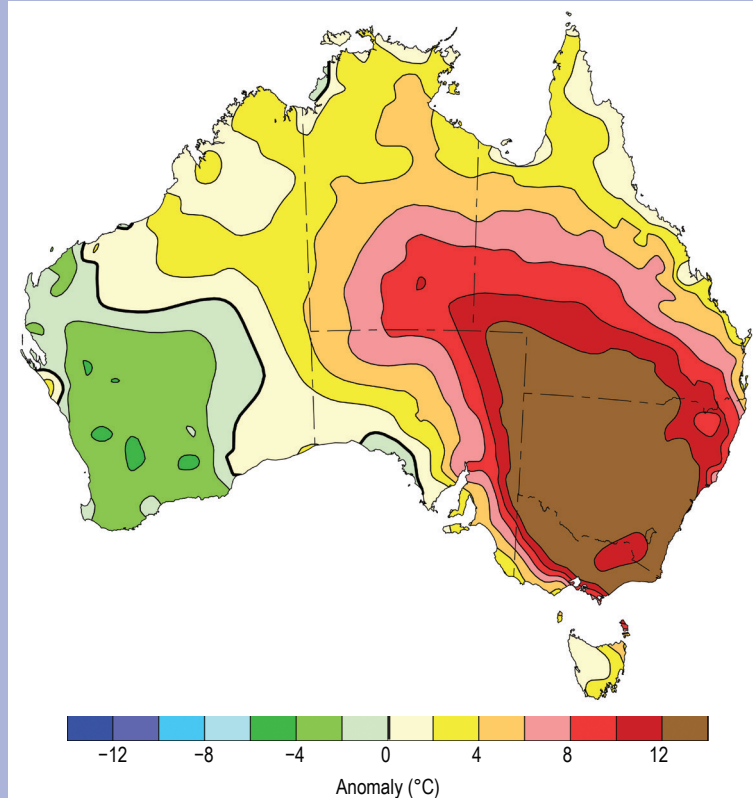


FIG. SB7.6. Maximum temperature difference (°C) from the 1981–2010 average for 23 Sep 2017. (Source: Australia Bureau of Meteorology.)

The heat returned in mid-to-late November when the southeastern states of Victoria and Tasmania experienced an unusually long run of warm days and nights. A long-lived blocking high was again responsible for the high temperatures, but this time the center was over the southern Tasman Sea, directing the hot, dry air into southern states from Central Australia.

The extended warm spell lasted from 10 November until the start of December when a strong trough accompanied by heavy rain crossed the states. This heat wave was notable for its duration rather than its intensity, with many records set for consecutive days with maximum or minimum temperatures above thresholds and only a few records set for individual days. Events of this duration are unusual in spring when weather systems are normally more mobile than in late summer and autumn.

CONT' SIDEBAR 7.4: **SUMMER ARRIVES EARLY IN AUSTRALIA AS THE AUSTRAL SPRING BREAKS RECORDS**—S. TOBIN AND S. J. JACOBS

During this event Melbourne experienced six consecutive days with maxima of at least 30°C and nine consecutive days of at least 28°C—the latter breaking the previous record of six days set in 2009. Melbourne also experienced 14 consecutive nights above 15°C, solidly surpassing the previous spring record of nine days in 2009. A warm spell of this length had not occurred in Melbourne before mid-summer (January) in at least the 108-year record.

In Tasmania, the length of the late spring warm spell was unprecedented for any time of year, particularly in the south and west. Many locations set November records for consecutive days above 25°C. Strahan, on the west coast, had 18 consecutive days (from 13 to 30 November) of maximum temperatures 21°C or above, including seven consecutive days of 27°C or above, both records for any time of year. Hobart's six consecutive days of 25°C or above equaled the record for any time of year, while its five consecutive nights above 15°C was a November record.

The prolonged heat event also caused a marine heatwave to form around Tasmania due to the clear skies and light winds associated with the blocking high over the Tasman Sea. The surface waters increased to 3°C above the 1971–2000 November average and ranked among the highest values on record in that region. The marine heatwave persisted into the austral summer with November, December, and January 2018 monthly sea surface temperatures highest on record for large areas around Tasmania and extending to the western coast of New Zealand (Fig. SB7.7).

For further details on both events, see Special Climate Statement 62 and 63: www.bom.gov.au/climate/current/statements/scs62.pdf and www.bom.gov.au/climate/cur

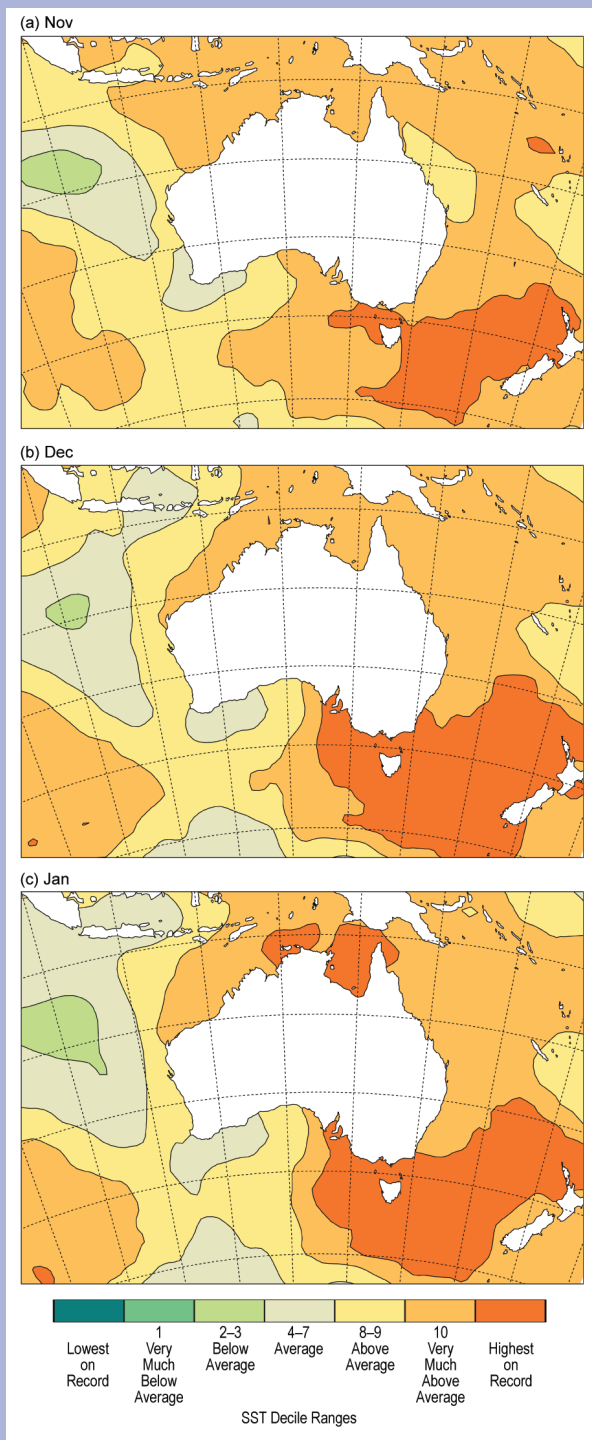


FIG. SB7.7. SST deciles for (a) Nov and (b) Dec 2017 and (c) Jan 2018, based on the 1900–2017 distribution using the NOAA ERSST v5 dataset. (Source: Australia Bureau of Meteorology.)